uOttawa

L'Université canadienne
Canada's university

FACULTÉ DES ÉTUDES SUPÉRIEURES ET POSTOCTORALES

uOttawa

L'Université canadienne
Canada's university

FACULTY OF GRADUATE AND POSDOCTORAL STUDIES

R. A. M. Dayani R. Mohottalage
AUTEUR DE LA THÈSE / AUTHOR OF THESIS

M.Sc. (Chemistry)
GRADE / DEGREE

Department of Chemistry
FACULTÉ, ÉCOLE, DÉPARTEMENT / FACULTY, SCHOOL, DEPARTMENT

Modulators of Proprotein Convertase, Subtilisin Kexin Isozyme-1 (SKI-1)/Site 1 Protease (S1P): Design synthesis and in vitro evaluation

TITRE DE LA THÈSE / TITLE OF THESIS

Dr. N. Goto
DIRECTEUR (DIRECTRICE) DE LA THÈSE / THESIS SUPERVISOR

Dr. A. Basak
CO-DIRECTEUR (CO-DIRECTRICE) DE LA THÈSE / THESIS CO-SUPERVISOR

EXAMINATEURS (EXAMINATRICES) DE LA THÈSE / THESIS EXAMINERS

Dr. R. Ben

Dr. W. Willmore

Gary W. Slater
Le Doyen de la Faculté des études supérieures et postdoctorales / Dean of the Faculty of Graduate and Postdoctoral Studies

Modulators of Proprotein Convertase, Subtilisin Kexin Isozyme-1 (SKI-1) /Site 1 Protease (S1P): Design, synthesis and in vitro evaluation

R. A. M. Dayani R. Mohottalage

Thesis submitted to the
Faculty of Graduate and Postdoctoral Studies
University of Ottawa
As partial fulfillment of the requirements for the degree of
Master of Science in Chemistry
Ottawa – Carleton Chemistry Institute
University of Ottawa
Ottawa, Ontario
CANADA, K1N 6N5

Candidate

.....
R.A.M. Dayani R Mohottalage

Supervisor

.....
Dr. Ajoy Basak

Co-Supervisor

.....
Dr. Natalie Goto

Your file Votre référence
ISBN: 978-0-494-59886-3
Our file Notre référence
ISBN: 978-0-494-59886-3

Abstract

Subtilisin Kexin Isozyme-1 (SKI-1) also called Site1 Protease (S1P) is a member of mammalian subtilisin family that is involved in cholesterol metabolism, lipid synthesis and viral infections. It is considered as a target for intervention of these diseases or disorders. Herein, vaccinia virus transfected HEK 293 expression system was used in the production of ~98 kDa C-terminally truncated soluble human hSKI-1 enzyme in enzymatically active form. Partial purification of recombinant (rec) hSKI-1 enzyme was achieved by using modified cell culture condition and affinity column chromatography. In addition, gel filtration size exclusion chromatography was also attempted as an alternative to column chromatography method to purify the enzyme. Purification of rec-hSKI-1 led to significant dimerization of the enzyme which results the partial loss of protease activity. Nonetheless, it was used to design novel SKI-1 inhibitors for biochemical and therapeutic applications.

Oxymethylene (-OCH_2-) based pseudo and multibranch peptide strategies were used for the design of new hSKI-1 inhibitors. The peptide sequences used in these approaches were obtained from SKI-1 prodomain near its autocatalytic cleavage sites. Depending on the length of the peptide sequence, competitive and mixed type inhibition was observed for the Oxymethylene based pseudo peptide inhibitors. However, most of them showed competitive inhibition of hSKI-1 activity, suggesting their interactions with the catalytic domain of SKI-1 enzyme. It also indicated that Oxymethylene function might be a good mimicry of peptidyl amide bond (-CONH-). In the pseudopeptide series, ~5 fold more inhibition was observed for the P_7-Tyr mutant peptide. This suggested the preference of aromatic residue at P_7 position of the substrate is important for hSKI-1 enzyme recognition. In the multibranch peptide series, the 2- and 4- branch peptides displayed ~8.6

and ~13 fold increased inhibition of hSKI-1 enzyme respectively compared to the single branch linear peptide. This suggests that increasing the number of inhibitory peptide chain within a core molecule may be an interesting concept for the design of enzyme inhibitors and should be explored not only for convertase but also for other protease inhibition as well.

Table of content

Chapter 3: Materials and Methods

Dedication

TO :

My husband Susantha, our daughters Dhanuddara and Medhani and to my mother and my late father

Acknowledgement

I would like to convey my sincere gratitude to my supervisors Dr. Ajoy Basak and Dr Natalie Goto for their guidance, direction and support extended to me throughout the entire period of my studies. I would like to express my special gratitude to Dr Ajoy Basak for accepting me as a graduate student and providing me an opportunity to study under his broad experience and knowledge by facilitating me to continue my research in his protein chemistry laboratory at OHRI. I admire Dr Goto's guidance and extensive support in bringing my research and this thesis up to the standard. I was privileged to gain great experiences in research and to explore my knowledge in the field of science under the supervision and direction of excellent supervisors.

I am grateful to Drs M. Chrétien, M. Mbikay and J. Mayne of "Convertase Group" of the Chronic Disease Program of OHRI, for their inspiration and advices extended to me especially during the difficult time of my studies. Thanks to Dr. N.G. Seidah and Ms. M.C. Asslin at Clinical Research Institute of Montreal for providing the SKI-1 construct and the cell line used in this study. My special acknowledgements go to Ms Francine Sirois for teaching me cell culture studies, Andrew Chen for assisting me in peptide synthesis and amino acid analysis and Charles Gyamera-Acheampong for his help in gel electrophoresis. I express my gratitude to Dr. Thierry Ducat, a former member of Dr Goto's lab, for his kind assistance in my FPLC work. I would like to pass my earnest thanks to all the former and present members of Dr. Basak's lab and Convertase Group at OHRI and Dr Goto's lab at the Department of Chemistry, University of Ottawa, for their corporation, friendship and support. I would also like to extend my gratitude to Ms. JoAnn McDonald, and Ms Denise Joanisse for their assistance in preparation of this thesis and administrative work during my stay at OHRI. I am grateful to NSERC for the Discovery grant to Dr A. Basak, which provided the financial support for my studies.

At last my heartfelt thanks go to my family for their endless patience and numerous sacrifices, which allowed me to work extended hours during the nights and weekends. I would like to convey my warmest gratitude to my husband Dr. Susantha Mohottalage for his continuous support, encouragement and constructive criticisms on my work and to my dearest daughters Dhanuddara and Medhani for their love and support.

List of figures

List of tables

Abbreviations

AEBSF	4-(2-aminoethyl benzene) sulfonyl fluoride
BSA	Bovine serum albumin
BDNF	Brain derived neurotrophic factor
BTMD	Before Trans Membrane Domain
CCHFV	Crimean Congo Haemorrhagic Fever Virus
Cmk	Chloromethyl Ketone
DEAE	Diethyl amino ethyl
DMF-	N, N-Dimethylformamide
DCM	Dichloromethane
DTT	Dithiothreitol
EDTA	Ethylene diamine tetraacetic acid
ER	Endoplasmic reticulum
FBS	Fetal bovine serum
gp	Glyco protein
HEK	Human Embryonic Kidney
HCMV	Human Cytomegalo virus
IQF	Intramolecularly quench fluorogenic
LCV	Lymphocytic Choriomeningitis Virus
MCA	Methyl coumaryl amide
NARC	Neural apoptosis-regulated convertase
PACE	Paired basic amino acid cleaving enzyme
PC	Proprotein Convertase
PCSK	Proprotein Convertase Subtilisin Kexins
QGPC	Quench Lassa virus Glyco Protein
"RSL"	Reactive site loop
rec-hSKI-1	Recombinant human Subtilisin Kexin Isozyme-1
SREBP	Sterol Regulatory Element Binding Protein
SPC	Subtilisin like Proprotein Convertases
S1P	Site 1 Protease
TFA	Trifluoroacetic Acid

CHAPTER 1:

Introduction Part-I: Background of Subtilisin Kexin Isozyme (SKI-1)

1.1 Overview of Subtilisin Kexin Isozyme (SKI-1)

Subtilisin Kexin Isozyme 1 (SKI-1) is an important member of proteolytic enzymes of subtilisin family that has drawn considerable interest in health research ever since its discovery in 1999 (1-6). The proteolytic enzymes, also called proteases or proteinases, cleave inactive protein precursors at specific sites to generate biologically and functionally active peptides. These enzymes constitute a large number that regulate normal metabolism, physiology, growth and many other biological functions in mammalian systems. Any irregularities in their levels of expression and activity lead to disorders or disease conditions and hence collectively they comprise a major target for the development of new therapeutics. Studies revealed that SKI-1 possesses important clinical and functional role particularly in viral infections, cholesterol regulation and lipid metabolism.

Extensive research on SKI-1 enzyme has been conducted during past decade leading to our increased knowledge about the function and the role of this enzyme in human health and diseases. In the sections below, a comprehensive literature review on various aspects of this enzyme including its discovery, enzymological, biochemical and functional properties is presented.

1.2 Discovery of SKI-1

Subtilisin Kexin Isozyme-1 (SKI-1) also known as **Site 1 protease (S1P)** was discovered in 1999 simultaneously by two research groups in Canada and USA (2;5). It was first identified as a protease that cleaves specifically at the site-1 position of human sterol regulatory element binding protein-2 (hSREBP2) and it was given the name S1P (2). At the same time, this enzyme was identified as the processing enzyme for Pro-BDNF (precursor of brain derived neurotrophic factor) intermediate form (28 kDa). The activity of this enzyme was found to be related to the bacterial subtilisin and yeast kexin and hence it was named as the Subtilisin Kexin Isozyme-1 (5). Since from its discovery, a lot of research has been conducted to understand the enzymological and biochemical properties and the function of this enzyme, using *in vitro, ex vivo* and animal models.

1.3 Classification of hSKI-1

SKI-1 is a widely expressed mammalian subtilase of the serine protease family with unique cleavage specificity. It is defined as the first known mammalian member of secretory subtilisin-like proprotein convertase that cleaves at the carboxyl side of the nonbasic amino acid residue (5;7;8). SKI-1 belongs to a group of nine mammalian **Proprotein Convertases (PCs)**, which are now more commonly referred to as **Proprotein Convertase Subtilisin Kexins (PCSKs)**. Previously they were also referred to as **Subtilisin like Proprotein Convertases (SPCs).** In order to avoid confusion with multiple names of the same enzyme, Alan J. Barrett and Neil Rawlings introduced a common system of nomenclature for all proteolytic enzymes (9;10). In this new system of classification proteases are divided into "clans" based on catalytic mechanism, and families on the basis of their common ancestry.

According to this new classification which include proteases of all types, SKI-1 and all other PCSKs belong to the clan SB (subtilisin-like). They are further grouped into the family of serine proteases (S8) which are mostly active at neutral-to-mild alkaline pH condition and thermo-stable with a preference to cleave after hydrophobic or basic amino acid residues. According to the similarities of their amino acid sequence and substrate specificity, serine protease family members have again been subdivided into sub types (http://merops.sanger.ac.uk/). All PCSKs are grouped in three major subtypes (i) kexin type (ii) pyrolysin type and (iii) proteinase-K type.

As summarized in **Table 1**, seven out of nine, PCs or PCSKs are of kexin type and they all cleave peptide bonds at the carboxyl side of Arg within the sequence motif **R/K/H-X-X-R↓** or **R/K/H-X-R/K-R↓**. These are PC1/PC3 (PCSK1), PC2 (PCSK2), furin/PACE (paired basic amino acid cleaving enzyme) (PCSK3), PC4 (PCSK4), PC5/PC6 (PCSK5), PACE4 (PCSK6), and PC7/PC8/LPC (PCSK7). Among these PCs, furin, PC5 and PC7 are membrane bound enzymes although they may undergo C-terminal shedding to produce active soluble forms. The remaining two PCs are known as non-basic amino acid cleaving subtilases. These are membrane bound Subtilisin Kexin Isozyme-1 (SKI-1) and NARC-1 (neural apoptosis regulated convertase 1) (PCSK9). These PCs are of pyrolysin and proteinase K types respectively (Table 1).

SKI-1 (PCSK8) belongs cleaves precursor proteins (substrates) at the C terminal side of a non basic amino acid residue characterized by the general motif of **R-X-L/I-L↓** (5;11;12).

Table: 1.0 *Nomenclature of mammalian Proprotein Convertases Subtilisin/Kexin-Like and their various alternative names.*

Subtype	Adopted Name (aliases)	Cleavage Specificity
Kexin-like	**PCSK1** (PC1, PC3, SPC3) **PCSK2** (PC2, SPC2) **PCSK3** (furin, PACE, SPC1) **PCSK4** (PC4, SPC5) **PCSK5** (PC5, PC6, SPC6) **PCSK6** (PACE4, SPC4) **PCSK7** (PC7, PC8, LPC, SPC7)	(H/R/K) –$(X)_n$ - R ↓ X or (H/R/K) –$(X)_n$ -K/R ↓ X
Pyrolysin-like	**PCSK8** (SKI-1,S1P)	R/K-X- (L,I,V)-Z ↓ X
Proteinase K-like	**PCSK9** (NARC-1)	V-F-A-Q ↓ S-I-P

Furin: Fes upstream protein; LPC: Lymphoma protein convertase; NARC-1: Neural apoptosis-regulated convertase-1; PACE: Paired basic amino acid cleaving enzyme; PC: Proprotein convertase; SIP: Site-one protease; SKI-1: Subtilisin kexin isozyme-1; SPC: Subtilisin-like proprotein convertase and where X= any amino acid, Z= small or hydrophobic amino acid

1.4 Mechanism and enzymatic action of serine proteases

All serine proteases contain three crucial amino acid residues in the active site, namely aspartic acid (Asp), histidine (His) and serine (Ser) (**Figure 1.0**). Serine proteases

cleave the peptidyl amide bond of their protein substrates via the formation of an acyl enzyme intermediate.

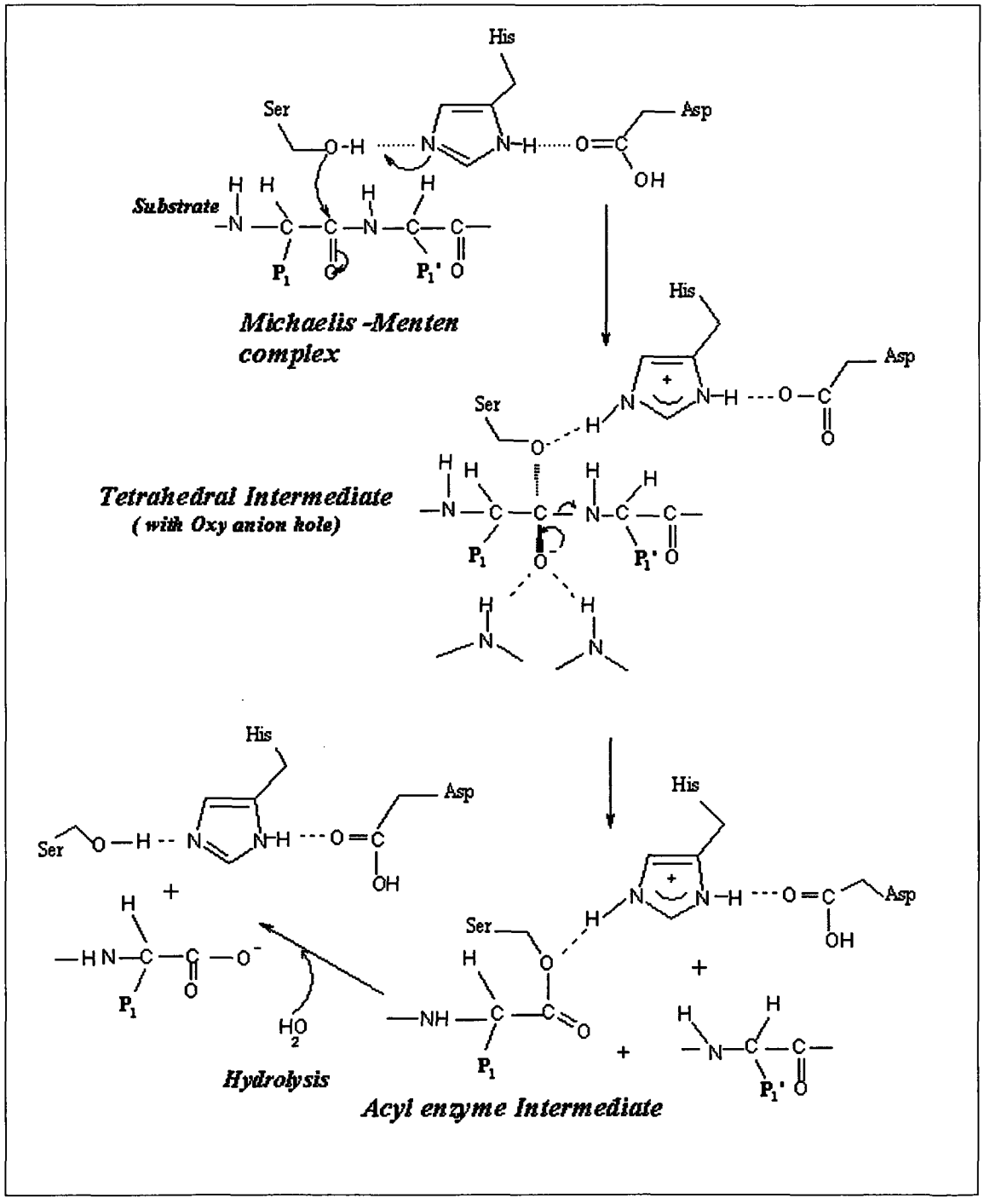

Figure 1.0: Mechanism involved in the enzymatic reaction catalyzed by serine protease family (13)

SKI-1 is believed to act via the same mechanism typically used by all serine proteases. In this reaction, catalysis is facilitated by the active site histidine, which abstracts a H^+ from the active site serine hydroxyl group to form a reactive oxyanion that undergoes a nucleophilic attack on the substrate peptide carbonyl group. This leads to the formation of a tetrahedral intermediate, which is stabilized by an "oxyanion hole". This oxyanion hole is usually formed by two backbone –NH- groups (and sometimes by the side chain of an Asn residue) while forming H-bonds to stabilize the negatively charged carbonyl oxygen atom. In the next step the intermediate collapses to re-form the carbonyl double bond, simultaneously eliminating the leaving group. The result is an "acyl enzyme" intermediate formed by the N-terminal portion of the peptide (substrate) that was cleaved and bound to the active site serine residue. Then hydrolysis of this intermediate releases the N-terminal peptide fragment and regenerates the active enzyme.

1.5 Localization and biosynthesis of SKI-1

SKI-1 is expressed in bones, teeth, striated muscles, cardiac muscles, brain (especially in cerebellum, pituitary & sub-maxillary) and even in the endocrine system related organs; for instance, in the thyroid and adrenal glands. It was also found to be present in the molar, thymus and in internal organs like kidney and intestine (5;14).

Active SKI-1 enzyme is reported to be found in the cis/medial of golgi apparatus of the cells (15;16). However, the full length SKI-1 (known as preproSKI-1) is synthesized in the nucleus as a membrane-bound, 1052 amino acids long protein with 148 kDa molecular weight. Once its signal peptide is removed by a signal peptidase cleavage at LVVLLC1^{17}↓GKKHLG site it migrates to the ER. It then undergoes sequential auto catalytic cleavage first at the N terminus and then at the C- terminus ultimately leading to active soluble form of the enzyme (5).

Three sequential N-terminal auto processing sites within the prodomain of the SKI-1 have been identified as RRLL^{186}↓RAIP (primary cleavage site), PQRKVFR^{134}↓SLKYAESD and PQRKVFRSLK^{137}↓YAESD (8), (secondary cleavage sites). Within the endoplasmic reticulum, the first cleavage at the RRLL^{186} site still forms an inactive enzyme since enzyme still remains associated with its cleaved 24 kDa prodomain protein. This prodomain protein is then further processed into 14, 10, and 8 kDa

intermediates, leading to its dissociation from the enzyme complex, generating active SKI-1. These multiple cleavages of the prodomain are believed to be mediated by the enzyme itself via an auto catalytic mechanism (8). These prodomain fragments dissociate and are ultimately degraded in the golgi apparatus and/or endosomes, leading to the generation of SKI-1 in enzymatically active form.

In support of these findings, it has been reported that prosegments of cysteine and other serine proteases act as intermolecular chaperones by catalyzing the protein folding of the enzymes. They function by binding transiently to newly synthesized polypeptides, thus combating the tendency of these chains to aggregate under intracellular conditions. In addition, prosegments were also found to regulate activity of the associated enzyme by strongly binding with the catalytic domain of the enzyme. Removal of this bound prodomain via proteolytic cleavage is a prerequisite to generate fully enzymatically active enzyme (17).

Later in the secretory pathway some of the membrane-bound SKI-1 enzyme sheds its cytosolic tail via cleavage at the C-terminal and 98 kDa active soluble form of the enzyme is then secreted into the extracellular milieu (5). This cleavage has been shown to take place at $KHQKLL^{953}\downarrow SID$ and is known as shed site. It is also mediated by SKI-1 itself. Thus the active soluble form of SKI-1 enzyme is represented by the sequence $hSKI^{187\text{-}953}$. Both membrane bound and soluble (shed) SKI-1 forms were found to be equally active (5). Even though most SKI-1 is found intra-cellularly, a significant portion is also secreted into the medium by C-terminal autocatalytic cleavage (18). Subcellular localization studies have also revealed that active (soluble) enzyme can be found in the cis/medial-golgi and it directly sorts to the endosomes/lysosomes without being transferred to the cell surface (16).

This biosynthetic path makes SKI-1 unique among the mammalian subtilases, since both the C-terminal and internal cleavages of its pro-segment occur in the endoplasmic reticulum (ER). In addition during its migration through the golgi apparatus, the enzyme is not transferred to the cell surface like other PCs (16). Hence, this enzyme does not appear to require an acidic environment for activation. By analogy with other subtilases, it is assumed that prosegment release and its degradation are important events for activation or maturation of this enzyme (8).

1.6 Biochemical and enzymological properties of SKI-1

The proteolytic activity of SKI-1 has been well demonstrated via the discovery of a number of physiological substrates. As mentioned above, the prodomain of SKI-1 itself is a substrate for the active hSKI-1 enzyme (8). In addition, several proteins have been found to be processed and activated by SKI-1. For example, the membrane-bound transcription factor, sterol regulatory element-binding protein-2 (SREBP-2), is one of the first described substrates of SKI-1. SREBP-2 is cleaved by SKI-1 in the luminal region at RSVL↓ site (2;14). Another substrate of SKI-1 is the 32 kDa pro-BDNF, which is cleaved by SKI-1 at $RGLT^{57}\downarrow$ to generate an intermediate 28 kDa form which is further cleaved by furin to produce the final bioactive 14 kDa BDNF protein (19). SKI-1 is also involved in the proteolytic activation of endoplasmic reticulum stress response transcription factor (ATF6) (20).

More recently SKI-1 has been shown to cleave prosomatostatin at the N-terminal site, generating a new form of somatostatin called antrin in Zebra fish (21;22). Here the cleavage occurs at $RQFL^{11}\downarrow$ site, consistent with the SKI-1 recognition sequence. Besides these physiological protein substrates, SKI-1 has also been shown to cleave surface glycoproteins of several viruses, particularly of hemorrhagic type. These include surface glycoproteins (gp) of Lassa virus (3), gp protein of Crimean Congo Hemorrhagic Fever Virus (CCHFV) (23) and the glycoprotein of Lymphocytic Choriomeningitis Virus (LCV) (1). Additionally, we recently reported using model peptides that cytomegalovirus protease may also be activated by the host protease SKI-1 (24).

SKI-1 exhibits its proteolytic activity at pH ranging from 5.5 to 7.4. It is mostly inactive outside this range (5). Interestingly most substrate cleavages by SKI-1 occur at neutral pH, however auto catalytic cleavage of the internal, prosegment at $PQRKVFRSLK^{137}\downarrow YAESD$ was found to be optimal at pH 8. In contrast, the optimum pH of SREBP-2 cleavage by SKI-1 was found to be 6.5, suggesting that the processing of SREBP occurs outside of the ER, perhaps in the golgi where pH is 6. The processing of pro-BDNF by SKI-1 was also found to be most effective in the slightly acidic range. In fact, pro-BDNF and its derived peptides all appear to be well cleaved even at pH 5.5, suggesting that SKI-1 could cleave this substrate (and possibly other substrates) in acidic

endosome-like compartments where it was previously localized (23). *In vitro* analysis confirmed that SKI-1 cleaves pro-BDNF very efficiently at pH 6.5. In addition, *in vitro* cleavage studies with SKI-1 showed that the pH optimum of SKI-1-mediated proteolysis differs from substrate to substrate and is most likely closer to the neutral pH values (i.e. pH 6.5- 7.5) (8). During the discovery of SKI-1 enzyme it was observed that metal chelators such as EDTA and o-phenanthroline effectively inhibited the processing of pro-BDNF by SKI-1, suggesting that SKI-1 could be a Ca^{2+} dependent protease. This was substantiated by the demonstration that the calcium ionophore A23187 inhibited the *ex vivo* cleavage of pro-BDNF. These experiments also indicated that SKI-1 functions most efficiently in the presence of 2–3 mM Ca^{2+} concentration (5). In later studies using metal chelation chromatography-purified SKI-1, it was shown that Ca^{2+} ion chelators also affected the cleavage of hSREBP-2 peptide. The same study indicated that 2 mM Ca^{2+} is required for optimal cleavage (8).

In contrast to these observations suggesting a Ca^{2+} requirement for SKI-1 activity, other studies indicated that SKI-1 activity is not dependent on calcium ion. Specifically, it was shown that hamster SKI-1 does not require Ca^{2+} and is only weakly inhibited by high concentrations of Ca^{2+} chelators (14). In recent studies using transfected insect cells (Spodopetera frugiperda ovarian cells, Sf9 and Sf21) it was reported that Ca^{2+} can stimulate hSKI-1 activity, but they claimed that hSKI-1 is a non-calcium dependent enzyme. Instead, the possibility that a variety of mono and divalent cations could modulate SKI-1 activity was raised (25). In addition, one report stated that the bivalent transition metal ions Cu^{2+} and Zn^{2+}, but not Ni^{2+} or Co^{2+} inhibit SKI-1 activity at mM concentrations.

Although the divalent ion requirements of SKI-1 have not yet been resolved, the disparity between the thoughts about Ca^{2+} dependency of SKI-1 may possibly be related to the source and purity of the enzyme used in respective studies. However, when isolated from mammalian cells (i.e. SKI-1 transfected HEK 293 cells) the available evidence seems to suggest that SKI-1 is a Ca^{2+} dependant enzyme (5).

1.7 Substrate specificity of hSKI-1

Based on cleavage sites of various SKI-1 substrates (**Figure1.1**) it was suggested that SKI-1 has an extended substrate-specificity pocket (5) with a preferred cleavage motif of

$$P_7\ P_6\ P_5\ P_4\ P_3\ P_2\ P_1\ P_1'$$

$$\phi\text{- X- X- }\psi\text{- X- }\theta\text{- }\Omega\downarrow x$$

Where the vertical arrow represents the cleavage site and; ϕ is aromatic hydrophobic residue (such as F/Y), X is any amino acid except Cys, ψ is any basic amino acid residue (such as R/K/H), θ is aliphatic and bulky side chain containing amino acid (such as L/I/V), Ω- is either small or alkyl side chain containing amino acids i.e. Ala, Leu or Thr and *x* is either Gly or Ser.

	Cleavage site							↓							
Substrate	**P8**	**P7**	**P6**	**P5**	**P4**	**P3**	**P2**	**P1**	**P1'**	**P2'**	**P3'**	**P4'**	**P5'**	**P6'**	**P7' P8'**
hproBDNF	Lys-Ala-Gly-Ser-**Arg**-Gly-**Leu**-**Thr**								**Ser**-Leu-Ala-Asp-Thr-Phe-Glu-His						
rproBDNF	Lys-Ala-Gly-Ser-**Arg**-Gly-**Leu**-**Thr**								Thr-Thr-Ser-Leu-Ala-Asp-Thr-Phe						
hproSKI-1	Arg-His-Ser-Ser-**Arg**-Arg-**Leu**-**Leu**								Arg-Ala-Ile-Pro-Arg-Gln-Val-Ala						
	Arg-Lys-Val-Phe-**Arg**-Ser-**Leu**-Lys								Tyr-Ala-Glu-Ser-Asp-Pro-Thr-Val						
hSREBP-2	Ser- Gly-Ser-Gly- **Arg**-Ser-**Val**- **Leu**								**Ser**-Phe-Glu-Ser-Gly-Ser-Gly-Gly						
hSREBP-1a	His-Ser-Pro-Gly- **Arg**-Asn-**Val**-**Leu**								**Gly**-Thr-Glu-Ser-Arg-Asp-Gly-Pro						
rproRelaxB	Ala-Ser-Val- Gly-**Arg**-Leu-**Ala**-**Leu**								**Ser**-Gln-Glu-Glu-Pro-Ala-Pro-Leu						
hproCCK-5	Arg-Ile-Ser-Asp-**Arg**-Asp-**Tyr**- Met								**Gly**-Trp-Met-Asp-Phe-Gly-Arg-Arg						
rproSomat.	Asp-Pro-**Arg**-**Leu**-**Arg**-Gln-**Phe**-**Leu**								Gln-Lys-Ser-Leu-Ala-Ala-Ala-Thr						
ATF6	Ala-Asn-Gln-Arg-**Arg**-His-**Leu**-**Leu**								**Gly**-Phe-Ser-Ala-Lys-Glu-Ala-Gln						
Lassa GPC	I le-Tyr-Ile-Ser-**Arg**-Arg-**Leu**-**Leu**								**Gly**-Thr-Phe-Thr-Trp-Thr-Leu-Ser						
CCHFV (gp-siteA)	Ser-Ser-Gly-Ser-**Arg**-Arg-**Leu**-**Leu**								**Ser**-Glu-Glu-Pro-Ser-Asp-Asp-Cys						
CMV-protease						**Arg**-Gly-Val-Val-Asn-**Ala**			**Ser**-Ser-Arg						
SKI-1 shed site						**Lys**-His-Asn-Lys-**Leu**-**Leu**			**Ser**-Ile-Asp						

Figure 1.1: *Cleavage sites of various substrates of SKI-1 (Important P_1, P_2 and P_4 basic and hydrophobic residues are shown in bold).*

1.8 Intramolecularly Quenched Fluorogenic (IQF) substrates for SKI-1 assay

Knowledge of preferred SKI-1 cleavage sites has allowed the development of fluorescent probes that can be used to measure *in vitro* the rate of proteolytic activity for this enzyme. Fluorescence based assays have the advantage of high sensitivity and the added benefit to develop them to use in high throughput systems (26). For this purpose, **intramolecularly quenched fluorogenic (IQF)** substrates have been introduced and used to identify inhibitors of SKI-1 enzyme (27-31).These IQF peptides contain a SKI-1 cleavage site with an electron donor fluorescent group on one terminus, and an electron acceptor fluorescence quench group at the other terminus of the peptide. In the intact form, quenching occurs through spectral overlap of electron donor and acceptor group which results the significant suppression of fluorescence. Hydrolytic cleavage of IQF substrate at any internal site leads to eliminate this quenching effect where the free electrons in the electron donor group (fluorescence group) become available. This leads to the release of fluorescence in to the assay media. The released fluorescence per unit of time gives a measure of cleavage efficiency. Thus the rate of fluorescence release is directly proportional to the rate of the enzymatic reaction.

In vitro hSKI-1 protease activity has been measured by using three intramolecularly quenched fluorogenic (IQF) peptides derived from known physiological substrates of SKI-1. One of the best synthetic substrates for SKI-1 was derived from the lassa viral glycoprotein and is known as Q-GPC (**Figure 1.2**) (25;32). A related substrate was derived from the surface glycoprotein of the Crimean Congo Hemorrhagic fever virus near its site-A cleavage domain and is called Q-CCHFV (**Figure 1.3**) (23). Both the above IQF substrates consist of an N-terminal Abz (2-Amino benzoic acid) as the donor group (fluorescence group) and a C-terminal 3-nitro-tyrosine residue as the acceptor or quench group.

A third IQF substrate was later designed also to measure SKI-activity *in vitro*. It is derived from the hSKI-1 cleavage site of the human cytomegalovirus protease (Q-CMV) and utilizes Edans as the fluorescent donor group at the C-terminus while Dabcyl as the electron acceptor quench group at the N-terminus (**Figure 1.4**) (24).

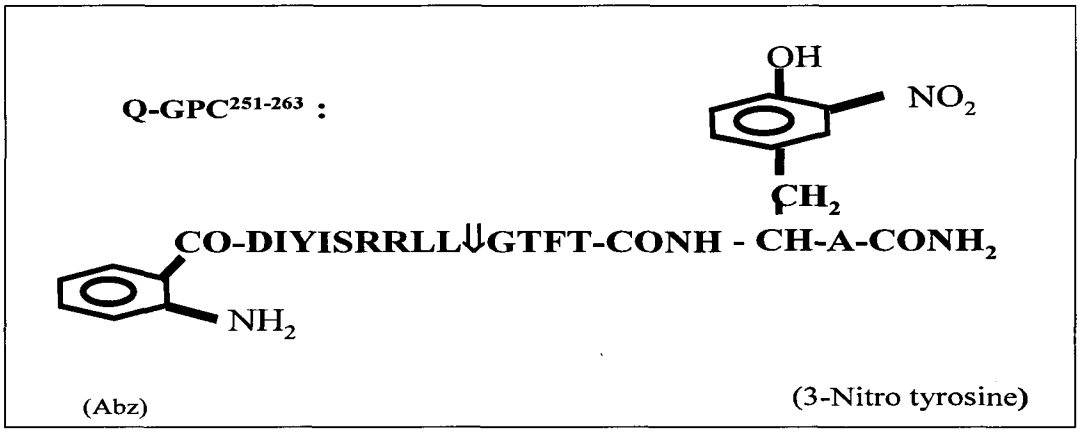

Figure 1.2: *Chemical structure of Q-GPC (containing amino acid sequence from 251-263 of lassa virus glycoprotein).*

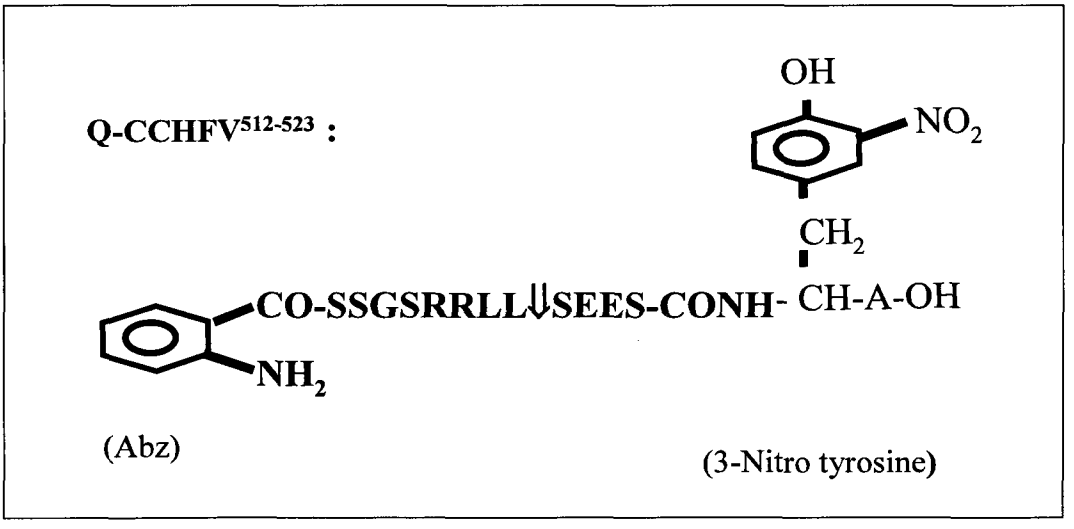

Figure 1.3: *Chemical structure of Q-CCHFV (Containing amino acid sequence from 512-523 of surface glycoprotein of CCHF virus).*

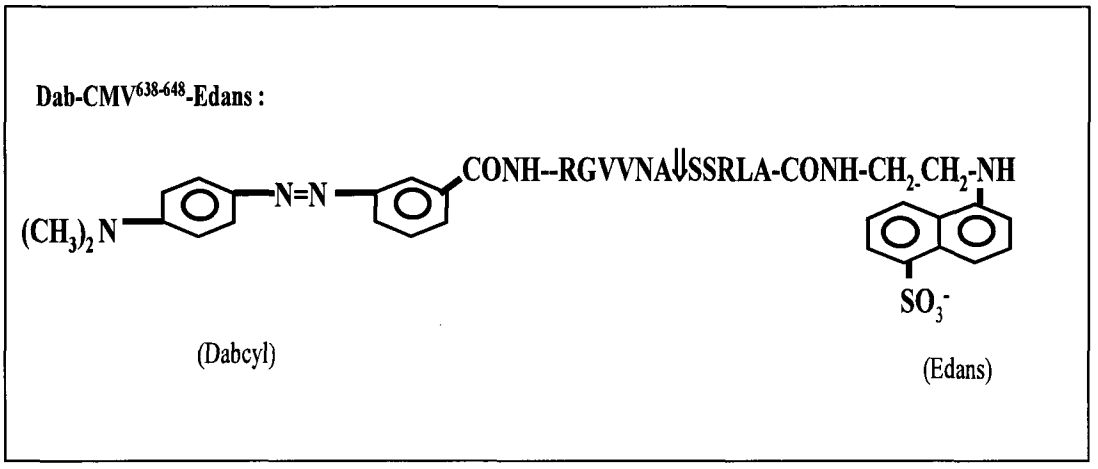

Figure 1.4: *Chemical structure of Q-CMV (Contains amino acid sequence from 638-648 of CMV- protease).*

1.9 Clinical implications of hSKI-1

The impact of SKI-1 on many human diseases and disorders has been revealed in a number of biochemical studies examining the role of this enzyme in human health and diseases. This was reflected by the findings that show the role of this enzyme in the cleavage of many vital protein precursors associated with the diseases. One such example is sterol regulatory element-binding proteins (SREBPs), which are membrane-bound transcription factors that promote cholesterol homeostasis and lipid synthesis in mammalian cells. Processing of SREBPs depends on the level of cholesterol. At low level of cholesterol, the sterol sensor protein, SCAP (SREBP cleavage-activating protein), which binds SREBP within ER, escorts it to the golgi, whereby the complex meets SKI-1 and the first cleavage at **RSVL↓** site occurs, followed by a second cleavage by a metalloproteinase called (S2P) at **DRSRILL↓** site. This generates a soluble cytosolic basic helix-loop-helix transcription factor, which enters the nucleus, binds to nuclear sterol regulatory elements and up-regulates the transcription of the various mRNAs needed for cholesterol and lipid synthesis and metabolism (33;34). In fact it enhances and activates transcription of genes encoding the low density lipoprotein (LDL) receptor and multiple enzymes of cholesterol and fatty acid biosynthesis (35). This suggests that SKI-1 plays an important role in the regulation of cholesterol and lipid synthesis in humans (2;14;36).

At the time of discovery of SKI-1 in 1999, it was shown that SKI-1 besides furin is also involved in the processing of pro-brain-derived neurotrophic factor (pro-BDNF), leading to bioactive products that protect neuron function and its degradation. Thus it has been suggested that SKI-1 may be associated with age-related neurological diseases via its role in cleaving precursor form of BDNF (5;19;19;37).

In addition, the proteolytic activation of ATF6, a membrane bound transcription factor by SKI-1 has been demonstrated. SKI-1 mediates ATF6 cleavage that activates several genes involved in ER stress response in protein unfolding (20). Evidence suggests that SKI-1 activity regulates the unfolded protein response to enhance the protein folding or refolding capacity in the secretory pathway (6;38). Since accumulation of unfolded proteins seems to contribute to the progression of neurodegenerative cerebro-vascular diseases like Alzheimer's, Parkinson's, Huntington's disease and amyotrophic lateral sclerosis (ALS), SKI-1 has become a potential therapeutic target for the intervention of these diseases as well (39).

Several studies revealed that the enzymatic activity of SK1-1 is required for several type of viral infections, particularly during the invasion and fusion with the host cell. One example is lassa virus. It is a member of the arenaviridae family, which causes lassa fever in humans. It was shown that the cleavage of lassa virus glycoprotein C (GP-C) into its active fragments GP1 and GP2 (3) is mediated by SKI-1. The cleavage of such surface glycoproteins of virus, initiates the fusion of virions with the host cell membrane. In a similar manner, SKI-1 was also shown to mediate site A cleavage of CCHFV glycoprotein (23), and also the surface protein of Lymphocytic Choriomeningitis Virus (LCV) (1) suggesting its role in these hemorrhagic infections in humans. Owing to these findings, SKI-1/S1P has become a major target for development of antiviral therapeutic agents.

As previously suggested by us, cleaving human cytomegalovirus (hCMV) protease by SKI-1 at maturational (M) site may possibly contribute to the CMV infection in humans (24), In the absence of extended biological studies, such a concept is still speculative at this stage, However, this cleavage induces the viral replication (40). hCMV is the most common opportunistic viral infection in immunodeficient patients. Thus by cleaving the maturational site of CMV protease, SKI-1 may play a role in these congenital viral infections in humans.

Besides, studies relevant to several human diseases, involvement of SKI-1 enzyme in cartilage development in zebrafish and mice has been presented in previous studies (21;41).

1.10 Inhibitors for hSKI-1 enzyme

Based on above clinical and biochemical studies implicating SKI-1 activity to several diseases and conditions, it is easily understandable why development of SKI-1 inhibitors has become so attractive objective to many researchers in the field. Several naturally occurring activators, inhibitors and binding partner proteins have been described for a number of PCs, but so far no such physiological regulators have yet been described for SKI-1 *in vivo*. Nonetheless, in recent years, interest in finding a physiological inhibitor for SKI-1 has grown considerably. It has stimulated the process and already several synthetic SKI-1 inhibitors have been reported. Based on structure, these inhibitors have been grouped into two general categories, namely (i) macromolecules such as proteins and (ii) small peptide molecules.

1.10.1 Macromolecule inhibitors of SKI-1

Bioengineered variants of serpins (**Serine Protease Inhibitors**), and SKI-1 prodomain proteins or polypeptides have been used as macromolecule inhibitors of SKI-1. For example, inhibitors based on α–1-Antitrypsin (AT) serpin protein have been developed as SKI-1 inhibitors. In this strategy the reactive site loop ("RSL") sequence **AIPM^{358}↓S** (arrow indicates the serpin cleavage site) was mutated to include a SKI-1 recognition motif (42). Among those tested only RRVL^{358}, RRLL^{358}, and RRIL^{358} variants showed the best inhibition of cellular SREBP-2, ATF6 and modified pro-PDGF processing by SKI-1 enzyme. Thus 4 μg of such an inhibitor representing 1:4 inhibitor: substrate ratio, exhibited 55-80% cellular inhibition of SREBP-2, ATF6 and modified PDGF cleavages by SKI-1 (42). In the same study it was shown that a 198 amino acid long hSKI-1 prosegment (SKI-1$^{1-198}$) containing the RRLL^{186}↓ cleavage site also possesses strong inhibitory activity against hSKI-1. In addition several bioengineered recombinant propeptides of SKI-1 were also developed in this study. And among these, the variant with the R^{134}E mutation was identified as the best inhibitor of SKI-1 activity (42).

Besides above findings, several short proteins derived from prosegment sequence of SKI-1 enzyme have been reported as moderate to strong inhibitors of SKI-1 enzyme (8). Prosegment proteins encompassing SKI-1 primary processing site ($RRLL^{186}$) were tested for SKI-1 inhibitory property and compared with that of full length prodomain hSKI-1 protein ($hSKI\text{-}1^{18\text{-}188}$) ending at the primary cleavage site ($RRLL^{186}\downarrow RA$) as well as one additional C-terminal extended prodomain and another C-terminal shortened protein ($hSKI\text{-}1^{18\text{-}197}$ and $hSKI\text{-}1^{18\text{-}169}$). The measured apparent inhibition constants (K_i app) were found to be within 97–182 nM, depending on the nature of the peptide. Prosegment construct ending at R^{188} remains potent among all the prodomain proteins tested (8).

1.10.2 Small peptide inhibitors of SKI-1

Small peptide inhibitors are more favoured as drug candidates in the pharmaceutical industry since they tend to be more proteolytically and thermally stable and can be engineered to be more bioavailable. There is also an opportunity to perform structure activity work with these compounds since they are easily accessible by synthetic means. In addition the process can be adapted to suite large-scale production. For these reasons several small prodomain based peptides have been studied as inhibitors of SKI-1 enzyme.

Previously our group reported a peptidyl analog as a SKI-1 inhibitor using the peptide sequence (VFRSLK) from the primary activation site of SKI-1 prodomain (43). This analog contains an AEBSF (aminoethyl benzene sulphonyl fluoride) moiety at the C-terminal of a peptide sequence. This molecule Ac-VFRSLK-AEBSF was shown to inhibit SKI-1 activity in a competitive manner with K_i ~58 nM when measured against the Q-$GPC^{251\text{–}263}$ substrate. This hexapeptidyl-AEBSF analog also showed similar SKI-1 inhibition when tested against other fluorogenic substrates suggesting that the measured inhibition is independent of the substrate used for the assay (43).

Earlier peptidyl chloromethyl ketones (cmks) containing a SKI-1 recognition sequence were also shown to behave as irreversible inhibitors of SKI-1. In those studies 4 mer decanoyl-RRLL-cmk was shown to be the best SKI-1 inhibitor with an IC_{50} value of 9 nM, which is ~250 fold more potent than either 6 or 7 mer cmk-peptides (Dec-YISRRLL-cmk and Dec-IYISRRLL-cmk) (44).

A few small molecule nonpeptide inhibitors of SKI-1 have also been reported These include AEBSF, which inhibited SKI-1 activity in a competitive manner against a number of intramolecularly quenched fluorogenic peptide substrates (IC_{50} ~200 to 800 nM) (43). 3, 4-dichloroisocoumarin (DCI) has also been shown as another nonpeptide molecule that inhibited SKI-1 activity with relatively high degree of potency (apparent inhibitory constant K_i app ~ 6.8 μM) (25).

1.10.3 Comparative evaluation of SKI-1 inhibitors

While there are at least a few SKI-1 inhibitors reported in the literature, only a limited number possess any high degree of potency or selectivity towards the enzyme. In most cases these inhibitors were tested *in vitro* against small peptide substrates, which may be less effective substrates than the proteins those are naturally cleaved *in vivo*. However, in a few instances inhibitors were also tested against protein substrates in cells. For example, in CHO-K1 cells, the bioengineered α 1-AT serpin as well as the SKI-prosegment mutant (ppSKI-1 $R^{134}E$) were identified as relatively potent cellular inhibitors of SKI-1 with 53–74% inhibition of endogenous SREBP-2 cleavage at concentrations within 10-100 μM range. In addition, they also reported inhibition of SKI-1 processing of exogenous ATF6 by prosegment mutant (42). Most SKI-1 prodomain peptide inhibitors showed significant SKI-1 inhibition only at high nM to low μM concentration levels.

Peptide analogs with C-terminal modification were found to be particularly potent SKI-1 inhibitors *in vivo*, with a measured K_i for Ac-VFRSLK-AEBSF of ~58 nM. *In vitro* assay using succinyl- MCA peptide substrate in the reported study it is found that decanoyl-RRLL-cmk inhibited SKI-1 activity with a much higher degree of potency than its seven mer peptide with the IC_{50} value of 9 nM. In the same study it was reported that *ex vivo* processing of pro-PDGF-A cleavage by SKI-1 was blocked only by 2% using 110μM dec-YISRRLL-cmk peptide. This suggested that c-terminal modified peptide analogs could be a good option to design potent inhibitors for hSKI-1 enzyme (43;44). However, the AEBSF peptide was found to be toxic to vero cells, indicating their incompatibility in *in vivo* applications.

In this connection it is important to point out that C-terminal peptides of PCs may also behave as regulators of their cognate enzyme (45). Even though such observation has

not yet been substantiated for SKI-1 enzyme, C-terminal tail peptide of SKI-1 was shown to act as an inhibitor of PC1 activity against some of its substrates in the endoplasmic reticulum and golgi apparatus (46).

1.11 Objectives of the study

Although SKI-1 plays an important role in a number of diseases and disorders, therapeutic agents to control its effects have not yet been identified. So far only a limited number of inhibitors have been identified from *in vitro* and *ex vivo* studies to modulate the activity of this enzyme. Most of these are protein-based and therefore are prone to proteolytic and thermal degradations. Although a few small molecules such as peptides or their analogs have been described as SKI-1 inhibitors there is always a need to develop strong and more potent inhibitors. The known pseudo peptide approach or the novel multi branch peptide strategies were never pursued to develop inhibitors of SKI-1 enzyme. In addition such inhibitors may be more potent, selective and bio available for biochemical and other applications. Since small molecule based inhibitors are more effective for therapeutic purposes, one of the objectives of this study was to develop small peptide inhibitors of hSKI-1 using the above mentioned strategies. However in order to develop and study inhibitors of SKI-1 enzyme, it is necessary to produce pure form of soluble and active form of this enzyme. So far there is only one reported instance of production and purification of recombinant SKI-1 enzyme (25). The availability of significant quantities of pure and soluble active SKI-1 would not only allow the inhibitors to be tested *in vitro*, but would also help to expand our understanding about the structural and physiological properties of this enzyme. For this reason the other objective of this project was to produce and purify soluble and active recombinant hSKI-1.

CHAPTER 2:

Introduction Part-II: Background related to thesis objectives

2.1 Overview of inhibitor design

In an enzyme catalyzed proteolytic reaction, any compound that decreases the measured rate of hydrolysis of a given substrate is generally termed as an inhibitor. Inhibitors play a vital role in our understanding of enzymatic activity in many biological processes. Knowledge about natural inhibitors in the physiological systems and the use of synthetic inhibitors in the characterization of such activity are particularly important in the search for therapeutic applications. Synthetic inhibitors also afford more practical use in biochemical and pharmacological research (13).

2.2 Selected inhibitor design strategies relevant to the project

i) Prodomain approach

It has been well established that the pro-segments of most proteases function as *in vivo* regulators of cognate enzymes (47). The prodomain sequence has frequently been used as a starting point in inhibitor design, as shown for cathepsins-B and L as well as papain, subtilisin, pepsin and stromelysin. As mentioned before this concept has been extended for design SKI-1 inhibitors. Thus prodomain and serpin inhibitors (42) and prosegment derived short protein / peptide inhibitors (8) have been reported. In this study specific prodomain sequences of SKI-1 were selected to design inhibitors for the enzyme.

ii) Pseudo peptide approach

Pseudo peptides are known to be very potent inhibitors of proteases as they mimic the peptide bond in their transition state but resists proteolysis. Pseudo peptide inhibitors are considered as transition state or substrate analogs. Here the strategy is to replace the scissile P_1-P_1' peptide bond of a potent substrate of the enzyme by a non-cleavable pseudo-peptide or isosteric bond. Various types of pseudo peptide linkages have been used in the past to generate peptide-mimetic compounds with high degree of stabilities and inhibitory potencies (24). Typical examples are: -C_αH-CH_2-NH- (amino), -C_αH-CO-CO- (oxalyl), C_αH-NH-CO-NH- (aza peptide), -C_αH-SO_2-NH- (sulphonamide), -C_αH-CH (OH)-NH-

(statin), -C_αH-CH_2-O- (methylene-oxy), -C_αH-CH_2-CH_2- (dimethylene) and -C_αH-CS-NH- (thioamide). This approach provides pseudo-peptides with essential structural features that can be easily recognized by the enzyme active site such that binding can occur (48;49).

By having a similar bond length and bond energy to the amide bond, methylene-oxy (or oxymethylene) is one of the best mimic pseudo peptide linkages for the amide bond (50;51). Besides this it is a neutral group that do not carry any charge and therefore would not alter the structure of the peptide that contains such functionality. Considering all these facts, we decided to use methyleneoxy (oxymethelene) factional group as the mimic of peptidyl-amide bond in our design paradigm.

iii) **Branch or oligomeric peptide approach**

This is a novel concept and according to our understanding this has never been applied for enzyme inhibition. Earlier this strategy has been used to enhance other biological properties of peptides such as antimicrobial and immunogenic properties. With the availability of several branches of inhibitory peptide in an oligomer peptide, it is expected that such molecules will exhibit higher potency of enzyme inhibition than the monomer since it may interact multiple molecules of the enzyme. In fact branch peptides have been successfully used in the past for enhancement of antigenicity and immunogenic response compared to their monomeric peptide counterpart (52), and consequently they have been used to raise antibodies against proteins or enzymes . In addition to above, it was also reported that such peptides possess higher antibiotic properties compared to their monomeric counterparts (53).

It was further observed that multimeric peptides had enhanced cell-attachment ability compared to the corresponding monomeric form. More importantly, relevant to our study, it was reported that the affinity of these multimeric peptides towards to certain highly malignant tumor cells are much higher than the monomer peptide and thus they were used as inhibitors of tumor growth and metastasis (54). Based on these observations, we propose that similar strategy of oligomeric peptide assembly can be adopted to enhance enzyme inhibitory property.

2.3 Thermodynamic factors in inhibitor design

Enzyme inhibitor association [equation (I)] can be characterized by an association constant (Ka, equation II), which gives a measure of enzyme binding affinity.

$$[E] + [I] \underset{}{\overset{Ka}{\rightleftharpoons}} [EI] \quad \text{..... (I)}$$

$$Ka = [EI] / [E]\,[I] \quad \text{..... (II)}$$

This binding affinity can be related to the standard Gibbs free energy of binding (ΔG^{o});

$$\Delta G^{o} = -RT \ln Ka = \Delta H - T\Delta S \text{ ..... (III)}$$

Where R is the gas constant, T is the temperature in absolute scale, ΔH is the enthalpy change, and ΔS is the entropy change associated with the interaction. The enthalpy change largely reflects the formation of new covalent or electrostatic types of interactions between the two molecules (e.g. hydrogen bonds, Van der Waals and charge-charge interactions). Since binding occurs in aqueous medium, the magnitude of binding is also modulated by interactions between solvent water and the inhibitor or protein. Hence the net contribution must reflect the difference between those interactions that occur in the free and bound states. This is also important when considering the potential sources of entropy changes. In particular, the change in solvent entropy that occurs upon ligand binding can significantly influence the binding equilibrium. For example, if ligand binding leads to a decrease in hydrophobic surface area that is exposed to water, water molecules are released from motionally restricted solvation layers, leading to significant gains in the number of degrees of freedom. In this case the net entropy increases contributing to favourable binding. This entropic increase upon binding is a characteristic signature of interactions that are largely hydrophobic in nature. Another entropic factor to consider is that of the protein and/or ligand itself. For example, upon inhibitor binding flexible regions of the enzyme may become involved in the interaction resulting in loss of conformational degrees of freedom. This would decrease conformational entropy and consequently contribute unfavourably to the binding energy. Overall, all these factors demonstrate that a good inhibitor must

maximize the number of favourable interactions with its target protein while minimizing the entropic cost that may be associated with this binding event (55).

2.4 Michaelis-Menten model for enzyme inhibition

Many enzymes follow Michaelis-Menten kinetics and hence types of inhibition are often explained in the context of the Michaelis-Menten model. In this model, it is assumed that the concentration of enzyme (E) is much lower than the substrate concentration (S) ([E] << [S]), a condition that is similar to physiological conditions where enzyme concentration is the limiting factor.

$$E + S \underset{k_{-1}}{\overset{k_1}{\rightleftharpoons}} ES \xrightarrow{k_2} E + P \quad \text{..... (IV)}$$

Michaelis-Menten assumed that equilibrium existed between ES and free enzyme (E) and the substrate (S). In practical this equilibrium state can be explain by the Briggs/Haldane (steady state) model. In the steady state condition, reaction reaches the steady state concentration where concentration of the ES complex is not changing with time, thus d[ES]/dt =0. Therefore in order to maintain these conditions in the experimental set-up initial rates are measured where no reverse reaction, no inhibition by products and no inactivation of enzyme is observed (56).

Therefore for steady state $k_1[S]_0[E]_0 = (k_1+k_2)[ES]$ .....(V)

For enzymes obeying the Michaelis-Menten theory the initial reaction velocity versus the substrate concentration yields a hyperbolic curve **(Figure 2.0)** that can be described by the Michaelis-Menton equation (VI). Thus highest velocity (V) of the reaction = Vmax

$$V = V_{max}\,[S] / K_m + [S] \quad \text{..... (VI)}$$

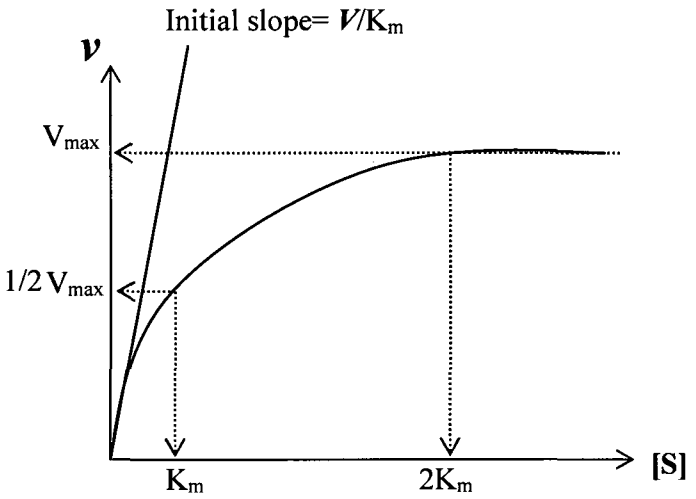

Figure 2.0: *Dependence of initial rate V on the substrate concentration [S], for a reaction obeying the Michaelis-Menten equation(56)*

In this graph the substrate concentration at which the velocity or the rate (***V***) of reaction is half maximum (1/2Vmax) is referred to as Km, or the Michaelis-Menten constant. Km can be considered to be an "apparent" dissociation constant and represented by the following equation.

$$Km = [E]\,[S]_0 \,/\, [ES] \quad \ldots\ldots\ldots\ldots \quad (V)$$

Hence Km gives a measurement for the affinity that an enzyme has for a given substrate. The higher the Km the lower is the affinity and vice versa. For the steady state enzyme reactions Km can be given by equation (VI).

$$Km = k_{-1} + k_2 \,/\, k_1 \quad \ldots\ldots\ldots\ldots\ldots \quad (VI)$$

2.5 Reversible inhibition

Reversible inhibitors interact with the enzyme via non-covalent interactions such as hydrogen bonding, van der Waals and ionic interactions.

$$E + I \underset{k_{-1}}{\overset{k_1}{\rightleftharpoons}} EI \quad \ldots\ldots\ldots \quad (VII)$$

Figure 2.1*: Scheme for reversible inhibition*

Reversible inhibition can be characterized as equilibrium between the complex form (EI) and free enzyme (E) (**Figure 2.1**) where Ki is the equilibrium constant can be given by following equation (VIII)

$$Ki = [E]\,[I] / [EI] = k_{-1} / k_1 \quad \ldots\ldots\ldots \text{(VIII)}$$

Thus lower values of Ki indicate stronger enzyme-inhibitor complexes and higher inhibition.

Reversible inhibition can classified in four main categories namely (i) competitive, (ii) un competitive (iii) mixed and (iv) non competitive types.

2.5.1 Competitive inhibition

In competitive inhibition, the inhibitor binds to the active site of the enzyme where the substrate normally binds, thereby competing with the substrate. Substrate analogs or transition state based compounds are often seen to behave as competitive inhibitors for the enzyme as they designed to mimic the enzyme substrate or transition state complex. In the case of protease inhibitors, this is often done by substitution of a scissile peptide bond by a non peptide bond. This allows enzyme to bind to these inactive structural analogs, thereby blocking the entry of the natural substrate into the enzyme active site (57).

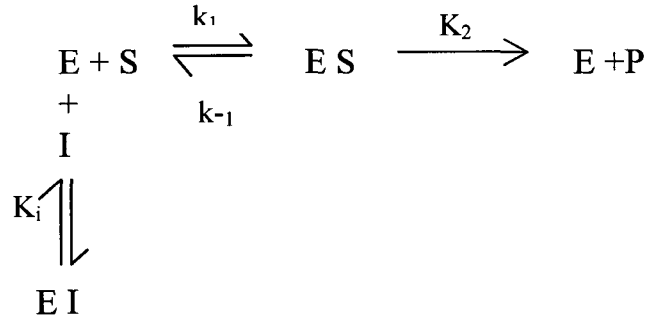

Figure 2.2: *Scheme for the mechanism showing competitive inhibition in presence of substrate* (58)

By interfering with substrate binding, competitive inhibitors change the apparent value of Km but do not affect V_{max} for the substrate, as they cannot bind to the ES complex (***Figure 2.2***)

2.5.2. Non-competitive inhibition

Non-competitive inhibitors bind to the free enzyme as well as the enzyme substrate complex (ES). Since they have identical affinities for both enzyme and ES complex, dissociation constant for both steps would be equal $K_i = K_i^1$ (**Figure 2.3**). In non-competitive inhibition, inhibitor binding does not interfere with substrate binding hence Km is not affected, while V_{max} is reduced. Here the inhibitor bind to the non catalytic domain of the enzyme and modify its activity.

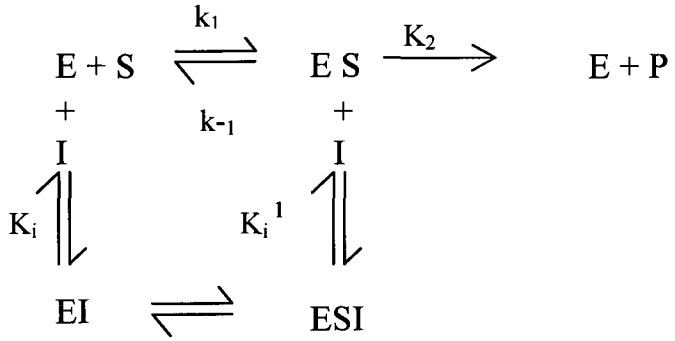

Figure 2.3: *Scheme for the mechanism associated with non- competitive inhibition (58;59)*

2.5.3 Mixed type inhibition

Mixed inhibitors are able to bind both the free enzyme and the enzyme bound to substrate (**Figure 2.4**). They possess kinetic characteristics of both competitive and non-competitive inhibition. Contrast to non competitive inhibition, in the mixed type inhibition dissociation constants for EI and ESI would not be equal $K_i \neq K_i^1$. Apparently mixed type of inhibitors increases the Km and decreases the Vmax.

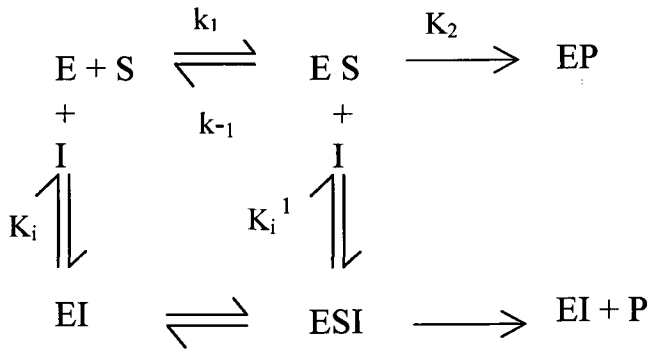

Figure 2.4: *Scheme for the mechanism showing mixed type of inhibition (58;60)*

2.5.4 Un-competitive inhibition

Un-competitive inhibitors do not bind to the free enzyme but bind to the enzyme substrate complex (ES) (**Figure 2.5**). Therefore reduction of effective concentration of enzyme substrate complex (ES) by uncompetitive inhibition increases the enzyme's apparent affinity for the substrate thus lowers the Km and decreases the maximum enzyme velocity (V_{max}).

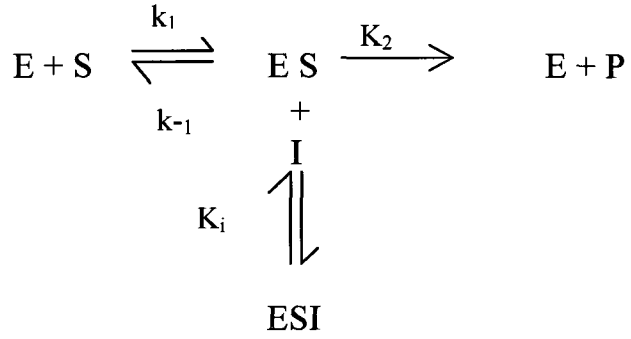

Figure 2.5: *Scheme for the mechanism associated with un- competitive inhibition (58;59)*

2.6 Kinetic evaluation of inhibition

Inhibition of enzymatic reactions can be kinetically characterized *in vitro* by measuring Ki (the inhibition constant) and IC_{50} (concentration needed for 50% inhibition of activity). Other important parameters include Km (Michealis-Menten constant) and Vmax (maximum velocity) values. There are many graphical methods available to determine Ki values in *in vitro* studies. Some more commonly used graphical techniques are the Lineweaver-Burk plot, Dixon plot and Cornish-Bowden plot.

Lineweaver-Burk plot

This plot is also known as a double reciprocal plot (1/V verses 1/[S] plot) of the Michaelis-Menton equation:

$$1/V = Km/Vmax\ 1/[S] + 1/Vmax \quad \text{..... (IX)}$$

Where, V is the initial reaction velocity (the reaction rate), Km is the Michaelis-Menten constant, Vmax is the maximum reaction velocity, and [S] is the substrate concentration. According to this equation, if the inverse initial reaction rates are plotted against the reciprocal of the substrate concentrations, Vmax can be determined from the Y intercept and Km is given by the slope of the graph where Slope = Km/Vmax. Subsequently Lineweaver-Burk plot can be used to compare efficiency of the different enzymes.

This is far the most widely used plot in enzyme kinetics, due to the fact that small experimental errors in the reaction rate can lead to significant error in the calculated Vmax value (60). Hence Dixon and Cornish Bowden plots are the most frequently used methods to determine Ki values.

Dixon Plot

The Dixon plot is a convenient way of calculating K_i of a competitive inhibitor. This plot is based on the following relationship (61).

$$1 / v = \frac{Km\,[I]}{Vmax[S]\,Ki} + \frac{1}{Vmax}\left(1 + \frac{Km}{[S]}\right) \quad \ldots\ldots\ldots\ldots\ldots (X)$$

In this approach the reciprocal of the reaction velocity (1/v) is plotted against inhibitor concentration ([I]). Each series of measurements is done with a fixed (constant) concentration of the substrate and a variety of inhibitor concentrations. This is repeated at different substrate concentrations to generate a series of lines that should intersect at a common point where [I] = - Ki. This approach has some restrictions in that it can't be used to calculate K_m, and cannot differentiate between mixed inhibition and competitive inhibition. Therefore in order to distinguish between competitive and mixed inhibitors, the Cornish Bowden plot should also be performed (60).

Cornish Bowden plot

A Cornish Bowden plot is another graphical method that allows the type of inhibition to be determined and the dissociation constant (Ki) measured for the enzyme inhibitor complex. In this method the initial reaction rate (V) is measured at two or more substrate concentrations ([S]) over a range of inhibitor concentrations ([I]).
According to the rate equation derived from the Michaelis-Menten theory following equation can be obtained.

$$S/V = Km/V (1 + I / Ki) + S/V (1+I/Ki') \quad \text{..... (XI)}$$

According to this relationship a plot of S/V versus I for each substrate concentration should represent a straight line. When performed for a number of different substrate concentrations, a series of lines should be produced that intersect at I=-Ki and S/V =Km/Vmax for uncompetitive inhibitors or on the abscissa (S/V=0) at I=-Ki for non-competitive inhibitors. For competitive inhibition the lines would be parallel (60).

IC_{50} value determination

IC_{50} or the molar concentration of an inhibitor at half maximal (50%) inhibitory response is another parameter that is used in the pharmacology studies. Thus IC_{50} is a measure of the effectiveness of a compound in inhibiting biological or biochemical function. This value is commonly used in the quantitative comparison of the compounds, for their biological activity.

The Cheng-Rusoff equation (XII) derived from enzyme kinetic theory describes the relationship between IC_{50} value, dissociation constant Ki and the substrate dissociation constant (Km) with substrate concentration [S] (62).

$$Ki = IC_{50} / 1 + [S]/Km \quad \text{..... (XII)}$$

However, this relationship is valid only for completely competitive inhibition and hence it is less frequently used in the kinetic evaluation studies.

2.7 Selected chromatographic methods for PC purification

Enzyme kinetic studies are facilitated by the availability of pure enzyme samples and hence another goal of this thesis was the development of a production and purification strategy for recombinant SKI-1 enzyme. Several chromatographic techniques have been used in the past to purify recombinant PCs that includes SKI-1. They can be classified as (i) affinity chromatography, (ii) ion exchange chromatography, and (iii) size exclusion chromatography. Metal affinity chromatography is one of most commonly used affinity techniques. Mainly it can be seen as columns with an immobilized nickel ion (Ni^{2+}). This most frequently used method requires the presence of a poly His tag on (N or C terminal) the protein of interest to purify (8). Besides these, depending on the overall charge of the enzyme one can use either anion or cation exchange columns to achieve purification for the protein (63). Size exclusion chromatography is an another widely used chromatographic technique which separates proteins according to their size (64).

In the past a combination of these methods were successfully applied to purify various recombinant PC enzymes. Thus an affinity column e.g. concanavalin-sepharose and size exclusion chromatography were used to purify recombinant PC-1/PC-3 enzyme (65). Recombinant PC-2 was purified by using an anion exchange column followed by size exclusion chromatography (Superdex 75HR) (66). Anion exchange chromatography was also employed to purify recombinant PC-4 and the PC-5 enzymes (29). Very recently secreted recombinant soluble hSKI-1 enzyme which lacks its transmembrane domain and expressed in insects cells (Sf9 and Sf21) was purified using IMAC (immobilised metal affinity chromatography) with Co^{2+} affinity column (25). However, since this expression system (insect cells) is non-mammalian, it is possible that these secreted proteins possess different translational modification, potentially leading to differences in human SKI-1 structure and function (67;68). Hence in our study we attempted to produce and purify the hSKI-1 enzyme from a mammalian expression system (transfected HEK-293-cells).

CHAPTER 3:

Materials and methods

3.1 Recombinant human (h) SKI-1 expression and production

Vaccinia virus infected human embryonic kidney cells (HEK 293) stably expressing hSKI-1 BTMD (before trans membrane domain) were used to express human SKI-1 enzyme. The construct used begins with sequence ^{1}MKL and ends at PGRYNQE^{997} with an added six-histidine residues at the C-terminus (PGRYNQE^{997}-H_6). Construct without SKI-1 CDNA or empty vector (EMV) was concurrently used as control. This hSKI-1 construct and the EMV were kindly provided by Dr. N.G. Seidah (Director of the Molecular biology and Biochemical laboratories, Clinical Research Institute of Montreal, (CRIM) (8;18;42) Biochemical laboratory. Standard cell culture condition was used for expression of both SKI-1 and control constructs containing HEK 293 cells (69;70).

Accordingly, cells were grown for 48 hours in Dulbecco's modified Eagle's medium (DMEM) (Sigma Aldrich, Saint Louis, Missouri, USA) with 10% heat inactivated fetal bovine serum (FBS) (Gansera Intentional Inc ON, Canada) and 0.6µl/ml of gentamicine sulphate (GTM) (Invitrogen Corporation, ON Canada) to inhibit the bacterial growth and with geneticin (G 418) 50µg/ml (purchased from GIBCO, New Zealand) under 5%CO_2 conditions. G 418 was added to the media as an antibiotic for selective growth of mammalian cells and to maintain stable eukaryotic cell lines. Phenyl red indicator was used in the preparation of cell culture medium to detect any possible bacterial growth or the cell death resulting from high growth of the cells, which would indicate as changes of pH in the culture medium.

The culture media containing secreted SKI-1 enzyme was collected at 85-90% confluency of cell growth. Media was centrifuged to remove all the unwanted cell debris at 4°C at 8,000 rpm using Beckman Coulter, Allegra^{TM} centrifuge instrument for 5 min to separate cell debris and cell culture medium then the clear supernatant containing active soluble SKI-1 enzyme was collected. The medium was further concentrated ~13 fold using ultra centrifugation (centricon-10, Amicon, USA at 4^0C and 1.2 X 10^3 rpm). EMV medium

or the medium of the cells transfected with the parent vector (control) was collected and concentrated using the same protocol. **Please note that for simplicity's sake, throughout the text of this thesis, our recombinant soluble human SKI-1 will be referred to only as "rec-SKI-1".**

3.2 Recovery and purification of rec-SKI- 1

Enzymatic activity of collected medium was examined using intra molecularly quenched fluorogenic peptide substrate. The substrate used for the study was Q-GPC$^{251\text{-}263}$ (25;32) and possessed the sequence Abz-^{251}DIYISRRLLGTFT^{263}-Tyx-A-$CONH_2$. Where Abz: 2-amino benzoic acid and Tyx: 3-nitrotyrosine. All assays were performed at 37°C in a buffer consisting of 25 mM Tris, 25mM Mes and 2.5 mM $CaCl_2$ at pH 7.4 (5;8).

The Abz containing highly fluorescent N-terminal peptide fragment was released upon cleavage by hSKI-1 enzyme following incubation. Using Dab-CMV$^{638\text{-}648}$-Edans (Dabcyl-^{638}RGVVDASSRLA^{648}-Edans) as a substrate, [where Dabcyl is 4,4'-dimethyl amino phenazo benzoic acid and Edans is 5- {(2'-amino ethyl)-amino} naphthalene 1-sulphonic acid}] (24) one can monitor SKI-1 activity.

The released fluorescence was measured using spectrofluorometer (Dynamax fluorescence detector, model FL-2) with the excitation and emission wavelengths at 320 nm and 420 nm for Abz containing substrate and at 355nm and 495nm for Edans containing substrate respectively. Enzymatic activity of the each hSKI-1 batch was checked against the EMV (control vector medium). The presence of 98 kDa active soluble form of the enzyme in every batch was verified by western blot analysis with SKI-1 primary antibody [SKI-1 (D-19): sc-9786] (Santa Cruz Biotechnology Inc., Europe) and with donkey anti goat IgG –HRP (Santa Cruz Biotechnology Inc., Europe) as the secondary antibody.

The presence of histidine tag at the C-terminus of soluble rec-SKI-1 enzyme was verified by the Western blot analysis using His6 primary antibody [His-probe mouse monoclonal (H-3): sc-8036) and donkey anti-mouse IgG-HRP secondary antibody (Santa Cruz).

3.3 DEAE column purification

Diethyl aminoethyl (DEAE) Sepharose® Fast Flow weak anion exchange column was used as the first column for our efforts to purify rec-SKI-1. This DEAE resin (with 0.11-0.16mM highly cross-linked agarose with 45-165 μm particle size) was purchased from Pharmacia Biotech, Canada. The column was packed in house with the resin (height 8.5 cm, diameter 2.5 cm, the column bead resin volume 12 ml). First, the column was equilibrated with 5 column volumes of buffer consisting of 25 mM Tris, 25 mM Mes and 2.5 mM $CaCl_2$, pH 7.4. Then 13 fold concentrated rec-SKI-1 medium (500 μl) was loaded on to the column and left for 1hr at 4^0C for efficient binding. It was then eluted with the buffer containing three different salt concentrations at 4^0C. The flow rate was maintained at 1ml/min and first elution was done with 2 column volumes of 10 μM NaCl in Tris Mes Buffer (low salt pool). Then 5 column volumes of 50 μM NaCl in Tris Mes buffer (medium salt pool) and finally with 2 column volumes of 500 μM NaCl in Tris Mes buffer (high salt wash) was used for the elution. Fractions (1.5 mL) were collected at the 1ml/min flow rate. Column clean up was carried out at pH 7.4 with 4M guanidine hydrochloride in Tris Mes buffer. Following equilibration with buffer, the column is ready to be used again. The fractions were tested for Ski-1 activity using the fluorogenic assay based on O-GPC. The active fractions were pooled for further analysis and characterization.

3.4 FPLC purification of rec-SKI-1 using Mono-S column

Purification of rec-SKI-1 was also attempted with AKTA-FPLC (GE Healthcare) system with a Mono S 5/50 GL (Tricorn column™, Amersham Bioscience, NJ, USA). Matrix of the column is polystyrene / divinyl benzene of 10 μm particle size with the column dimension of 5 x 50 mm and 1ml bed size. The column contains a strong cationic resin with the ionic capacity of 0.12-0.15 mM H^+ /ml gel.

Mono S 5/50 GL column was equilibrated with 20-column volumes of 20 mM Mes starting buffer. Then 500 μl of 13 fold concentrated crude rec-SKI-1 sample that was dialyzed overnight against the starting buffer, was injected into the column. The column was eluted with 20-column volumes of 20 mM Mes+1M NaCl buffer at room temperature. pH was maintained at 6.5 for all buffer systems and flow rate used was 1ml/min. Protein

content and rec-SKI-1 activity of the collected fractions were checked and analyzed by SDS-PAGE, Western blot and *in vitro* assay

3.5 FPLC purification of rec-SKI-1 using Mono-Q column

In our second purification attempt, strong anion Mono Q 5/50GL (Tricorn column^{TM}, Amersham Bioscience, NJ, USA) column from GE Health Care was employed in AKTA FPLC system for this purification. Matrix of the Mono Q 5/50GL column is polystyrene/divinyl benzene in 10 μm particle size and column's dimension of 5X50 mm with ionic capacity of 0.27-0.37 mmol, Cl^-/ml gel.

Thirteen-fold concentrated crude rec-hSKI-1 sample that was dialyzed overnight at 4^0C using the starting buffer was used for purification. The column was equilibrated with 20-column volume of 20 mM Tris HCl starting buffer at pH 7.4. rec-SKI-1 (500 μl) sample was injected into the column. Elution was done with 20 mM Tris HCl at pH 7.4.

3.6 FPLC purification of rec-SKI-1 purification using Size exclusion column

In our next attempt of utilizing AKTA-FPLC (GE Health Sciences) for SKI-1 purification, a Superdex 200, 10/300 GL size exclusion column was employed. The column is a composite of cross-link agarose and dextrin with 10x (300-310) mm bed with an approximate volume at 24 ml. Average particle size was 13 μm with separation range from Mr 3,000 to 600, 000. Column was washed with double distilled water at 2ml/min flow rate. Then column was equilibrated with 2-column volume of 25 mM TisHCl and 150 mM NaCl contain buffer at 0.5 ml/min flow rate. A ~15 fold concentrated hSKI-1 cell culture medium sample, which was previously dialyzed in the same buffer system was injected into the column at the same flow rate. UV absorbance of the eluted fractions was monitored at 280 nm wavelength using UV detector. Collected fractions were further concentrated using 10 kDa Amicon MWCF and tested for the enzymatic activity. Selected active fractions were analysed by SDS-PAGE and immuno-blot using SKI-1 antibody.

3.7 Modified cell culture condition using reduced FBS concentration

Modification to the standard cell culture condition for SKI-1 expressing HEK-293 cells (Human Embryonic Kidney cells) was made in order to increase the purity of the

expressed rec-SKI-1 enzyme in the medium. Cells were initially grown in 10% FBS containing standard cell culture medium until 85-90% confluence had been reached. The cells were then transferred and adapted to 5% FBS, 1% FBS, 0.25% FBS and serum free culture media (SFM) respectively. Cells were incubated at 37^0C and the growth was monitored during incubation. Medium was collected at ~95% confluence for each condition and then centrifuged at 4^0C to remove cell debris. The supernatant containing active soluble form of rec-SKI-1 enzyme was collected. Media was then concentrated (~50 fold) using Centricon 30 kDa MWCF (Molecular Weight Cut off) at 3.2 $X10^3$ rpm for 30 min at 4^0C. Harvested medium containing enzyme was tested for enzymatic activity with fluorogenic substrate and analyzed by the SDS-PAGE and Western blot analysis.

3.8 Application of Cibacron 3GA column for hSKI-1 purification

This method was applied to remove BSA (Bovine Serum Albumin) in the cell culture media of hSKI-1. Cibacron blue 3GA dye with agarose beads in saline suspension (Sigma Aldrich) was used to prepare a column (size 13 cm x 6.5 cm). Column bead height; 6.5 cm (half from the total height), resin volume 40 ml, binding capacity of the resin for BSA 10-20mg/ml. Flow rate was maintained at 2 ml/min by gravity and protein purification was carried out at 4^0C. The column was equilibrated in 8-column volume of 10 mM Tris. HCl buffer at pH 7.4. Then the sample was loaded on to the column and left for 1hr in order to facilitate the binding of the proteins with dye resin. The column was then washed with the same buffer 10 column volumes to remove unbound proteins. Bound residual proteins were eluted with 8-column volumes of buffer containing 10mM Tris. HCl +1.5 M NaCl, pH 7.5.

The column was then cleaned by washing with 10-column volumes of 0.1M Sodium Borate (Boric acid and NaOH mol/mol) +1.0 M NaCl and then 0.1 M Borate alone at pH 9.8 followed by other 10-column volumes of de-ionized water. Finally column was stored at 2M NaCl at 4^0C for the purpose of reuse.

3.9 SDS-PAGE and Western blot analysis

Either tris tricine or tris glycine gel with 8% resolving and 4% stacking phase was used for SDS PAGE. Denaturation of the protein samples were done by heating at 95^0C for

5 min with sample loading buffer contain 1% SDS, 10% glycerol, 10 mM Tris-Cl and 5% of reducing agent either dithiothreitol (DTT) from Sigma Aldrich (Saint Louis, Missouri, USA) or 2-mercapthoenthanol (EM science, NJ, USA) at pH 6.8.

Goat polyclonal anti-SKI-1 IgG primary antibody (raised against an epitope mapping within an internal region of SKI-1 of rat and identical to corresponding human sequence) and donkey anti-goat IgG-HRP secondary antibody (both from Santa Cruz Biotechnology, USA) were used for immunodetection of rec-SKI-1 protein in Western blot analysis. For primary and secondary antibodies, 1:500 and 1:5,000 dilutions were used respectively. Proteins in the sample were then separated by electrophoresis and transferred to an Immobilon-P membrane (0.45 μm) (PVDF-poly-vinylidene difluoride) (Millipore Corporation, Bedford USA) for immunological detection. Chemiluminescence reagents (PerkinElmer LAS Inc USA) were used for detection of immuno reactive bands. Images were then captured using Kodak X-OMAT Blue autoradiography film (PerkinElmer LAS Inc., USA).

3.10 Enzyme activity assay

In vitro enzymatic assay for SKI-1 activity was monitored both on line as well as stop-time method using intramolecularly quench fluorogenic (IQF) substrates (QGPC and QCMV) at room temperature at the final volume of 50 μl in 96- well (flat-bottom black) plates (Micro-fluor, Dynatec, Va, USA). Activity was measured as fluorescence released from the cleaved fluorogenic substrate. Released fluorescence at the excitation wavelength 320 nm and the emission at 420 nm were monitored by a spectrofluorometer (Perkin–Elmer LS50B). Readings were taken following incubation at 37^0C in buffer containing of 25 mM Tris, 25 mM Mes and 2.5 mM $CaCl_2$ at pH 7.4 for both assays. On line assay (progress curve) was monitored over a period of 60 min for enzyme kinetic measurements. Stop time and end point assay was conducted by measuring raw fluorescence units (RFU) at various time points starting from 0 to 6 hours after incubation of rec-SKI-1 (10 μL) with fluorogenic substrate (100 μM) in buffer condition as described above.

3.11 Protein assay

Protein assay dye (Bio Rad) was used to determine the amount of protein in each sample. Sample fractions were mixed with protein assay dye and absorption was measured at 595 nm wavelength using Multiskan® Spectrum (Thermo) plate reader. The amount of protein in each sample was calculated using a standard curve, which was drawn using various concentrations (0 μg /μL-10 μg /μL) of BSA standard (Bovine Serum Albumin) sample.

3.12 Synthesis of peptides

All peptides were synthesized on a solid phase support using an automated peptide synthesizer (Pioneer model, PE-PerSeptive Biosystems, Framingham, Mass, USA), following HATU (O-hexafluorophospho-[7-azabenzotriazol-1-yl]-N,N,N',N'-tetramethyl uronium)/DIEA (Diisopropyl ethyl amine)-mediated by Fmoc (9-Fluorenyl methoxy carbonyl) chemistry. Fmoc-PAL-PEG-PS [PAL, a polyamino linker namely, 5-(4-amino methyl 3,5-dimethoxy phenoxy) valeric acid, PEG-PS = polyamino linker (poly ethylene glycol polystyrene)] resin (substitution = 0.55 meq/gm resin) was used with Fmoc amino acids using an extended cycle of 20 minutes for each coupling step.

Fmoc and side chain protected natural amino acids (L configuration) and the unnatural amino acid derivatives were used for peptide synthesis. All amino acids, coupling reagents namely HATU, DIEA, Fmoc-PAL-PEG-PS resin and the solvents were purchased from Applied Biosystems (Foster city, CA, USA), Calbiochem Novabiochem AG (San Diego, CA, USA), Chem-Impex International (Wood Dale, IL, USA) and Aldrich Chemical (Milwaukee, WI, USA). Following side chain protecting groups were used for various amino acids as indicated: pbf (2, 2, 4, 6, 7-pentamethyldihydrobenzofuran- 5-sulfonyl) for Arg; tBut (tertiary butyl) for Ser and tBoc (tertiary butyloxy carbonyl) for Lys. The unnatural amino acids used in this study, include Fmoc-Aoa (aminooxy acetic acid) and Fmoc-Adoa [8-amino-3, 6 dioxa-octanoic acid] and these were purchased either from Bachem Inc, King of Prussia, Pa, USA, Calbiochem-Novabiochem, San Diego, Ca, USA and Neosystems Inc, Ca, USA. All Fmoc-protected loaded and unloaded resins were brought from PE-Applied Biosystems (Foster City, Ca, USA) and Calbiochem-Novabiochem (San Diego, USA) respectively (24;28;43).

3.13 Pseudo peptides

All pseudo peptides were synthesized on a solid phase support using an automated peptide synthesizer as described in the previous section (section 3.12) with slight modifications. For incorporation of hydrophobic amino acids and unnatural amino acids, extended cycle with double coupling was used.

3.14 Amino acid analysis

Quantitative amino acid analysis was performed following 24 hour hydrolysis of various peptide samples in 6 N HCl in a sealed tube at 110^0C under vacuum. Hydrolyzed samples were lyophilized and reconstituted in the 0.01 N HCl. Using anion exchange chromatography system (Dionex BioLC system model ICS-2500, Oakville, ON, Canada) and a gradient system containing of double distilled water, 0.25 M NaOH and 1 M Sodium acetate system, eluted amino acids were detected by conductance detector (ED 50)(electro chemical detection). A precise volume of 5 μL of each sample was injected in to the system by auto sampler unit. Prior to each analysis the instrument was standardized using a standard sample of known amino acids. The retention time of the eluted peak and the area of the peak provided information about the nature of various amino acids and their relative amounts (28).

3.15 Synthesis of oligomeric or branch peptides

2-branch peptide was prepared by coupling the regular PAL- PEG resin following Fmoc deprotection with $Fmoc_2$-Lys in the first cycle followed by subsequent couplings of rest of the amino acids one at a time. Four- branch peptide was obtained by coupling $Fmoc_4$- Lys_2-Lys-Ala-Wang resin (substitution = 0.1 meq/g resin) with each amino acid one after another (24).

3.16 De-protection and recovery of crude peptides

Synthesized peptides were washed with DMF to remove remaining reagents from the synthesis, then swollen in DCM to separate the resin particles and then peptide-bound resin was allowed to react with a deprotection cocktail (Reagent B) containing TFA,

phenol, water and triisopropylsilane (5ml). After 3 hours of treatment and stirring at room temperature, free peptide was released from the resin and recovered by evaporating residual TFA under suction vacuum. Finally crude peptide was precipitated with diethyl ether at -80^0C (24;43).

3.17 Purification of synthetic peptides

All synthesized crude peptides were dissolved in a solvent containing of 0.1% TFA in double distilled water and ACN in different ratios depend on the nature of the peptide. Dissolved peptides were filtered clean and purified by using reverse phase high performance liquid chromatography (RP-HPLC) on a Rainin Dynamax instrument using 10micron, 300 Å, C18 semi preparative column (1x25 cm, Jupiter, Phenomenex). The buffer system comprised of an aqueous 0.1% (v/v) TFA solution and an organic phase of ACN containing 0.1% (v/v) TFA. Peptides were eluted with a 1 mL/min linear gradient (5 to 60%) of 0.1% aqueous TFA/CH_3CN at a flow rate of 2 ml/min for semi preparative column and 1ml/min for analytical column. The elution of the peptides was monitored on line by the measurement of UV absorbency with wavelength set at 214 nm (8;24;43).

3.18 Characterization of purified peptides using MALDI-TOF MS

All purified peptides were characterized by mass spectrometry using Matrix Assisted Laser Desorption time of flight (MALDI-TOF) technique (Voyager DE (PE Biosystem Inc, Framingham, Ma, USA). Both linear positive and reflector positive detection modes were used for the analysis. Saturated solution of α-cyano-4-hydroxy cinnamic acid (CHCA) or 2,5 -dihydroxy benzoic acid (DHB) or sinapic acid (in 50% ACN:0.1%TFA in H_2O) was used as matrix. All samples were spotted according to the sandwich method (3) where 2 µl of the sample was spotted on the target plate followed by placing of 2µl matrix solution on top of the dried sample. The mass spectrometer was calibrated using calibration standard every time prior to sample analysis (8;24;43).

3.19 Fluorogenic substrates for SKI-1 assay

Intra molecularly quench fluorogenic (IQF) substrates namely Q-GPC and Q-CMV were either synthesised (solid phase synthesis) or purchased for enzyme kinetic studies. The Q-GPC substrate or Quench Lassa virus Glyco-Protein substrate (Amino acid sequence: Abz-DIYISRRLL^{259}GTFT-Tyx-A) was synthesized using automated peptide synthesizer (Pioneer model, PE-PerSeptive Biosystems, Framingham, Mass, USA) as described in the previous section. Fluorescence and quench amino acids, Abz (2-amino benzoic acid) and 3-nitro tyrosine (Tyx) were purchased from Chem Impex International IL, USA. For incorporation of hydrophobic amino acids, Leu, Tyr, 3-nitro tyrosine (Tyx), Abz (2-amino benzoic acid) and hydroxy amino acids like Thr and Ser into the elongating peptide chain, extended cycle (20 min) and double coupling steps were performed. De-protected crude fluorogenic peptide substrates were purified using HPLC as described in the previous section (Section 3.17).

The commercially available CMV (Cytomegalovirus Virus protease-site-1) fluorogenic substrate (Dabcyl-cmv-Edans of Dabcyl-^{638}RGVVNA↓SSRLA^{648}Edans), was purchased from Bachem, Chemical Inc (King of Prussia, PA, USA) and was used for kinetic assays.

Purity of the synthesized and purchased IQF substrate was checked by the characterization using MALDI TOF mass spectrometry.

For Q-GPC substrate, standard curves were obtained using known different concentrations of amino benzoic acid and measurement of respective released fluorescence units (RFU). This standard curve was used to convert released fluorescence units (RFU) into nano mole of cleaved fluorogenic substrate (8;24;43).

3.20 On line assay

Progress curve was monitored over a period of 60 min following incubation of rec-SKI-1 sample (10 µL) with Q-GPC$^{251\text{-}263}$ substrate (5 µM final concentration) in buffer (25 mM Tris, 25 mM Mes, 2.5 mM $CaCl_2$, at pH 7.4) in a total volume of 50 µL in 96-well plate. On line release of fluorescence was measured by slope at excitation and emission wavelengths fixed at 320 and 420 nm respectively. A similar procedure was used with

Dab-CMV$^{638-648}$-Edans substrate, but fluorescence release was monitored at excitation and emission wave lengths fixed at 355 and 495 nm respectively (8;24;43).

3.21 End point (Stop time) assay

End point assay was conducted by measuring raw fluorescence units (RFU) at various time points starting from 0 to 6 hours after incubation of rec-SKI-1 (10 μL) with Q-GPC $^{251-263}$ (50 μM final concentration) in buffer condition as described above. Similar methods were used for Dab-CMV$^{638-648}$ substrate (24).

3.22 Determination of K_i and IC_{50} value for inhibitors

For determination of K_i (inhibition constant) and IC_{50} (concentration required to inhibit 50% of enzymatic activity) values, varied inhibitor concentrations were selected, to yield residual activities of 20-80% respective to the control. Inhibition was measured following incubation with rec-SKI-1 enzyme in presence of fluorogenic substrate. Stop time data were collected as described (Section 3.13). Activity was recorded as RFU values given by the hydrolysed substrate. Kinetic parameters were evaluated using Sigma Plot (Systat Software Inc., USA) and Grafit software programs version 4.09 (Erithacus Software Limited, Staines, UK). Quench corrections were performed and measured RFU values converted to nano moles of substrate hydrolysis per hour using the standard curve as described previously in section (3.13). Non-linear regression analysis of plots of the hydrolysis rate vs. the inhibitor concentration was used. Data were collected in duplicates and mean value was calculated from two independent experiments (24).

CHAPTER 4.0

RESULTS

4.1 Production of recombinant soluble hSKI-1

As discussed in introduction, hSKI-1 is a membrane bound enzyme which is activated auto-catalytically following cleavage at the RRLL^{186}↓RAIP site (8), thereby removing the prodomain polypeptide which is ultimately degraded following a second internal cleavage. This active enzyme still remains membrane bound, but due to autocatalytic shedding at KHQKLL^{953}↓SIDL site (5) the enzyme loses its transmembrane domain including the cytosolic tail and is secreted as an active soluble enzyme (8;71). Based on this information, we decided to generate soluble recombinant hSKI-1 (rec hSKI-1) enzyme by designing a plasmid construct that contains the complete cDNA of hSKI-1 lacking the transmembrane domain ending at PGRYNQE^{997}. This form of hSKI-1 is also called BTMD-SKI-1. As shown in previous studies, this rec hSKI-1 retains catalytic activity and behaved similar to the full-length membrane bound form of active hSKI-1 (5). This form of recombinant hSKI-1 has been successfully used in the past to study its enzymatic properties (5;8;32). Accordingly in our study we decided to use hSKI-1 construct with an additional histidine (His_6) tag at the C-terminus to facilitate purification via nickel-affinity chromatography (8).

The crude culture media obtained from hSKI-1 expression following transfection with HEK293 cells under the standard optimum cell culture condition (69;70) was collected and then subjected to western blot analysis with SKI-1 primary antibody [(D-19: SC-9786), Santa Cruz, USA]. Each collected fraction was assessed for enzymatic activity against the known IQF (Intramolecularly quench fluorogenic) SKI-1 substrate namely Q-GPC (25;32). The level of cell growth for enzyme expression and the activity were all found to be significant under optimal condition of 10% FBS containing DMEM after 48 hours of incubation at 37^{0}C (69;70).

Western blot analyses

The molecular size of soluble active hSKI-1 has been previously determined as 98 kDa (5) close to the calculated molecular weight of 96 kDa based on its known amino acid sequence.

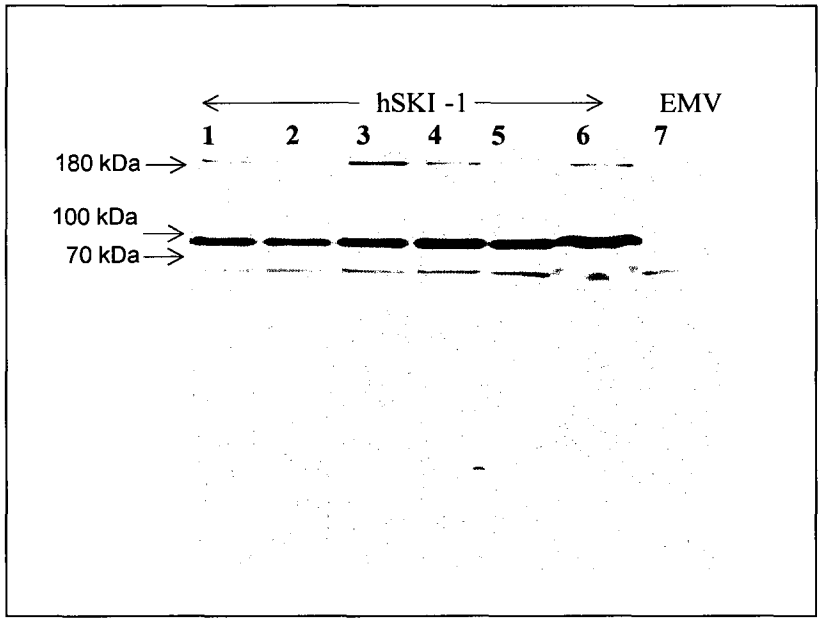

Figure 4.0: *Western blot (8% Tris tricine SDS PAGE) analysis of aliquots of the cultured non- concentrated hSKI-1 samples 20μl (lane 1-5), 13 fold concentrated hSKI-1 sample 2μl (lane 6) rec-SKI-1 and the control vector (lane 7) medium. Protein bands were visualized via immuno detection using anti SKI-1 (D-19: SC-9786) as the primary antibody. A strong immuno reactive band at ~100 kDa was observed for all rec-SKI-1 enzyme samples, which was absent as expected in EMV medium (lane 7).*

Hence we expected that our active soluble form of rec-hSKI-1 should also have a band with molecular weight at ~98 kDa and should be secreted into the culture medium. Our Western blot results shown in **Figure 4.0** revealed that the expected ~98 kDa immunoreactive band was only present in the media when cells were transfected with the plasmid encoding hSKI-1, and not present in the control samples from cells transfected

with parent or empty vector (indicated as EMV). To enrich SKI-1, media from each batch was concentrated ~13 fold using Centricon filtration unit with molecular weight cut off 10 kDa. For each rec-hSKI-1 sample an additional immunoreactive band (faint) at ~200 kDa was also observed. This is possibly due to the formation of a SDS resistant SKI-1 dimer. Such dimer forms have been noticed previously with other recombinant PC enzymes such as PC1 and PCSK9 (72;73). This suggested that our rec-SKI-1 is also prone to oligomerization under the conditions used. A weak immunoreactive band at ~70 kDa was also found in both crude concentrated control (EMV) and SKI-1 media, and was therefore not related to SKI-1. This was likely due to BSA (calculated MW 69 kDa) that was present in culture medium used.

The relative intensities of ~98 and ~200 kDa bands in SKI-1 sample were found to be variable and depend on the concentration of enzyme present in the sample. The absence of both bands in control (EMV) medium clearly confirmed that they are related to SKI-1.

***In vitro* enzyme activity**

The concentrated crude culture medium showed strong SKI-1-enzymatic activity against the intra-molecularly quenched fluorogenic Q-GPC substrate (50 μM) under the optimum assay conditions for SKI-1 (pH 7.4 and 2.5mM Ca^{2+}) (5;8). For all enzyme samples, a high level of activity could be observed with 400-500 RFU (Raw Fluorescence Unit) of fluorescence released upon cleavage of IQF (50 μM) substrate during the first 60 min of assay. Fluorescence measurements were recorded at fixed excitation and emission wavelengths set at 320 and 420 nm for the Abz and nitro tyrosine pair and monitored over a 60 minute period an example of which is shown in **Figure 4.1**

As expected, aliquots from the control vector (EMV) medium showed no fluorescence relaese at all. Instead there was a slight decrease in fluorescence occurring during the assay that may be due to time-dependent suppression of fluorescence of uncleaved IQF substrate (Q-GPC) by potential quenching compounds (e.g. antibiotic, methyl red dye, DMEM etc) present in the culture medium. This effect was not significant in our SKI-1 medium since the amount of fluorescence released is much higher; hence the background quenching effect is not noticeable.

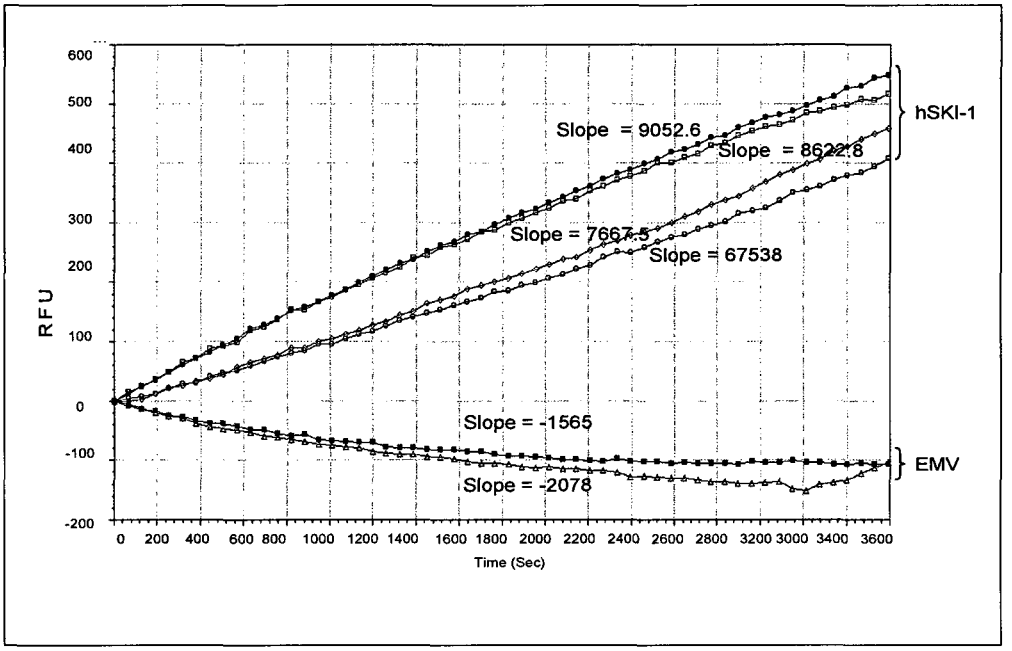

***Figure 4.1**: Raw fluorescence units (RFU) released by digestion of Q-GPC (50 uM) over time as monitored with excitation and emission wave lengths fixed at 320 nm and 420 nm, respectively. The figure showed results for duplicate samples from two different samples of media collected from hSKI-1-transfected cells and media from cells transfected with the control empty vector (EMV) in 25 mM Tris, 25mM Mes, 2.5 mM $CaCl_2$, pH 7.4.*

The presence of the His_6 tag was checked in all samples of hSKI-1 using Western blot analysis with anti His_6 antibody [(H-3): sc-8036, Santa Cruz, USA]. Unfortunately, our results did not show any immunoreactive bands for SKI-1(98kDa or ~200kDa) revealing the absence of the His_6 tag in our SKI-1 enzyme. Instead we observed only a nonspecific band at ~70 kDa due to the presence of a large amount of BSA in the cultured medium. This nonspecific binding was also observed in the control (EMV) medium (**Figure 4.2**). Thus findings confirmed that the loss of His_6 tag during SKI-1 expression, possibly due to proteolysis by endogenous enzymes present in the cell line. This created the potential difficulty for purification of rec hSKI-1 enzyme, since it was not be possible to utilize metal (Ni) affinity chromatography to purify expressed SKI-1 enzyme as we expected. Therefore alternative chromatographic methods needed to be considered.

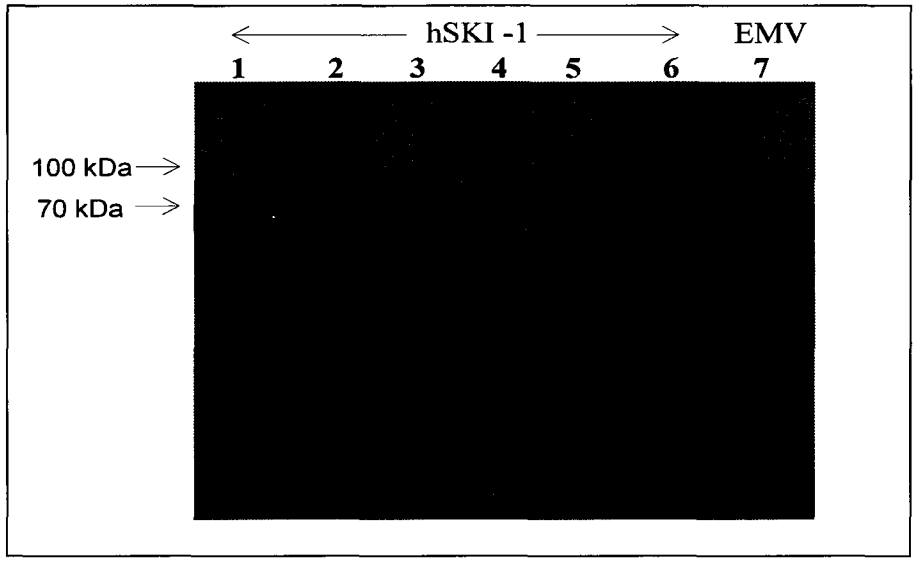

Figure 4.2: *Western blot Tris tricine 8%, SDS PAGE) analysis for samples of culture non concentrated (lanes 1-5), ~13 fold concentrated (lane 6) SKI-1 and control vector (EMV) media samples. Immuno detection was done with a* His_6 *primary antibody.*

4.2 Purification of rec-hSKI-1

4.2.1 DEAE column chromatography

Diethyl amino ethyl (DEAE) sepharose is a weak anion exchange resin (**Figure 4.3**) that was selected as a first choice for rec-hSKI-1 purification. This selection was made due to the fact that it had been successfully used to purify other related enzymes in previous studies (29). The pH was maintained at 7.4 throughout the chromatography which should maintain rec-SKI-1 in a positively charged state since its theoretical isoelectric point was ~8.

Under these conditions negatively charged contaminants in the SKI-1 medium should bind the DEAE column. As shown in **Figure 4.4**, after application to the column the bound enzyme was eluted with buffer containing increasing concentrations of salt. The protein content (by Bradford protein assay) and the enzyme activity (using the Q-GPC substrate) were monitored for eluted fractions.

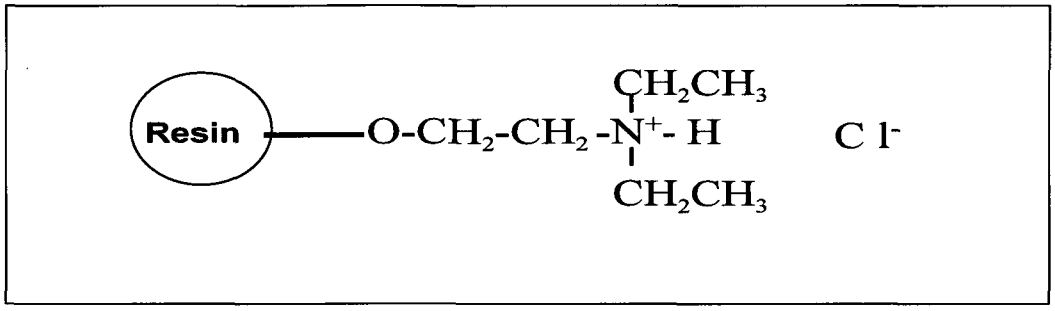

Figure 4.3: *Chemical structure of DEAE resin*

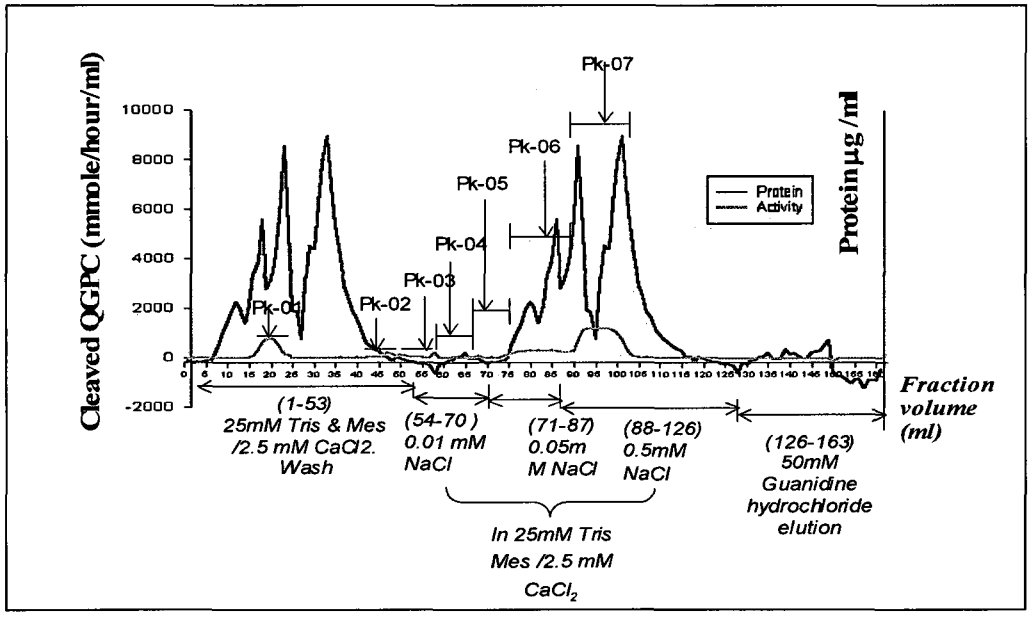

Figure 4.4: *Chromatography profile showing purification of rec-hSKI-1 by DEAE-sepharose column. Activity (orange line) and protein (brown line) profiles for the collected fractions are shown. The selected fractions for SDS PAGE and Western blot analysis shown in Figures 4.6 and 4.7 are indicated by vertical arrows labelled with the corresponding peak (Pk) number.*

This chromatography profile shows that some of the protein that did not bind to the column had some SKI-1 activity. However, more SKI-1 activity was obtained from fractions eluted at higher salt concentrations.

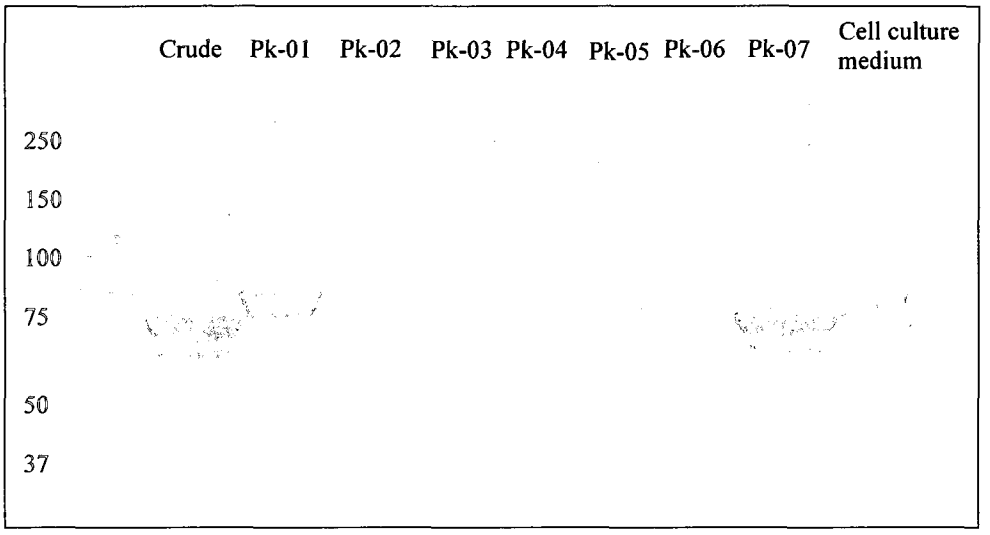

Figure 4.5: *Samples of fraction from the DEAE profile shown for the hSKI-1 purification in Figure 4.4 analyzed by SDS PAGE stained with Coomassie blue.*

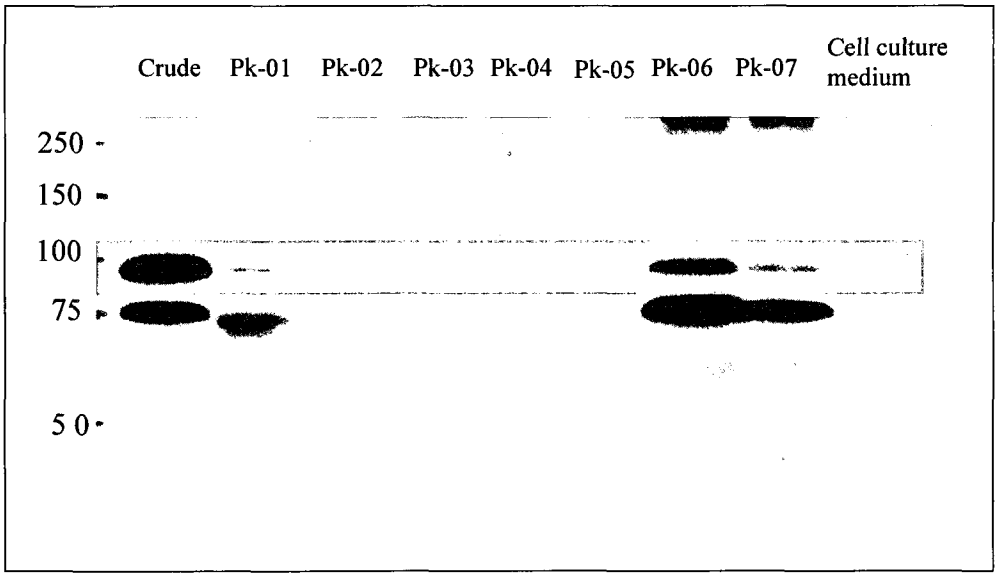

Figure 4.6: *Western blot analysis with SKI-1 primary antibody for a crude sample of hSKI-1 and several selected fractions (Peak # 1-7 from the profile shown in Figure 4.4. Crude hSKI-1 and DEAE fractions were concentrated (~13 fold) before immuno-detection. A SKI-1 immuno-reactive band at ~98 kDa was observed only in enzymatically active fractions.*

Enzymatically active and inactive fractions were concentrated (~13 fold) and then subjected to SDS-PAGE and Western blot analysis (**Figure 4.5 and 4.6**). As indicated by the Western blot in **Figure 4.6**, a strong immuno-reactive band at ~100 kDa was detected for 3 fractions with high enzymatic activity (Pk-01, Pk-06 and Pk-07). A similar band was also present in the crude enzyme sample but not in the enzymatically inactive fractions (Pk-02 – Pk-05). An immuno-reactive band at ~70 kDa for non-specific binding with BSA protein was also present in the control cell culture medium (**Figure 4.6**).

This purification was insufficient since major contaminants did not bind to the anion exchange column as expected hence some of it was eluted out with the enzyme.

4.2.2 Fast protein liquid chromatography (FPLC)

Due to heavy accumulation of FBS protein in the cell culture medium, we were unable to purify rechSKI-1 using DEAE column. We then decided to use other types of chromatography such as AKTA-FPLC system, which can provide better resolution than the previously used DEAE-chromatography.

4.2.2.1 rec-hSKI-1 purification attempt using the Mono S 5/50GL column

$$-O-CH_2-CHOH-CH_2-O-CH_2-CHOH-CH_2-SO_3^-$$

Figure. 4.7: *Functional moiety present in a mono S resin*

In our initial attempt for SKI-1 purification we utilized a strong cation exchange (**Figure 4.7**) Mono S 5/50GL column in an AKTA-FPLC system at pH 6.5.

Since the theoretical pIs (5.8) of the albumin, the major constituent of FBS, and rec SKI-1 (8.09) are significantly different from each other, it is expected that at pH 6.5, hSKI-1 should be positively charged while albumin will be negatively charged. However, none of the proteins in the sample were bound to the column under these conditions and instead all were eluted with the flow-through (**Figure 4.8**).

This observation suggested that the actual pI values of rec-hSKI-1 was actually lower than 6.5, since it did not bind to the column at this pH.

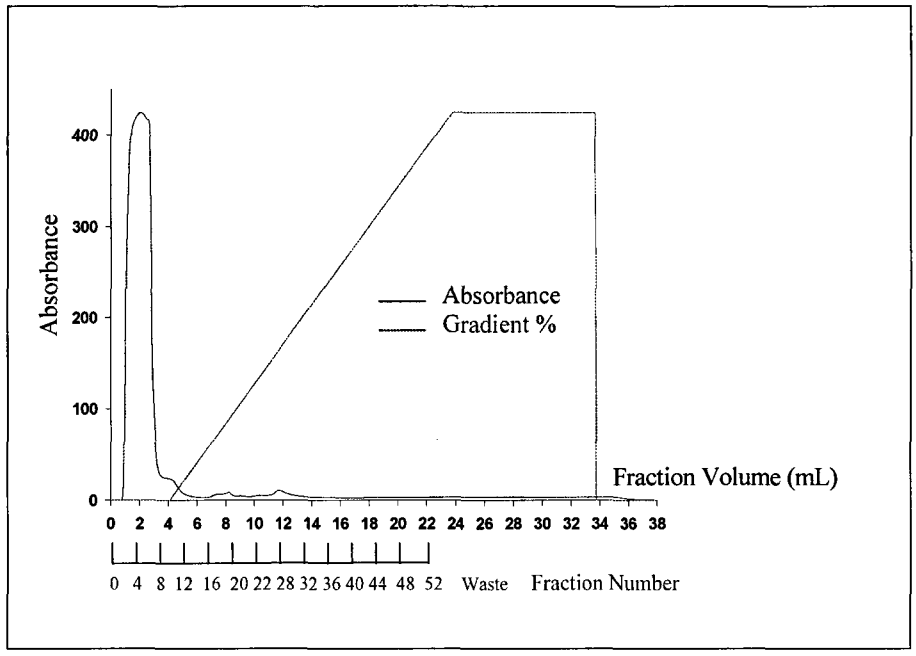

Figure 4.8: *Chromatography profile of rec-hSKI-1 from the Mono S 5/50GL column using the AKTA-FPLC system. The y-axis represents the absorbance (mAU or milli-AUFS) of each fraction at 280 nm wave length and the x-axis shows the elution volume and the fraction number. The sample was eluted at a flow rate of 1.0 ml/min with starting buffer containing 20 mM Mes, pH 6.5. The gradient (green line) shows the percentage of elution buffer (20 mM Mes, 1M NaCl, pH 6.5) which was run from 0 to 100 % over a 30 mL volume.*

In order to facilitate the binding of rec-hSKI-1 with the column, it may be necessary to conduct the purification under lower pH condition. However optimal pH range for hSKI-1 activity is very narrow (pH 6-7.5) leading us to consider alternative chromatographic methods for purification.

4.2.2.2 rec-hSKI-1 purification attempt using the Mono Q 5/50GL column

During our attempt to purify rec-SKI-1 using strong cation exchange column at pH 6.5; we noticed a significant destruction of SKI-1 enzymatic activity under these conditions. Therefore we decided to maintain the pH range that was closer to neutrality (i.e. pH 7.4), which will preserve most SKI-1 activity (**Figure 4.9**).

$$-O-CH_2-CHOH-CH_2-O-CH_2-CHOH-CH_2N^+(CH_3)_3$$

Figure 4.9: *Structure of the charged functional moiety present in a mono Q resin*

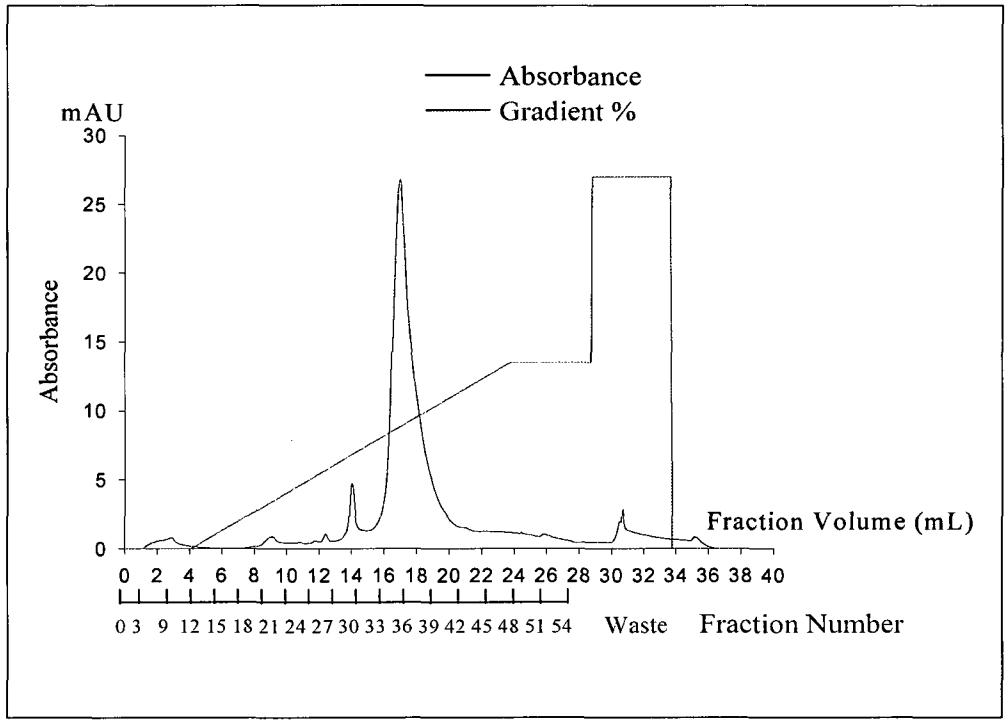

Figure 4.10 *FPLC chromatogram for rec-hSKI-1 purification on a Mono Q 5/50GL column. The purification is followed by measurement of absorbance (Y-axis) at 280 nm. The green line indicates the percent elution buffer used at each point in the purification, where the elution buffer consists of 20 mM Tris, 1M NaCl, pH 7.4.*

As shown in **Figure 4.10** most of the proteins were eluted within the fractions # 25-45 with corresponding volumes of 14-22 ml. Even if, according to the activity profile for the eluted

fractions (**Figure 4.11**) the highest enzymatic activity was observed for the fraction numbers ranging from 10-16.

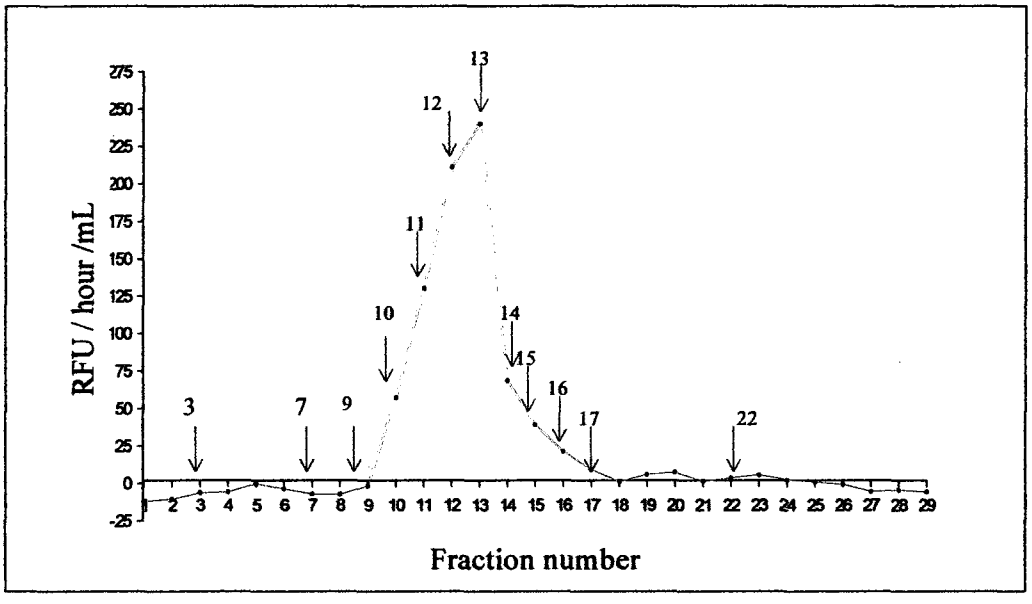

Figure 4.11: *Enzyme activity profile of various fractions collected following chromatography of crude rec-hSKI-1 medium through Mono Q5/50GL in an AKTA – FPLC. Activity was measured as Raw Fluorescence Units (RFU) against Q-GPC substrate at excitation and emission wave lengths fixed at 320 and 420 nm respectively. Y-axis represents the activity in RFU/hour/mL while the X-axis represents the fraction numbers or volumes. The fractions selected for analysis are represented by vertical arrows in the figure.*

Western blot analysis with anti-SKI-1 antibody for the enzymatically active fractions (**Figure 4.12B**) revealed that these fractions contained a SKI-1 immunoreactive band at the expected molecular weight of ~98 kDa. However as indicated by coomassie stained SDS PAGE (**Figure 4.12A**); these active fractions also contained a significant amount of BSA as a contaminant protein. Therefore we decided to change the column in an AKTA FPLC system for SKI-1 purification.

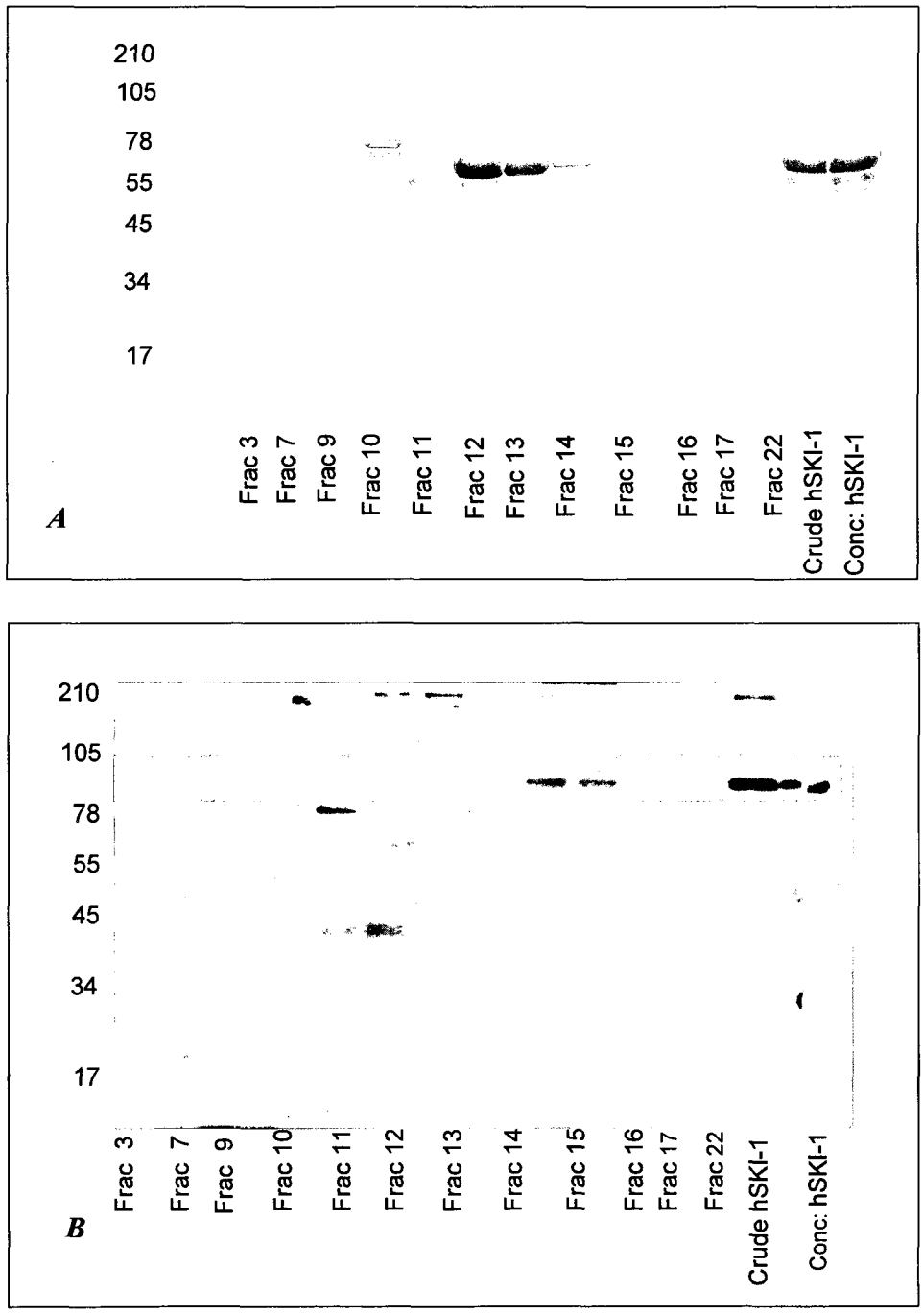

***Figure 4.12**: SDS-PAGE and western blot analysis of selected enzymatically active (Fraction # 3-17) and inactive (Fraction # 22) fractions (as shown in figure 4.11) of SKI-1 samples following chromatography via Mono Q column **A:** Coomassie stained 8% SDS-PAGE, **B:** Western blot with SKI-1 antibody (D-19: SC-9786)*

4.2.2.3 rec-hSKI-1 purification attempt using the Size exclusion (Superdex–200 10/300 GL) column

Since it was recognized that BSA (molecular size ~69 kDa) is the major contaminant in our SKI-1 enzyme medium, we then decided to utilize size-exclusion (SE) chromatography to purify rec-SKI-1. We choose the Superdex-200, 10/300GL FPLC column since it is known to be useful for separation of proteins with molecular weights ranging from 3 to 600 kDa. Thus FPLC chromatogram (**Figure 4.13**) and the respective activity profile (**Figure 4.14**) for rec-SKI-1 on a size-exclusion (Superdex200 10/300GL) column is shown below

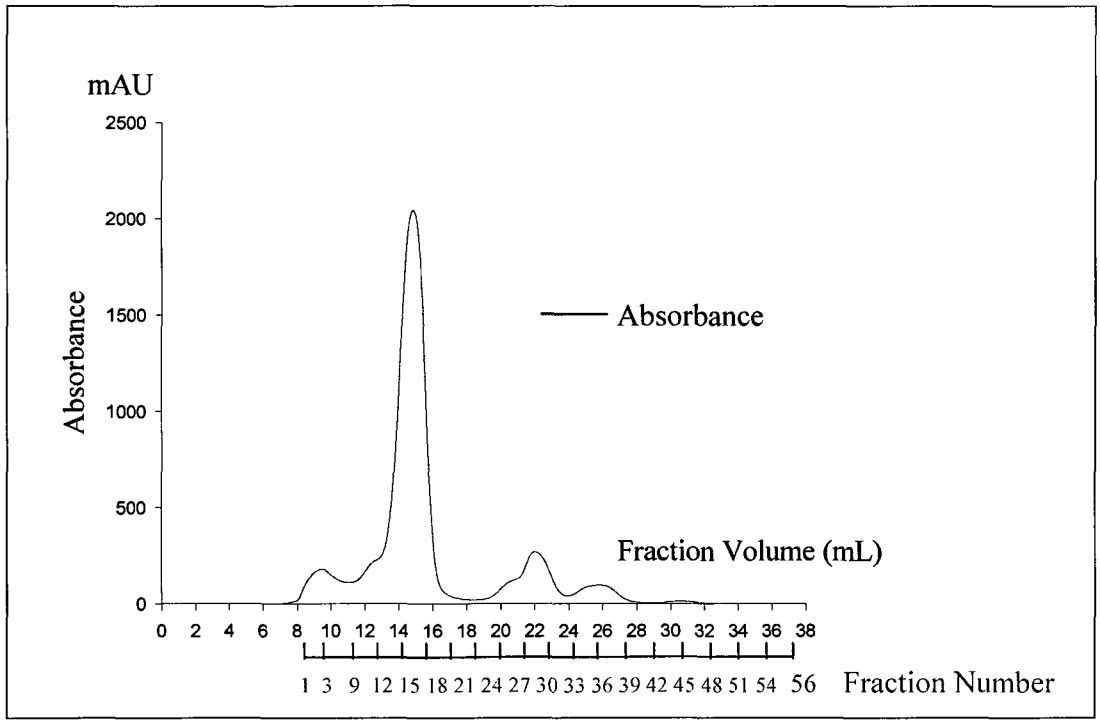

Figure 4.13: protein profile of *FPLC chromatogram for rec-hSKI-1 purification by size-exclusion (Superdex200 10/300GL) column. Absorbance (mAU) of each fraction (Y-axis) at the fixed wavelength of 280 nm was monitored as a function of elution volume. The sample was run at 1.0 ml/min with 25mM Tris HCl, 150 mM NaCl buffer, pH 7.4. The collected fraction numbers and the respective volumes are indicated on the x-axis*

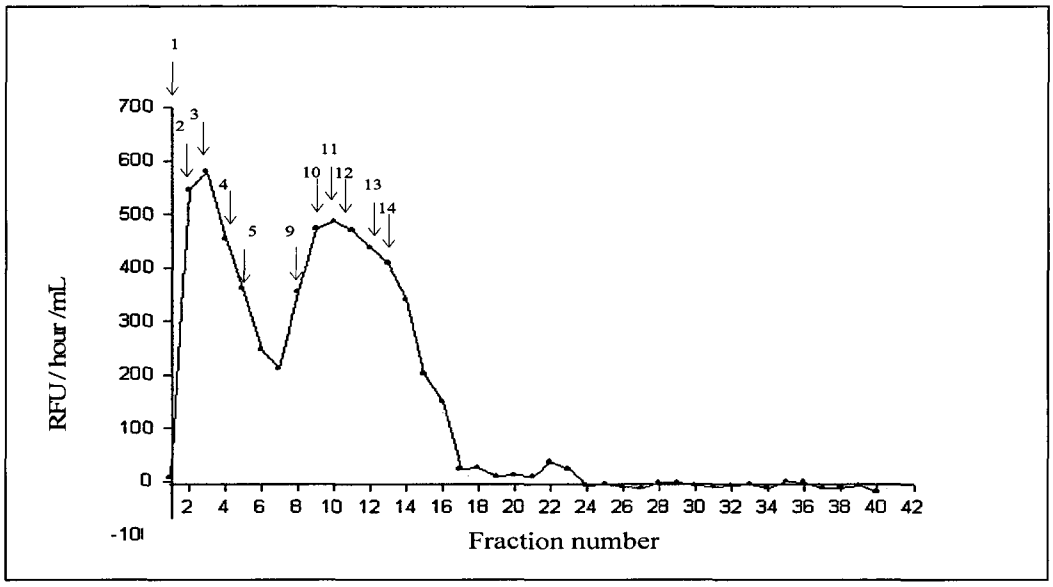

Figure 4.14: *Enzyme activity profile for various collected fractions of SKI-1 sample following chromatography through superdex200 10/300gl in an AKTA–FPLC system. Activity was measured as Raw Fluorescence Units (RFU)/hour/mL against Q-GPC substrate and it was plotted as a function of fraction number. Vertical arrows indicate those fractions selected for SDS-PAGE and Western blot analysis.*

The SDS PAGE and the Western blot analysis of various enzymatically active and selected non-active fractions are shown in **Figures 4.15** and **4.16** respectively.

Based on observed activity profile (**Figure 4.14**) and the Western blot results **(Figure 4.16)**, it was revealed that the fractions eluting at the beginning of the purification (fraction # 2-4) contain dimeric (based on MW) and monomeric forms of rec-hSKI-1 with much reduced level of residual protein. The remaining bound monomeric form of the enzyme was again eluted at a later stage with high amounts of residual cell culture protein. According to immuno blot results with SKI-1 antibody we concluded that SDS stable dimeric form of the SKI-1 and some monomeric SKI-1 were eluted at the very beginning of the chromatogram (fraction # 2-4). **This pool is reasonably pure since very little BSA protein is present in these fractions.** The later active SKI-1 containing fractions (fraction # 9-14) were found to contain only the monomeric form. No dimeric SKI-1 forms were detected in these fractions (**Figure 4.16**) but still contained a huge amount of contaminating BSA protein.

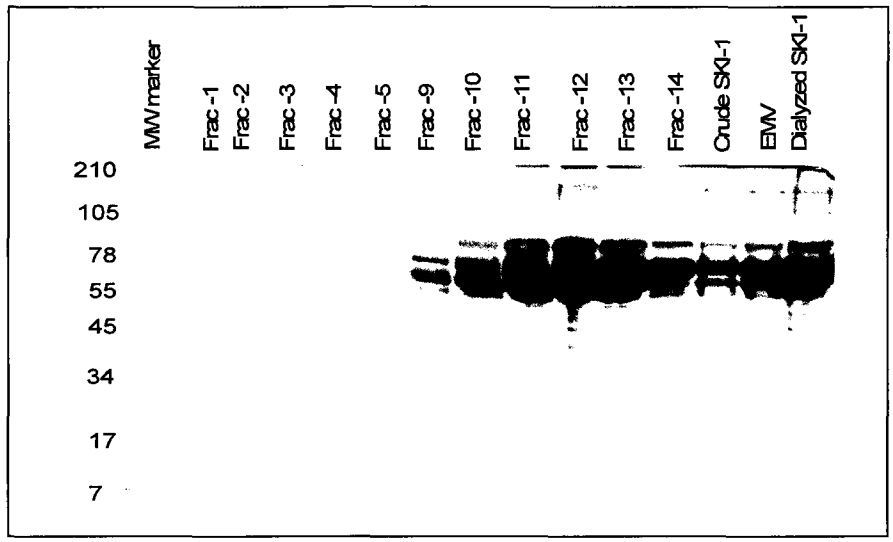

Figure 4.15: *8% Tris tricine SDS–PAGE for the enzymatically active fractions collected during the purification by size exclusion (Superdex 200 10/30GL) chromatography shown in* ***Figure 4.13****. Fractions are selected according to the activity profile (****Figure 4.14****).*

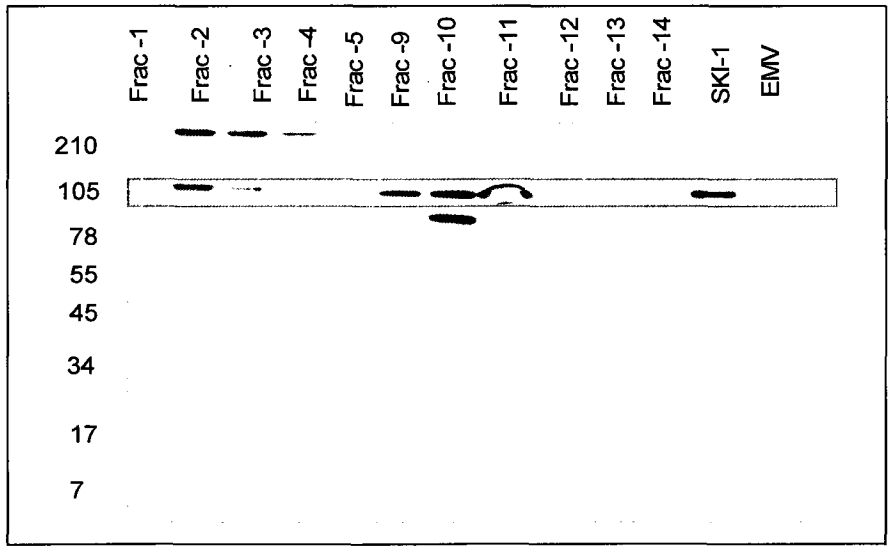

Figure 4.16: *Immuno detection of SKI-1 in enzymatically active fractions obtained from the size exclusion (Superdex 200 10/30 GL) chromatography. Note the presence of a SDS stable dimer of SKI-1 (~200 kDa) in fraction# 2-4.*

Our goal to purify rec hSKI-1 enzyme in an active form was greatly hampered by the presence of a large amount of BSA in various hSKI-1 fractions. To evaluate the feasibility of the purification we ran both hSKI-1 and the control (EMV) concentrated samples in parallel using same size exclusion column in an ALTA-FPLC system. The overlaid FPLC chromatograms for hSKI-1 and EMV samples are shown in the **Figure 4.17.**

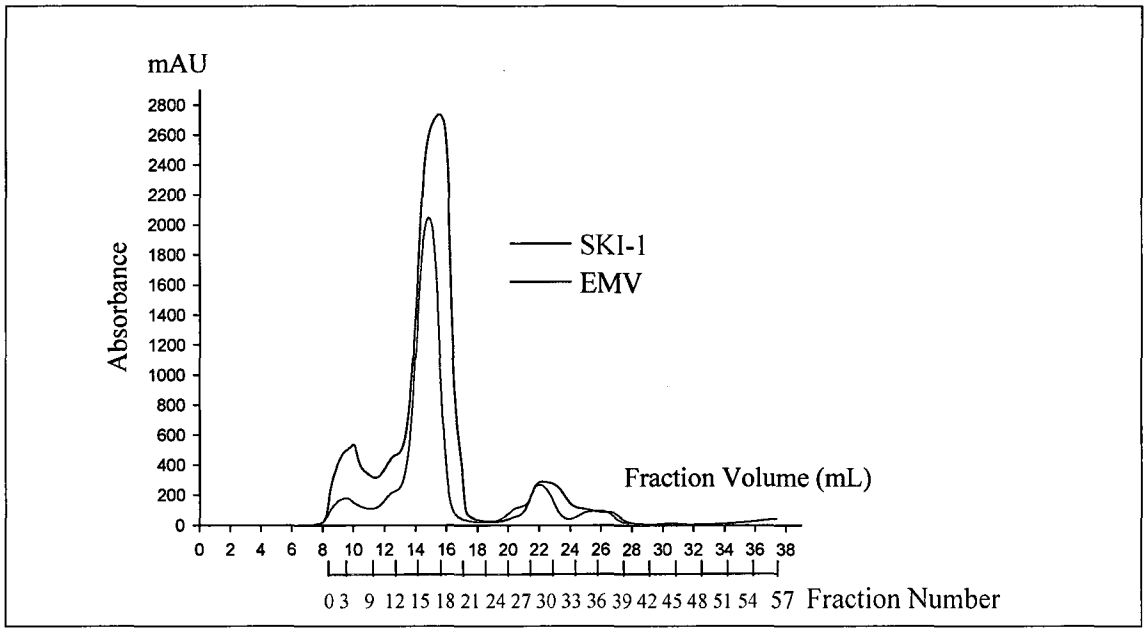

Figure 4.17: *Overlaid FPLC chromatograms for rec-hSKI-1 and EMV media using a size-exclusion column (Superdex200, 10/300GL). Each fraction was monitored by absorbance (Y-axis) measured at 280 nm wave length as a function of elution volume (X-axis). For each chromatogram, 1 ml of crude concentrated medium (~13 fold) of rec-hSKI-1 was loaded to the column and ran under identical conditions at 1.0 ml/min flow rate with 25 mM Tris HCl, 150 mM NaCl buffer, pH 7.4.*

Here we noted that both enzyme and the control have almost identical protein profiles. This suggests that the molecular sizes of SKI-1 and the contaminating BSA may be too close to one another rendering it difficult to purify rec SKI-1 via this chromatography method.

Hence we decided to use modified technique to reduce the amount of BSA used in the culture medium while maintaining cell growth and protein expression.

4.2.3 Effect of FBS concentrations in Culture medium on rec hSKI-1 production

Fetal Bovine Serum (FBS) is one of the major protein components required for HEK-293 cell growth and survival. The protocol used for optimum growth of HEK-293 cells for maximum SKI-1 production, contained 10% of FBS in DMEM (69;70). This FBS contains 90% of the serum albumin known as fetal bovine serum albumin protein (BSA), thus BSA appears to be main contaminant in our SKI-1 samples.

Since none of the tested chromatographic techniques were successful in purifying hSKI-1 due to the presence of BSA in very high level in the culture medium, we decided to modify the cell culture protocol for SKI–1 expression by using a reduced level of FBS in the medium. For this purpose SKI-1 or EMV (control construct transfected) HEK 293 cells were either adopted to or grown directly in culture medium containing low levels of (specifically 5%, 1%, 0.25%, 0.1% or 0%) FBS in DMEM.

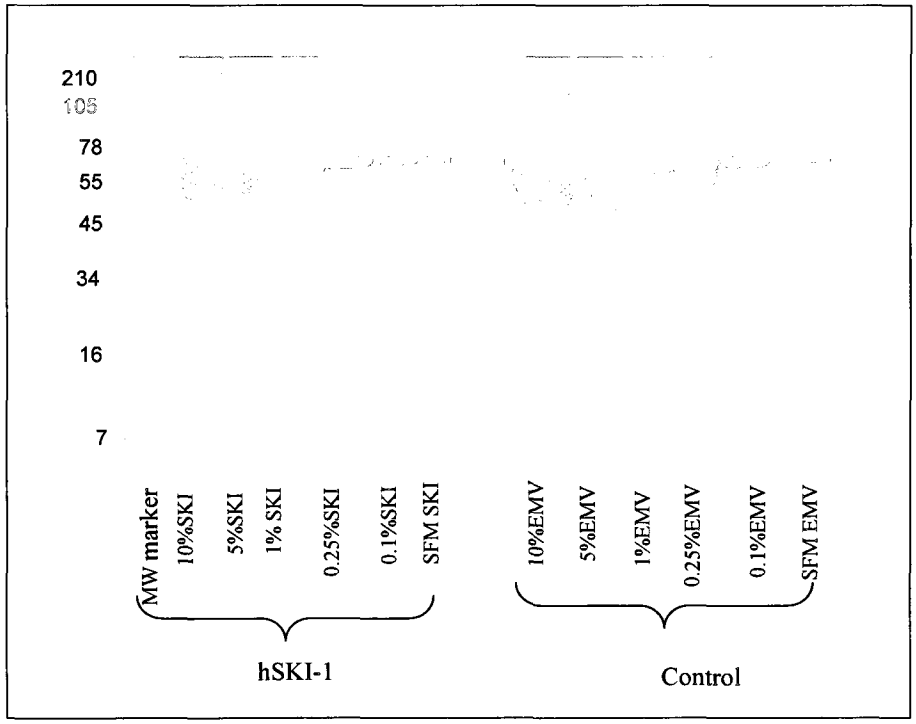

Figure 4.18: *Tris tricine SDS-PAGE (8%) analysis of 13 fold concentrated hSKI-1 and EMV (control empty vector) culture media under various concentrations of FBS protein.*

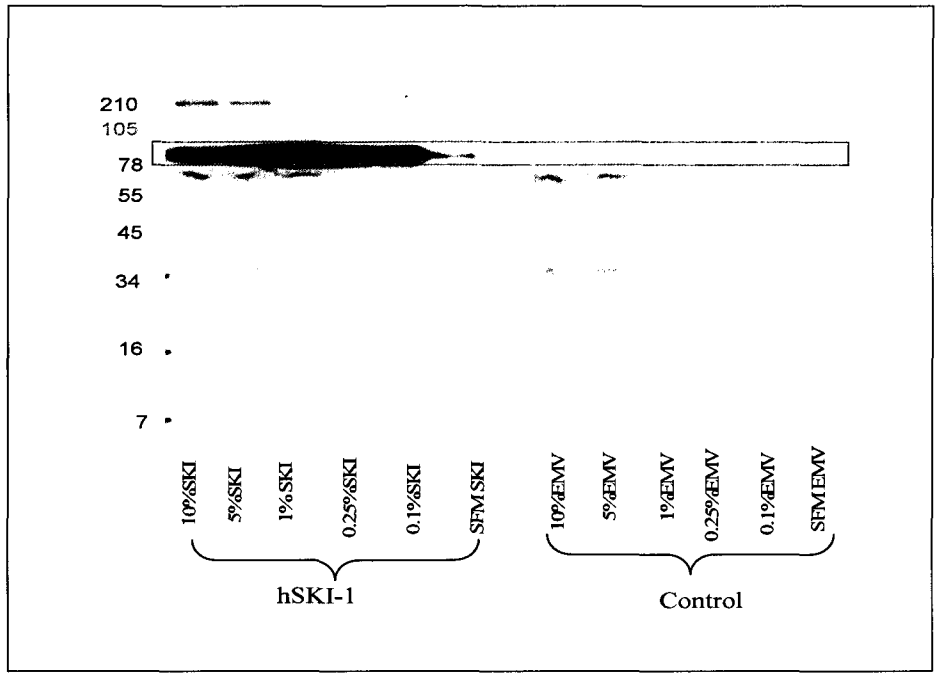

Figure 4.19: *Western blot analyses of SKI-1 and control empty vector (EMV) crude concentrate culture media (13 fold concentrated). Under various FBS conditions positive immuno reactive bands for dimer (~200 kDa) and monomer (~100 kDa) were observed for all hSKI-1 samples (lanes# 1-6) but not in control EMV (lanes # 8-13). In higher concentrations of FBS, strong non-specific bands for BSA protein at ~ 70 kDa were observed for both enzyme and control.*

Except for 0% FBS, all other conditions led to efficient cell growth during the initial 24 hours. However after this initial growth the cells started to shrink. Cells adapted in serum free medium (SFM) showed only slight growth at 24 hr incubation but then began to die. Therefore serum free condition could not be used for efficient production of recSKI-1.

The SDS-PAGE for the cell culture media from cells grown in different FBS conditions shows a steady decrease in the amount of ~70 kDa band for BSA protein as its concentration in the medium is gradually diminised (**Figure 4.18**). Positive immunoreactive bands (~100 kDa) for SKI-1 were noted in all enzyme samples cultured at various reduced FBS conditions indicating the expression of rec-SKI-1 in all of these conditions. (**Figure 4.19**).

Based on the efficiency of cell growth, the level of protein expression and the level of SKI-1 activity in the media, we observed that 0.25% FBS containing buffer condition is so far the best for SKI-1 production and subsequent purification.

4.2.4 Cibacron column purification

We then utilized a purification technique using a resin that selectively binds to serum albumin protein. For this we used rec-hSKI-1 enzyme medium that was cultured in 0.25% FBS condition. Although many proteins are known to non-specifically interact with dyes, it is known that Cibacron blue 3GA (**Figure 4.20**) binds specifically to serum albumin. Previously, this dye has been successively used to purify albumin from mixture of other proteins (74;75). Based on these reports we decided to utilize this property of the dye to separate our rec-SKI-1 enzyme from BSA protein. For this purpose we used a column containing Cibacron blue 3GA agarose resin.

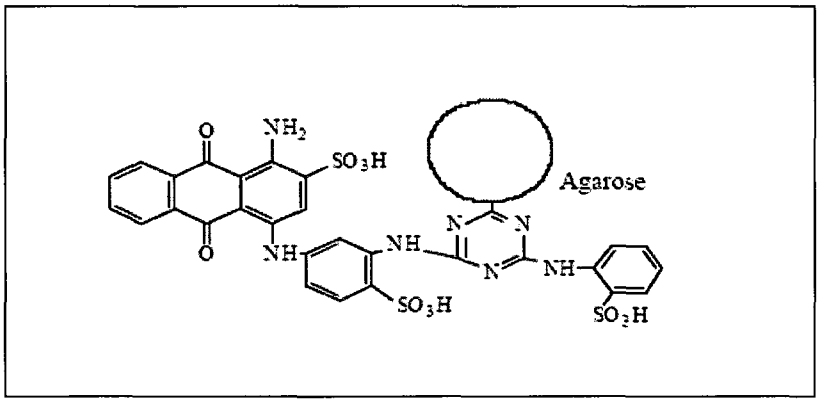

Figure 4.20: *Chemical structure of Cibacron blue 3GA dye immobilized on agarose resin.*

As we expected our Western blot, SDS-PAGE and activity assays for the preliminary application (data not shown) of Cibacron blue 3GA column revealed that rec-SKI-1 did not bind to the column thus enzyme was eluted with the flow through in first few buffer wash fractions. Most of the bound contaminant BSA protein (~70 kDa) was eluted in later with the strong buffer conditions. These findings confirmed that this methodology may be useful for removing BSA from our rec-hSKI-1 sample.

To achieve a higher degree of purity for rec-hSKI-1, the enzyme had been subjected to repeated chromatographies through Cibacron 3GA column. Following each

chromatographic step, activity was assayed in the collected fractions and then the active fractions were pooled and re-applied to the column. This process was repeated three times in total. Silver stained SDS PAGE and the Western blot analysis with SKI-1 primary antibody for the pooled fractions from the first, second and third purification steps were shown in **Figures 4.21** and **4.22** respectively. At each step significant amount of BSA was removed until it was almost undetectable after 3rd purification step.

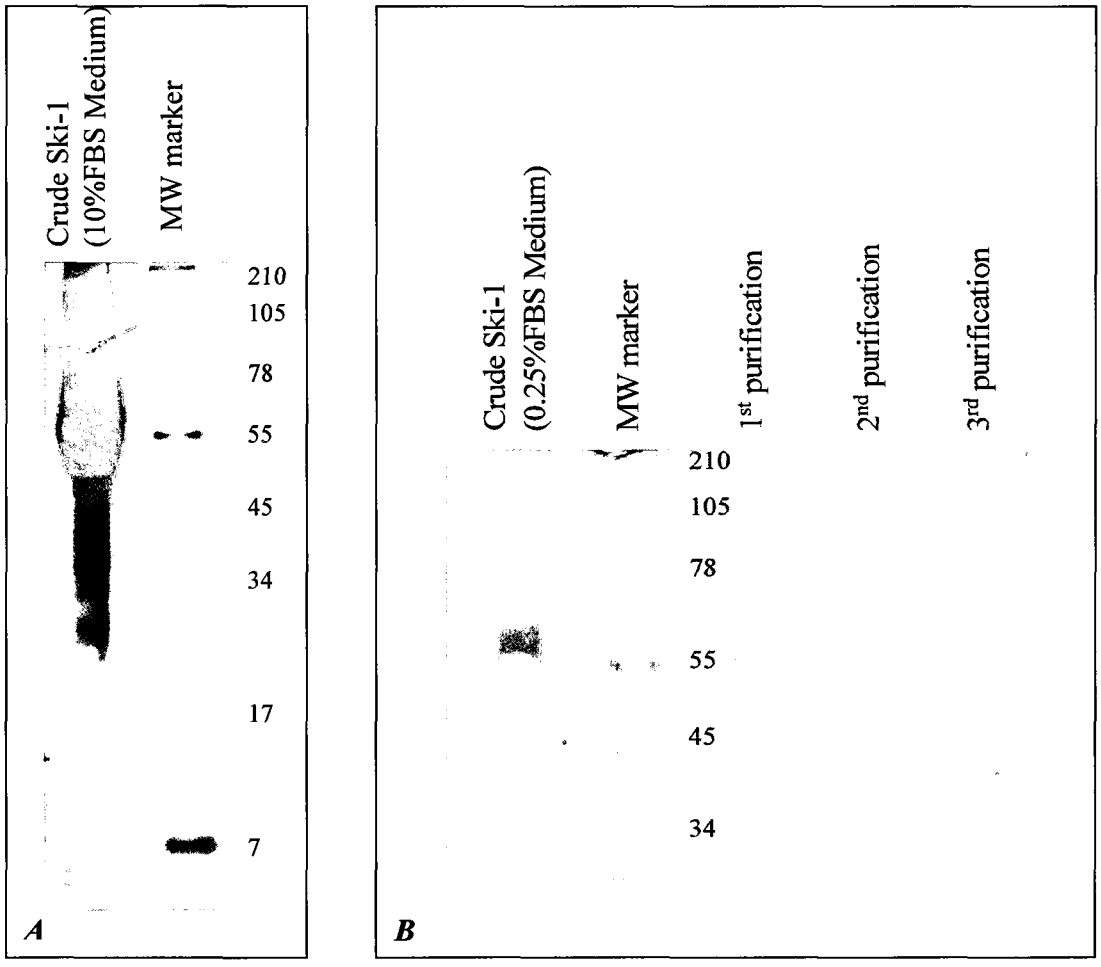

Figure 4.21: *Silver stained Tris tricine 8% SDS-PAGE on crude and Cibacron blue 3GA column purified rec-hSKI-1 samples. Equal volumes (1.5 μL) of each sample were loaded to each well. Figure A: shows higher amount of residual proteins present in rec-SKI-1 medium that was cultured in standard condition. Figure B: shows gradual removal of contaminant protein from rec-SKI-1 sample following Cibacron blue 3GA chromatographies on 0.25% FBS conditioned rec-SKI-1.*

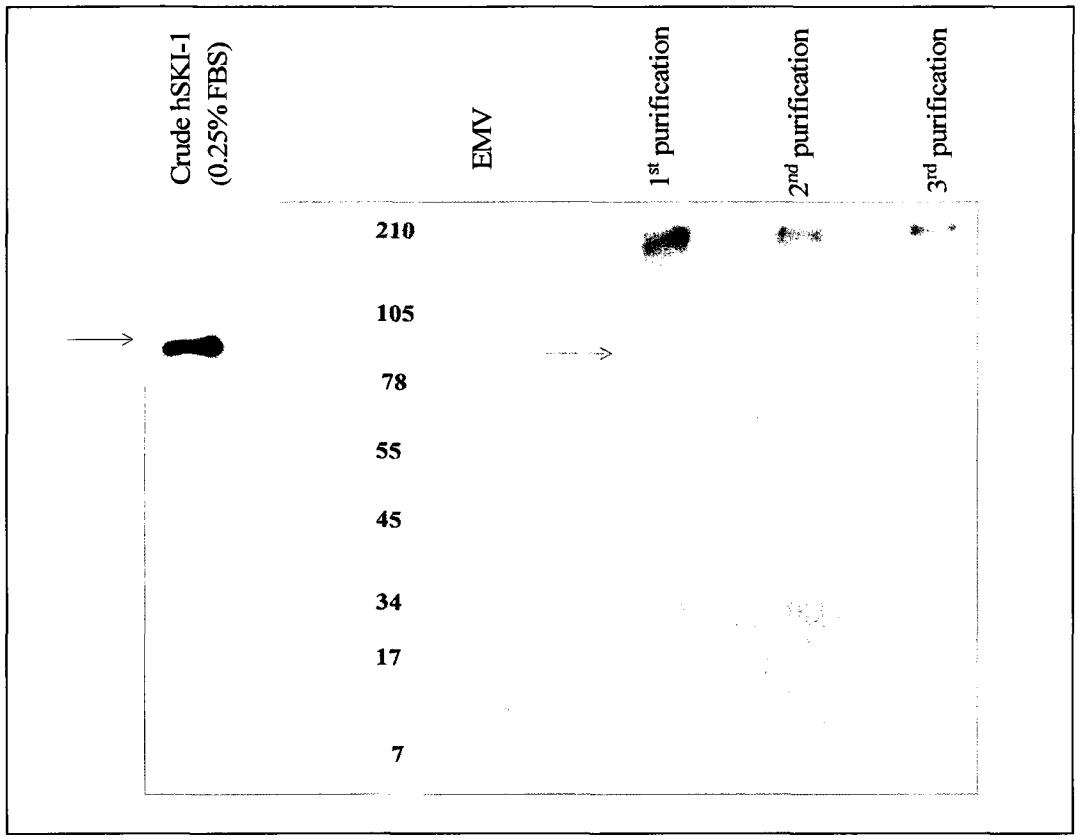

Figure 4.22: *Immuno-detection of SKI-1 with its specific antibody in crude rec-hSKI-1 medium (0.25% FBS condition) and various fractions following purification over Cibacron blue 3GA column. The immuno reactive bands at ~98 kDa for the monomer form (black arrow) of SKI-1 were detected in crude and first purified fractions. In addition to this, another immuno reactive band at ~200 kDa region (red arrow) was also detected.*

With the removal of the FBS from the enzyme following repeated Cibacron column chromatographies, we noticed that the disappearance of 98 kDa band and the emergence of a strong immunoreactive band at ~200 kDa in Western blot (**Figure 4.22**) as well as SDS-PAGE (**Figure 4.23**) analysis. Thus it was speculated as a possible dimerization form of SKI-1 enzyme. Hence this SDS stable dimer formation along with the purification suggested that SKI-1 is prone to oligomerization particularly in the absence of albumin. Given this information it is suggested that FBS might help in stabilizing the monomer form of the enzyme in the cell culture medium.

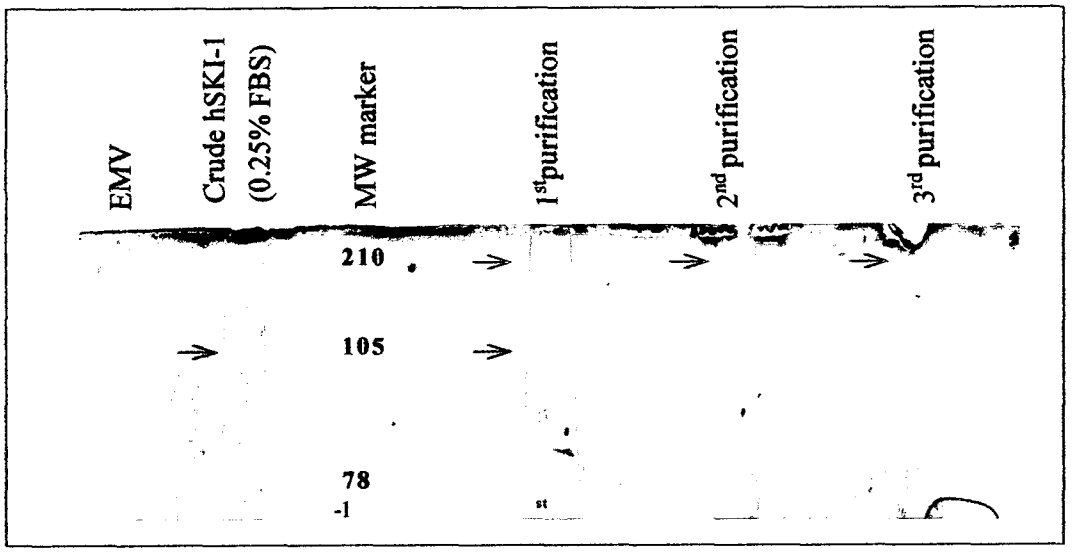

Figure 4.23: *Silver stained Tris-tricine SDS-PAGE for crude and Cibacron blue 3GA column purified rec-SKI-1 samples showing the presence of monomer form of SKI-1 at 98 kDa (black arrow) and for the dimer at ~200 (red arrow) respectively.*

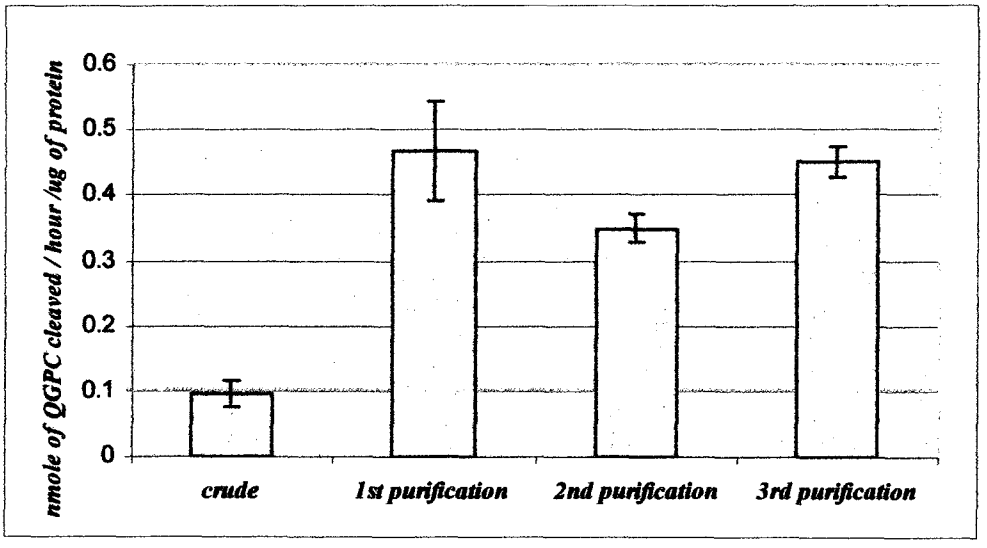

Figure 4.24: *Specific activity of crude hSKI-1(0.25% FBS conditioned medium) and aliquots from different steps in its purification via Cibacron blue 3GA column. Respective purification steps are indicated at the base of each bar chart.*

The specific activity of the enzyme was measured at different stages of purification and compared with that the of crude enzyme sample. The results (**Figure 4.24**) revealed a significant increase in specific activity after the first purification cycle. However, the specific activity did not increase after subsequent purification cycles suggesting that some active enzyme may remain bound to the column. Moreover a decrease in activity resulting from dimerization of rec-SKI-1 may have an effect on the final activity of the enzyme. However it is evident by Western blot analysis that immunoreactive SKI-1 band for dimer form (at ~ 200 kDa) became more visible following removal of BSA (**Figure 4.22**).

4.3. Design synthesis and in vitro evaluation of inhibitors of hSKI-1

4.3.1. Pseudo peptide approach

In previous studies it has been shown that peptides containing hSKI-1 prodomain sequence at RRLL^{186} RA, site (primary activation site) can be used as efficient substrates for hSKI-1 (25;42;44). Therefore for developing pseudo peptides as inhibitors for hSKI-1 enzyme we inserted a pseudo peptide bond (a bond that mimics the peptidyl amide bond) at the scissile site of this hSKI-1 prodomain sequence by either substitution or incorporation of an unnatural amino acid. A list of the various pseudo peptides prepared for this project is shown in **Table 4.0.** We selected the prodomain sequence at the hSKI-1$^{183\text{-}190}$ site containing the ^{183}RRLLRAIP^{190} sequence for first four pseudo peptides. Then we extended this prodomain sequence (towards the N-terminus) up to position 178 (prohSKI-1$^{178\text{-}190}$) to test if this would help enhance enzyme inhibitory property (peptide # 5 & 6 in the **Table 4.0**). All peptides in this series are therefore considered to be prodomain substrate-based pseudo-peptides.

Among the possible linkages that can be considered as good pseudo peptide bonds, the methylene-oxy bond was selected due to its similarities to the amide bond. Bond length and the bond angle of the C-O-C and C-N-C are quite close in size. Molecular weight, atomic size and the electro negativity of the N and O atoms are very close to each other (50;51). Thus oxygen containing methylene-oxy compounds was selected as our initial effort to prepare pseudopeptide inhibitors for SKI-1. In this study two oxymethelene containing unnatural amino acids Aoa (β amino oxy acetic acid) (-NH-O-CH_2-CO-) (also called Baa) and Adoa (8-Amino3,6- Dioxyoctanoic Acid) (-NH-CH_2-CH_2-O-CH_2-CH_2-O-

CH_2-CO-) were either incorporated or substituted in to the peptide sequence at the cleavable amide bond (-CO-NH-) between P1 and P1′ positions of prodomain of hSKI-1 sequence.

Thus in our preparation of a series of pseudo peptides, Aoa was incorporated to the P1-P1′ position of pro hSKI-$1^{183-190}$ while Adoa was used to substitute the entire "Leu-Arg" dipeptide or "Leu-Arg-Ala" tripeptide units of prohSKI-$1^{183-190}$ or pro hSKI-$1^{178-190}$ with this elongated pseudo-peptide linkage.

Table 4.0: *List of peptides and pseudopeptide analogs synthesized in the current study as potential inhibitors for SKI-1 along with the observed mass of the purified species as determined by MALDI TOF MS (spectra are all available in the appendix). The sequences were numbered based on prodomain sequence of h SKI-1.*

#	Amino acid sequence	Name of the inhibitor	Calculated MW	Observed MW
1	RRLLRAIP	hSKI-$1^{183-190}$	992	992.8
2	RRLL(Aoa)RAIP	hSKI-$1^{183-190}$ Aoa	1051*	1050.6
3	RRL(Adoa)AIP	hSKI-$1^{183-190}$ Adoa-1	868	868.5
4	Fmoc-RRL(Adoa)IP	hSKI-$1^{183-190}$ Adoa-2	1019	1019.9
5	GRHSSRRL(Adoa)AIP	hSKI-$1^{178-190}$ Adoa	1392	1392.4
6	GRYSSRRL(Adoa)AIP	hSKI-$1^{178-190}$ Adoa–Y mutant	1419	1418.8

** Represents mw for the de-aminated (-NH_2) form of the peptide detected by MALDI-TOF-MS*

All peptides were prepared by solid phase synthesis using Fmoc chemistry. Synthesised peptides were cleaved from the resin, deprotected, purified by HPLC (**Figure 6.0A to 6.5A**) and characterized by MALDI TOF mass spectrometry (**Figures 6.0B to 6.5B**) and data are summarized in the **Table 4.0.**

When synthesizing Amino-oxy acetic acid containing peptide we noticed that the main product that was isolated did not contain Aoa unit, likely due to the possible degradation caused difficulties in coupling the unnatural amino acid into the peptide chain.

Nonetheless, as shown in MS and HPLC data in the appendix (**Figures 6.0 A-6.1B**), it was possible to isolate the desired product though in poor yield. In addition amino acid analysis data for the purified Aoa (Baa) peptide (**Table 6.0**) and its non-Aoa analog (**Table 6.1**) confirmed the successful isolation of this peptide. In this amino acid analysis, incorporation of the unnatural amino acid Aoa was confirmed by the presence of a species that eluted at the same retention time as glycine, a residue not part of the synthesized peptide. This peak was confirmed to be Aoa using an authentic standard sample. Since this species was not present in the non-Aoa peptide, this provided excellent confirmation that the desired peptide had been isolated.

4.3.1.1 In vitro evaluation of pseudo peptides for SKI-1 inhibition.

Inhibitory effects of these peptides towards recSKI-1 activity were measured using the intra molecularly quenched fluorogenic $QGPC^{251-263}$ identified to be the most potent synthetic substrate of SKI-1 known so far (25;32). This substrate was synthesized using solid phase synthesis and fmoc chemistry and the characterization data are included in the appendix, (**Figures 6.11A and 6.11B**). The activity of this Q-GPC substrate with hSKI-1 was checked against hSKI-1 using control vector (EMV) at the optimum condition (69;70).

In order to measure the kinetic parameters for SKI-1 inhibition, released raw florescence units (RFU) were measured using a spectrofluorometer at an excitation wavelength of 320 nm and emission wavelength of 420 nm, since they are specific for the florescence unit (Abz: Aminobenzoic acid) of the substrate. Substrate cleavage by hSKI-1 should decrease with increasing concentrations of the inhibitor, which can be detected as a decrease in the rate of raw florescence unit (RFU) release.

This was monitored in a Dixon plot, where the reciprocal of the initial reaction rate was plotted against the concentration of inhibitor, to determine the inhibition constant. In addition, Cornish-Bowden plots (S/V vs. inhibitor concentration) (60) were also plotted for each inhibitor (**Figures 4.25A to 4.30B**).

Inhibition constants (Ki) were calculated by Dixon plots using three different concentrations of QGPC as summarized in **Table 4.1**. And the type of inhibition for each peptide analog was confirmed by the respective Cornish Bowden plot (**Figures 4.25 B – 4.30 B**) (60).

The observed Ki values for peptide # 2 RRLL (Aoa) RAIP, peptide # 3 RRL (Adoa) AIP and peptide # 6 GRYSSRRL (Adoa) AIP were comparatively lower (~4 to 8 folds lower) than the other peptide analogs and three of these pseudo peptides showed competitive inhibition. Even though competitive inhibition was observed for peptide # 5 GRHSSRRL (Adoa) AIP, calculated Ki for this peptide analog was higher than that of its Y mutant. The two shorter peptides in the each series, namely peptide #1 (RRLLRAIP) and peptide # 4 Fmoc-RRL(Adoa)IP exhibited mixed type inhibition with comparatively higher Ki value for hSKI-1 inhibition.

Furthermore our results suggest that complete replacement of the dipeptide unit "Leu Arg" by "Adoa" moiety is more effective than substituting the tripeptide unit "Leu-Arg-Ala". In addition, comparing results for peptide # 5 and # 6, suggest that a bulky aromatic residue at position P7 in the peptide analogs may be useful for efficient recognition by SKI-1, since the Tyr-containing mutant peptide (# 6 hSKI-$1^{178\text{-}190}$Adoa–Y mutant) is ~5 fold more potent (K_i~24.8 μM) SKI-1 inhibitor than the corresponding wild type peptide (# 5, hSKI-$1^{178\text{-}190}$Adoa).

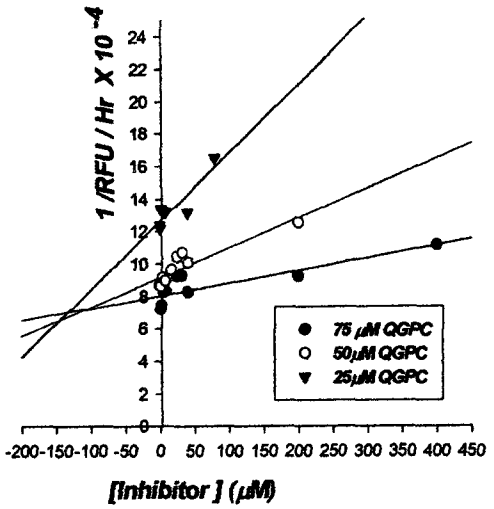

Figure 4.25A: *Dixon plot showing rec-hSKI-1 inhibition by RRLLRAIP peptide*

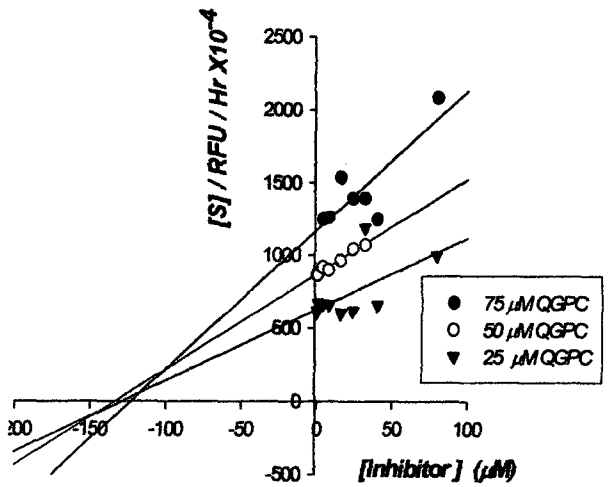

Figure 4.25B: Cornish *Bowden plot showing rec-hSKI-1 inhibition by RRLLRAIP peptide*

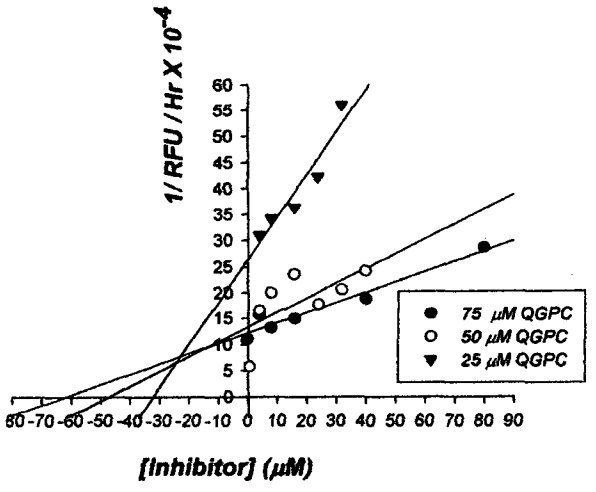

Figure 4.26A: *Dixon plot showing rec-hSKI-1 inhibition by RRL (Aoa)RAIP peptide*

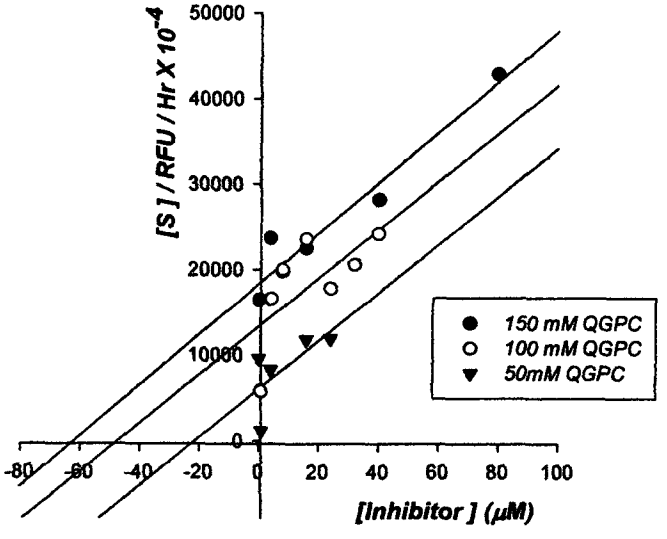

Figure 4.26B: Cornish *Bowden plot showing recSKI-1 inhibition by RRLL (Aoa)RAIP peptide*

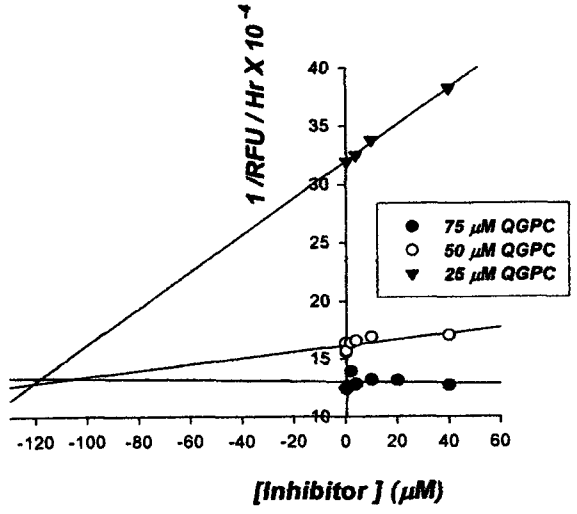

Figure 4.27A: Dixon plot for recSKI-1 inhibition by RRL (Adoa) IP peptide

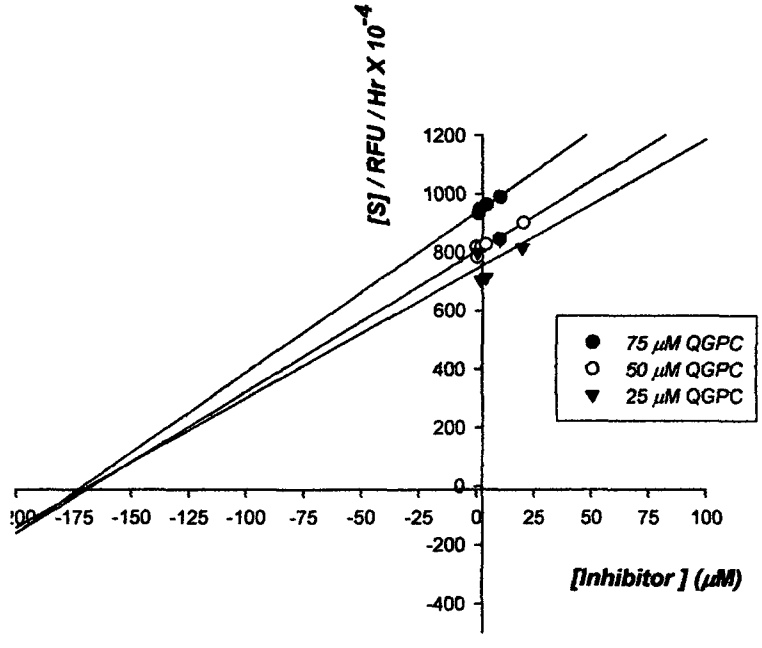

Figure 4.27B: Cornish Bowden plot for recSKI-1 inhibition by RRL (Adoa) IP peptide

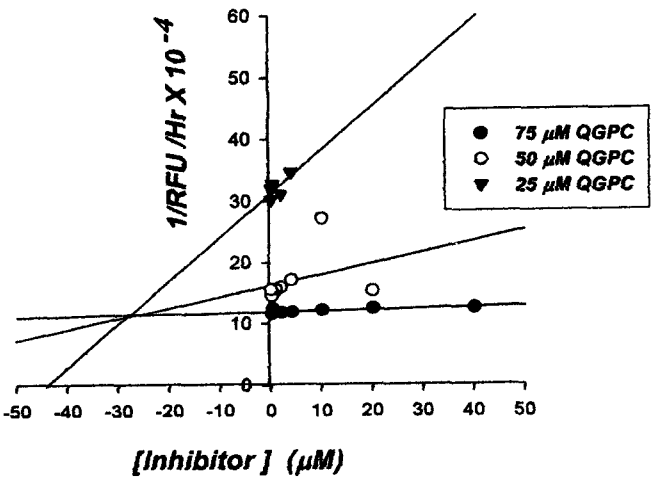

Figure 4.28A: *Dixon plot showing recSKI-1 inhibition by RRL (Adoa) AIP peptide*

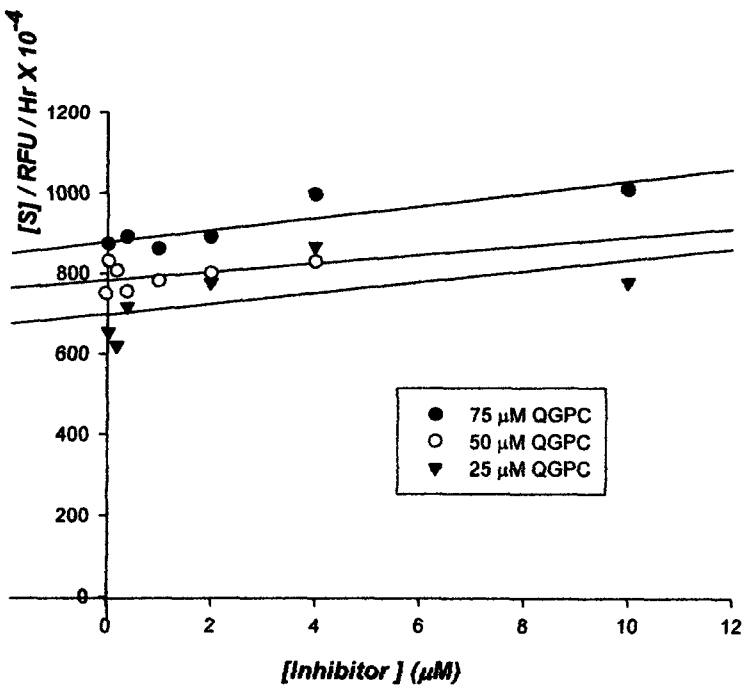

Figure 4.28B: *Cornish Bowden plot showing recSKI-1 inhibition by RRL (Adoa) AIP peptide*

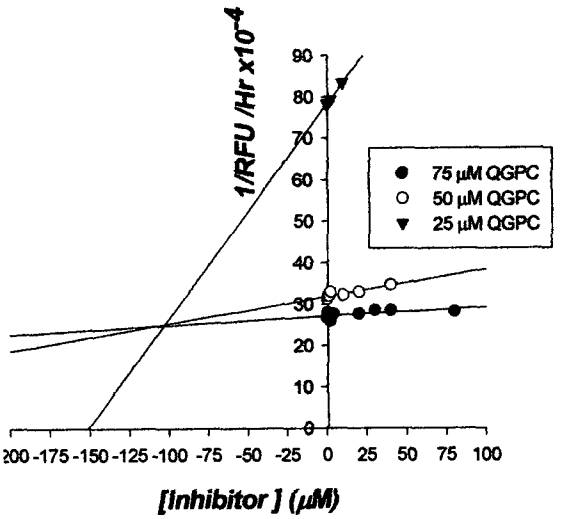

Figure 4.29A: *Dixon plot for recSKI-1 inhibition by GRHSSRRL (Adoa) AIP peptide*

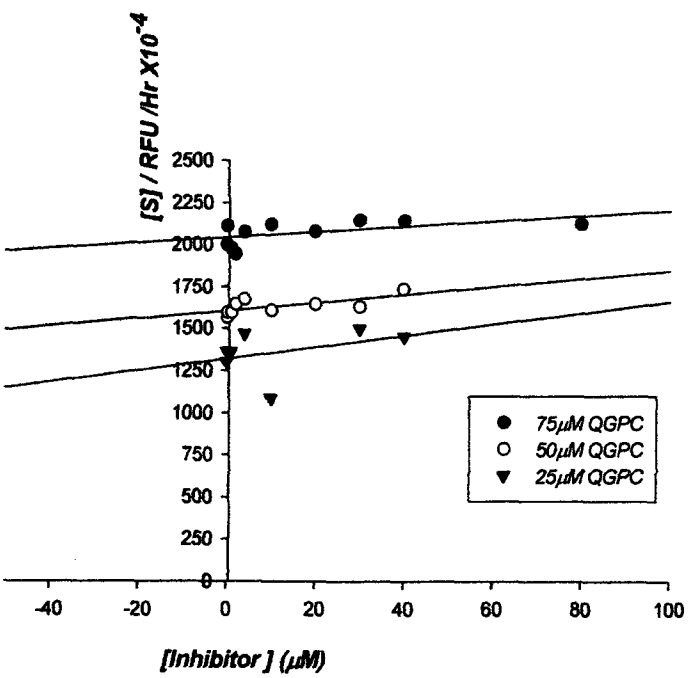

Figure 4.29B: *Cornish-Bowden plot for recSKI-1 inhibition by GRHSSRRL (Adoa) AIP peptide*

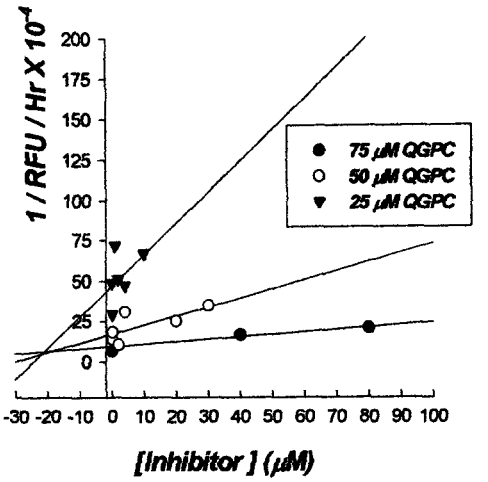

Figure 4.30A: *Dixon plot showing recSKI-1 inhibition by GRYSSRRL (Adoa) AIP*

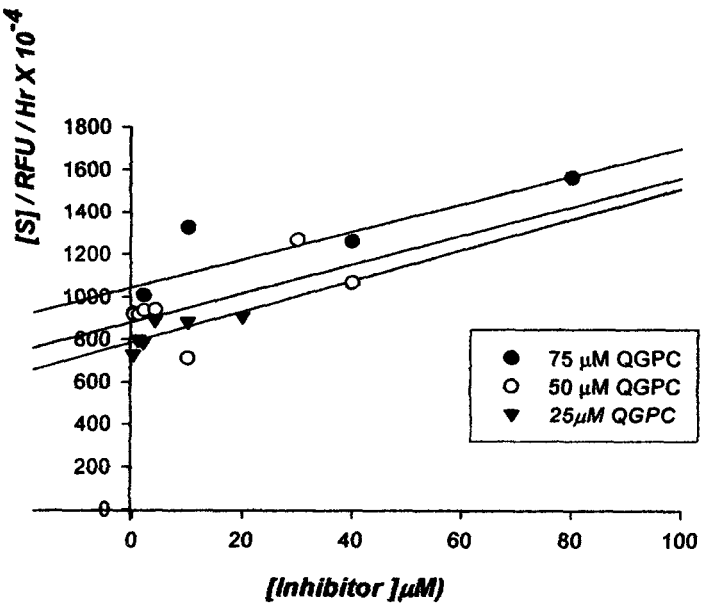

Figure 4.30B: *Cornish-Bowden plot showing rec-hSKI-1 inhibition by GRYSSRRL (Adoa) AIP*

Table 4.1: Enzyme inhibitory parameters of synthesized pseudo peptides against rec-hSKI-1 activity with QGPC substrate. Most potent inhibitors are shown in bold

#	Name of the Inhibitor	Measured K_i values (μM)
1	hSKI-$1^{183\text{-}190}$	135
2	**hSKI-$1^{183\text{-}190}$ Aoa**	**17+/-3.0**
3	hSKI-$1^{183\text{-}190}$ Adoa-1	28+/-2.7
4	hSKI-$1^{183\text{-}190}$ Adoa-2	110+/-9.5
5	hSKI-$1^{178\text{-}190}$ Adoa	109+/-10.4
6	**hSKI-$1^{178\text{-}190}$ Adoa "Y" mutant**	**24.8+/-0.8**

Basak et al Protein & Peptide Letters, 2006, 13, 847-860

4.3.2 Branch/oligomeric peptide approach

In our next approach to develop inhibitors for hSKI-1, the prodomain sequence at hSKI-$1^{128\text{-}137}$, containing the secondary cleavage site was selected. According to the previous findings this selected site is also known as one of the best recognizable sites for hSKI-1 .(8;25;32;42).

We assembled two and four of these peptide units on a single template, in an attempt to enhance protease inhibitory property, following previous studies utilizing a similar concept to enhance the inhibition of protein-protein interactions (52-54). In our design of multimeric peptides, we expected to improve enzyme inhibitor interaction via a multi-arm peptide.

Synthesis of linear peptides along with branched peptides containing two and four units of these peptide chains (peptides # 7-11), were accomplished by solid phase based Fmoc chemistry. All crude synthetic peptides were purified using RP-HPLC and identities were confirmed by MALDI TOF mass spectrometry. As shown in **Table 4.2**, this series included branched analogs containing two peptide inhibitory units, one without (peptide # 8) and the other with (# 9) a linker {two units of aminohexanoic acid, $[-NH(CH_2)_5CO-)]_2$ or $(Ahx)_2$}.

Table 4.2: List of branch and linear peptides synthesized as potential hSKI-1 inhibitors.

	Amino acid sequence	Name of the inhibitor	Calculated MW	Observed MW
7	Fmoc^{128}PQRKVFRSLK^{137}	Fmoc- (hSKI-1$^{128-137}$)	1480	1479.6
8	^{128}PQRKVFRSLK^{137}	(hSKI-1$^{128-137}$) Linear	1257	1256.5
9	(^{128}PQRKVFRSLK^{137})$_2$KA	(hSKI-1$^{128-137}$)2-branch	2696	2695.2
10	[^{128}PQRKVFRSLK^{137}(Ahx*)$_2$]$_2$KA	(hSKI-1$^{128-137}$) Ahx-2-branch	3147	3145.9
11	(^{128}PQRKVFRSLK^{137}(Ahx*)$_2$]$_4$KA	(hSKI-1$^{128-137}$) Ahx-4-branch	6339	6339.2

*Ahx = Amino Hexonic acid [-NH_2-CH_2-CH_2-CH_2-CH_2-CH_2-CO-]

hSKI-1 inhibition by synthetic linear and multibranch peptides were tested against the fluorogenic Q-CMV substrate (Dabcyl-^{638}RGVVNA↓ SSRLA^{648}Edans), which is derived from human Cytomegalovirus protease sequence (**Figure 1.4**), a substrate that has successfully been used in the previously reported fluorescence based assay studies (26). Despite the absence of a basic residue at the P_4 position, this substrate has a "SKI-1 like" recognition sequence; namely hydrophobic residues at positions P_2 and P_1 and a small amino acid residue at P_1' with a basic (Arg) residue at P_6 that composite the lack of a basic residue at P_4 position. In order to understand the affinity of the hSKI-1 for the substrate with P_6 basic residue (arginine) instead P_4 basic (arginine) residue, the Q-CMV substrate was selected for this study.

4.3.2.1. IC_{50} values for SKI-1 inhibition by branch peptides

IC_{50} values were obtained by measuring rec-hSKI-1 activity against 100 μM Q-CMV substrate in presence of a range of inhibitor concentrations. Released raw florescence units (RFU) by cleaving Q-CMV substrate, were measured using a spectrofluorometer with fixed excitation and emission wavelengths of 355 nm and 495 nm for Dabcyl donar and Edans acceptor groups in the substrate. The rate of RFU release was taken to be equivalent to the velocity of the enzymatic reaction and the rate at zero inhibitor concentration was considered as the initial (100%) velocity. The inhibitor concentration giving rise to half maximal (50%) reaction velocity was determined to be the

IC_{50} values for these compounds. Since only one substrate concentration (100 μM) was used data were not sufficient to plot Dixon or Cornish Bowden plots for respective peptides

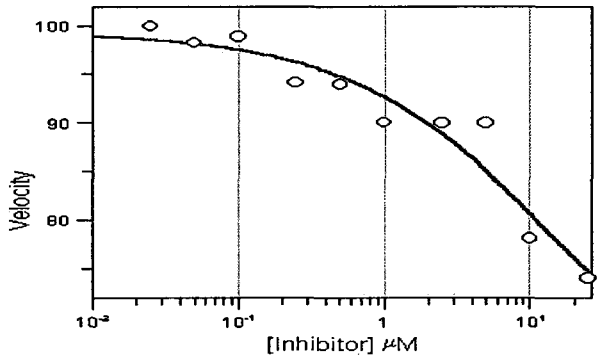

Parameter	Value	Std. Error
Y Range	42.2483	7.0363
IC 50	14.7009	7.8684
Slope factor	0.6279	0.1831
Background	57.1018	6.5639

Figure 4.31: *Sigmoidal graph (plot of activity vs log inhibitor concentration) showing* inhibition of recSKI-1 activity by *linear Fmoc-hSKI-*$1^{128\text{-}137}$ *peptide for determination of* IC_{50} *value.*

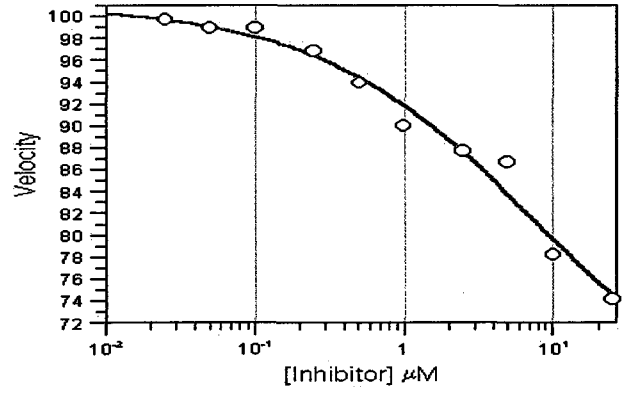

Parameter	Value	Std. Error
Y Range	39.9035	4.2303
IC 50	7.9356	2.8517
Slope factor	0.5904	0.1017
Background	61.0388	3.7212

Figure 4.32: *Sigmoidal graph (activity vs log inhibitor concentration) showing* inhibition of rec- hSKI-1 activity by *linear recSKI-*$1^{128\text{-}137}$ *peptide for determination of* IC_{50} *value.*

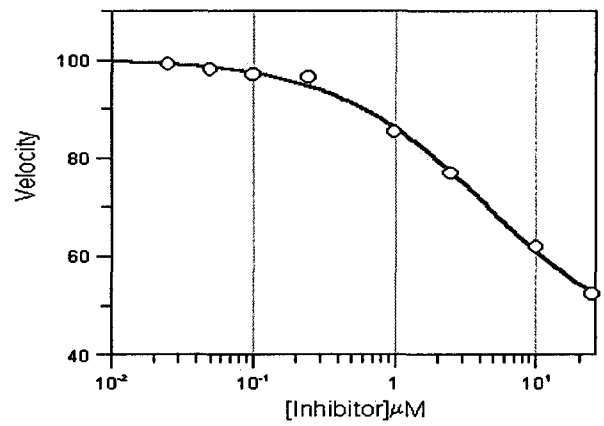

Parameter	Value	Std. Error
Y Range	59.4204	7.3104
IC 50	4.4503	1.3618
Slope factor	0.7977	0.1303
Background	40.6793	6.4413

Figure: 4.33: *Sigmoidal graph (plot of activity vs log inhibitor concentration) showing* inhibition of recSKI-1 activity by *2-branch hSKI-*$1^{128\text{-}137}$ *peptide for determination of* IC_{50} *value.*

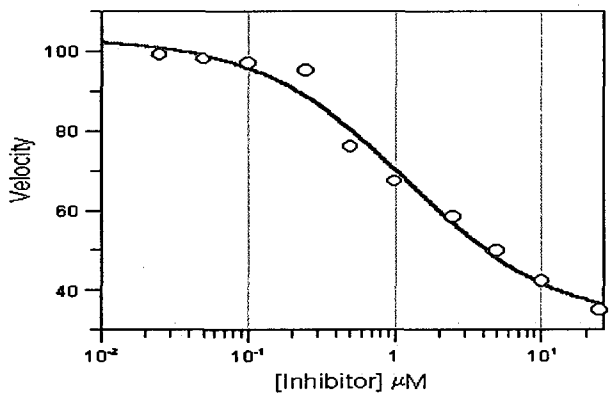

Parameter	Value	Std. Error
Y Range	71.3433	10.3632
IC 50	1.2012	0.3419
Slope factor	0.8640	0.2346
Background	31.8488	6.9765

Figure 4.34: *Sigmoidal graph (plot of activity vs log inhibitor concentration) showing* inhibition of recSKI-1 activity by *2-branch-Ahx-hSKI-*$1^{128\text{-}137}$ *peptide for determination of* IC_{50} *value.*

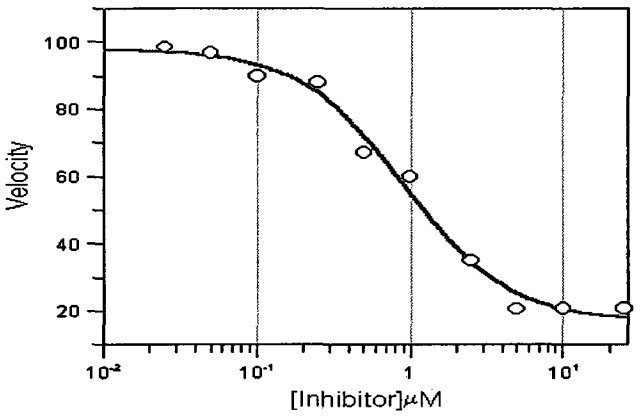

Parameter	Value	Std. Error
Y Range	80.8799	6.0163
IC 50	0.9201	0.1434
Slope factor	1.2749	0.2488
Background	16.9109	3.9911

Figure 4.35: *Sigmoidal graph (plot of activity vs log inhibitor concentration) showing inhibition of recSKI-1 activity by 4-branch hSKI-1*$^{128\text{-}137}$ *peptide for determination of* IC_{50} *value.*

Plotted sigmoidal graphs for IC_{50} calculations of each peptide are shown from figure 4.32 to 4.36 with IC_{50} values summarized in **Table 4.3**. Graphs obtained for the linear peptides (# 7 & # 8) for hSKI-1 inhibition exhibited the least sigmoidal shape while the best sigmoidal curve was observed for 4- branch peptide (# 11) inhibition.

The linker-containing 2-branch peptide (# 9) is ~3 fold more potent than its non-linker peptide (#8), while 4-branch peptide (IC_{50} = 0.9 μM) is the most potent among this series of peptides being ~1.3 and 8.6 fold more potent than the corresponding 2-branch and single-branch peptides respectively.

However, given the fact that the 4-branch peptide contained two times the number of inhibitory peptide units per mole compared to the 2-branched peptide, this increase in inhibition was lower than expected. Based on our hypothesis, it was expected to have 2 fold more inhibition for 4-branch peptide than corresponding 2-branch peptide. Possible steric hindrance in the four-branch peptide may be responsible for this lower level of inhibition.

An additional finding in this series of inhibitors is that the presence of highly hydrophobic Fmoc group at the N terminal P_{10} position reduces the inhibitory activity of the peptide since its removal enhances enzyme inhibition by a factor of ~1.9 (compare IC_{50} values between # 6 and # 7 peptides).

Table 4.3: *IC_{50} values for hSKI-1 inhibition by linear and branch peptides against* 100μM *Q-CMV (*Dab-CMV$^{638-648}$-Edans) *substrate*

#	Name of peptide	IC_{50} value (μM)
7	(Fmoc-hSKI-1$^{128-137}$)	14.8 (± 3.1)
8	(hSKI-1$^{128-137}$) Linear	7.9 (± 1.8)
9	(hSKI-1$^{128-137}$) 2-branch	4.4 (± 0.6)
10	(hSKI-1$^{128-137}$)-Ahx-2-branch	1.2 (± 0.3)
11	**(hSKI-1$^{128-137}$)-Ahx-4-branch**	**0.92 (± 0.04)**

***Basak et al Protein & Peptide Letters*, 2006, *13*, 847-860**

CHAPTER 5

DISCUSSION AND CONCLUSION

5.1 Production of rec-hSKI-1: Effect of FBS on rec-SKI-1 expression and activity

The construct used here for production of a soluble active form of human SKI-1 enzyme contains its signal peptide, prosegment, catalytic domain and the C-terminal P-(protease) domain terminating immediately before the trans-membrane domain. Its calculated molecular weight is ~100 kDa based on the known sequence hSKI-1$^{18-997}$. The 3D structure of this enzyme has not yet been determined due to the unavailability of pure enzyme in a considerably large quantity. However in a recent publication, Bodward et al (25) reported the production of rec-SKI-1 in soluble form using baculovirus expression system in insect Sf9 cells. They were also able to purify the enzyme to homogeneity with high enzymatic activity (indicating loss of prodomain) as tested against small fluorogenic peptide substrate (25). In our study rec-soluble hSKI-1 enzyme was produced in a similar manner but by using vaccinia virus infected HEK 293 cells (a mammalian cell line) since this expression system was known to produce a soluble form of human SKI-1 enzyme with a reasonably high level of activity based on initial work from our lab (43) This also confirmed by other studies (42;44;71). This expression system also has the potential to be used as an *in vivo* system to test the efficacy of SKI-1 inhibitors. However, a major drawback with this system was the requirement of high level of FBS in the culture medium, a factor that hindered our purification attempts of recombinant enzyme.

However our data suggested that under the standard cell culture condition rec-SKI-1 lacking the trans membrane domain was produced in enzymatically active form and was secreted as soluble protein in to the culture medium. The activity of the concentrated culture medium containing rec-hSKI-1, measured with the intramolecularly quench fluorogenic substrate (Q-GPC) was found to depend on FBS concentration.

In order to overcome heavy BSA accumulation in SKI-1 culture medium, vaccinia virus (VV) infected BSC-40 cells (an African green monkey kidney cells) could be used to produce active SKI-1 enzyme, since it was shown that serum free media can be used in this expression (8). However, the level of SKI-1 expression in this system was reported to be extremely poor and not sufficient for enzymological and biochemical studies. During that

study it was understood that there is a need to modify the culture condition particularly the level of FBS used in the culture medium. Herein, we for the first time carried a systematic study showing the effect of FBS concentration on SKI-1 activity and its production. Our data revealed that although 10% FBS culture condition yielded rec-SKI-1 with highest level of enzymatic activity, the 0.25% FBS condition also produced rec-SKI-1 with less but still significant levels of activity. Both 0.1% and 0% FBS culture medium did not yield any significant activity and therefore is not recommended for SKI-1 production.

Alternatively gradual cell adaptation technique could be examined to determine whether a slow reduction in the concentration of FBS might permit HEK 293 cells to be used to produce active SKI-1 in the complete absence of FBS, a possibility that remains to be explored in the future.

5.2 Chromatographic methods for purification of rec-hSKI-1.

Previously various types of chromatographic methods have been used for purification of recombinant PC-family enzymes with partial success, the most common being ion exchange chromatography. In the present study for purification of our recombinant hSKI-1, we used ion exchange, size exclusion, as well as FBS-specific cibacron dye affinity column chromatographies. While only a moderate level of purification was achieved using size exclusion column chromatography the best route appears to be to use a low (0.25%) FBS culture condition and Cibacron 3GA column chromatography. Our study reviled that this column removed a significant amount of FBS from the enzyme although some SKI-1 activity was also lost, suggesting that a strong affinity may exist between SKI-1 enzyme and BSA protein. Moreover, repeated application of sample to Cibacron 3GA column led to an improvement of purification of the enzyme but also led to a decrease in enzymatic activity. In addition, it was also observed that removal of contaminant FBS protein from rec-SKI-1 medium led to the formation of an SDS-resistant SKI-1 dimer. This dimmer was predicted on the basis of the molecular weight of the immunoreactive protein band. **The results raise the possibility that the enzyme became less stable when FBS concentration is reduced, suggesting that FBS possibly helps to stabilize this enzyme and protects its activity.** This would be

similar to previous studies showing that albumin protein can act as a thermal stabilizer to enzymes and other proteins potentially through hydrophobic interactions (76;77).

Although such formation of dimer for SKI-1 was quite unexpected and never reported before, other PC enzymes such as PC-1 and PCSK9 have been shown to exist in dimeric forms (72;73). These dimers are believed to be formed by interaction involving amphipathic helices at the C-terminal ends of these proteins (78). A similar mechanism is also possible for hSKI-1 dimerization.

Examination of entire amino acid sequence of hSKI-1, particularly its C-terminal P-domain, using Peptide Companion program (version 1.25) revealed the presence of a potential amphipathic helix region near the proximal C-terminal segment comprising the residues hSKI-$1^{654-671}$ (**Figure 5.0**).

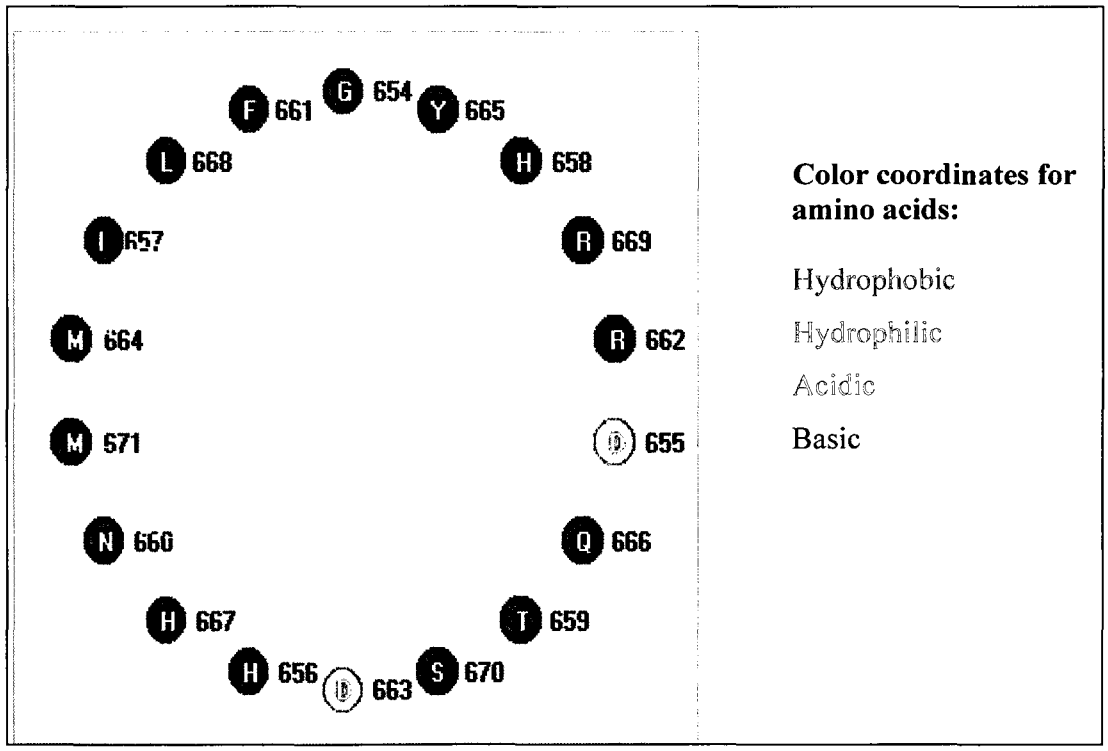

Figure 5.0: *Helical wheel diagram showing the potential amphipathic helix that exhibited by hSKI-$1^{654-671}$ segment as determined by Peptide Companion v1.2 program. The numbering corresponds to that of the hSKI-1 sequence (Accession number = NP_003782).*

This particular segment contains hydrophobic and charged residues on opposite side of the wheel. When viewed along the protein backbone chain a similar type of segment has been previously identified for PC1 (79) near its C-terminus. We propose that this region may be involved in self-association between two molecules of hSKI-1 enzyme leading to dimerization. This same amphipathic region may also be involved in its association with BSA protein. We propose that such associations may help to stabilize or destabilize the activity of the enzyme depending on the type of association, given that dimerization may hinder the conformational flexibility of the enzyme particularly its catalytic domain (80;81). This may provide a plausible explanation for the observed reduced hSKI-1 activity associated with dimerization.

5.3 Factors that influence the competitive inhibition of hSKI-1 activity

Most of the peptide based SKI-1 inhibitors developed in this study exhibited competitive inhibition even though different types of unnatural amino acids were used. However shortest peptides in each series (Aoa and Adoa) namely RRLLRAIP and RRL (Adoa) IP peptides displayed mixed type of inhibition, suggesting that length of the peptide may be important to bind with the active site of the enzyme. But close examination of the inhibition parameters of longer and shorter Adoa containing peptides revealed that the shorter RRL(Adoa)AIP is nearly 4-fold more potent than its N-terminal extended larger counterpart GRHSSRRL(Adoa)AIP. Thus introduction of 5 additional amino acid residues at the N-terminus led to poor interaction with the enzyme. This unexpected observation may be due to the effect of His residue, which can undergo partial protonation under the condition of pH used. However it may be pointed out that replacement of this P7 His by a Tyr residue greatly improved the inhibition parameter. This P7 Try-mutant peptide [GRYSSRRL (Adoa) AIP] exhibited almost the same SKI-1 inhibitory efficiency as the shorter RRL (Adoa) AIP peptide. This suggests that P5-P9 residues have little effect in terms of interaction with the enzyme. However the larger peptide may be more selective SKI-1 inhibitor than the shorter peptide owing to its extended interaction. Such hypothesis needs to be confirmed by further studies. To get a better idea about the catalytic pocket and size of SKI-1 enzyme it is necessary to get a crystal structure of the enzyme. Such a structure is not available currently. However based on the homology model of the catalytic

domain (Arg^{187} to Glu^{460}) of human SKI-1 (24), we speculate that the catalytic pocket of the hSKI-1 may not be so extended as initially thought.

5.4 Role of linker in multi-meric peptides for rec-SKI-1 inhibition

Our study revealed that the branch or multimeric peptide approach is an effective method for design of SKI-1 inhibitors. Although similar approach has been used to enhance the antibacterial property (53), protein binding efficiency and immunogenic property (54), according to our understanding this is the first reported study of multi-branch peptide approach for design of protease inhibitors. In this respect it may be considered as a general strategy. However it needs to be extended to other protease family members to confirm the efficacy and validity of this approach.

However one potential difficulty in this approach is the steric hindrance, which is caused by the presence of several peptide chains in close proximity. It is likely that higher steric hindrance may lead to a reduction in the ability of individual peptide segments to access to the active site of the enzyme. To eliminate this possibility we have introduced a linker with two units of amino hexanoic acid (Ahx) between each peptide segment and the core unit of the molecule. Our results indicated that such linker improved the inhibitory potential of the peptide to a certain extent. However more spatially distributed linker would be a better solution to this situation. For instance aromatic or ring type linkers can be good alternatives for this purpose, as shown by reported studies of inhibitors with aromatic linking groups that yielded significantly greater inhibition compared to analogs compounds with aliphatic linkers (82). During the final phase of correction of thesis, a new report showing the role of SKI-1 in bone mineralization was published in the literature (83).

5.4 Conclusion

Using HEK-293 cell lines and an expression system with a plasmid containing the cDNA of hSKI-1 lacking the transmembrane domain, a recombinant form of soluble hSKI-1 was produced in an enzymatically active form. Our data revealed that activity and the production of hSKI-1 was partially dependent on FBS concentration used in the cell

culture medium. Thus a 10% FBS culture condition-produced rec-SKI-1 with a highest level of activity followed by 5%, 2.5%, 1% and 0.25% FBS condition respectively. 0.1% and 0% FBS condition did not produce any significant level of active hSKI-1. The activity went down significantly as the FBS concentration is decreased to below 0.25%.

The secreted enzyme was recovered from the culture medium and a partial purification of the enzyme was accomplished using the media with reduced FBS concentrations (0.25% instead of 10%) and affinity chromatography. Western blot and gel electrophoresis data showed that purified hSKI-1 underwent dimerization to a significant extent depending on the purification method used. The effect is most prominent in low FBS concentration condition compared to the higher ones. Dimerization of rec-SKI-1 led to partial loss of activity, even though the dimer still retained significant activity when measured against the peptidyl fluorogenic substrates. It is speculated that the association of albumin protein that present in FBS with SKI-1 via non-covalent interaction may stabilize the monomeric form of the enzyme. Removal of FBS led to a self-assembly of SKI-1 enzyme.

Two types of small molecule hSKI-1 inhibitors have been developed in this study. These are pseudo and multi-branched peptides. In the pseudopeptide class, selected prodomain sequences and the alkyloxy based unnatural amino acid incorporation at the scissile P1-P1′ peptide bond led to the generation of peptide analogs that inhibited rec-hSKI-1 activity *in vitro* mostly in a competitive manner. They exhibited IC_{50} or K_i values in low micromolar ranges. This concept of introduction of alkyloxy pseudopeptides can further be developed to obtain more potent inhibitors of hSKI-1 enzyme in future studies using different peptide sequences.

In the multibranch series, steric effects caused some reduction in enzyme inhibition. However our results indicated that, 4-branch peptide is nearly 8.6 and 13-fold more potent SKI-1 inhibitor than the corresponding 2-branch and linear peptide respectively. Even though a comparatively high inhibition was observed with our novel multi branch inhibitors, minimizing the steric hindrance among the individual peptide chains through the use of a suitable linker in the structure of the branch peptides may lead to more potent and effective enzyme inhibitors in future.

In conclusion *in vivo and ex vivo* application of these SKI-1 inhibitors are recommended for future studies to determine their potential therapeutic and clinical values.

6.0 Appendix

Table 6.0: *Amino acid analysis data for RRLL(Aoa) RAIP or Baa peptide*

No.	Ret.Time	Peak Nam	Height	Area	Rel.Area	Amount	Type	Nor Ala	Nor Leu	Nor Baa	known seq
	min		nC	nC*min	%						
1	1.78	Arg	207.64	52.554	37.54	1013.502	BM *	1.8	3.6	2.6	3
2	6.72	Ala	83.883	18.096	12.93	554.142	BMb*	1.0	1.9	1.4	1
3	7.98	Gly	64.451	15.484	11.06	394.616	bMB*	0.7	1.4	1.0	0
4	12.1	Pro	64.776	25.364	18.12	524.943	BMB*	0.9	1.8	1.3	1
5	15.82	Ile	24.541	13.002	9.29	546.845	BMB*	1.0	1.9	1.4	1
6	17.35	Leu	21.227	10.744	7.67	569.618	BMB*	1.0	2.0	1.4	2
7	23.83	SYS	16.679	1.643	1.17	65.614	BM *	0.1			
8	23.97	n.a.	10.562	0.939	0.67	n.a.	MB*	#VALUE!			
9	25.75	n.a.	13.949	2.164	1.55	n.a.	BMB*	#VALUE!			
Total:			507.706	139.99	100	3669.28					

Table 6.1: *Amino acid analysis data for RRLLRAIP peptide*

No.	Ret.Time	Peak Nam	Height	Area	Rel.Area	Amount	Type	known seq	Nor Ala	1470.0
	min		nC	nC*min	%					
1	1.75	Arg	298.501	112.645	27.15	2385.958	BM *	3	1.4	1.6
2	6.7	Ala	240.892	60.4	14.56	1751.686	BMb*	1	1.0	1.2
3	7.97	Gly	51.808	12.899	3.11	333.856	bMB	0	0.2	0.2
4	11.95	Pro	232.944	101.019	24.35	1960.865	BMB*	1	1.1	1.3
5	15.38	Ile	87.97	52.746	12.72	2118.382	BM *	1	1.2	1.4
6	16.85	Leu	99.241	63.243	15.25	3096.898	MB*	2	1.8	2.1
7	23.82	SYS	19.954	1.439	0.35	48.817	BM *			
8	25.47	n.a.	4.976	0.535	0.13	n.a.	Ru*			
9	25.73	n.a.	53.212	9.904	2.39	n.a.	BMB*			
Total:			1089.497	414.83	100	11696.46				

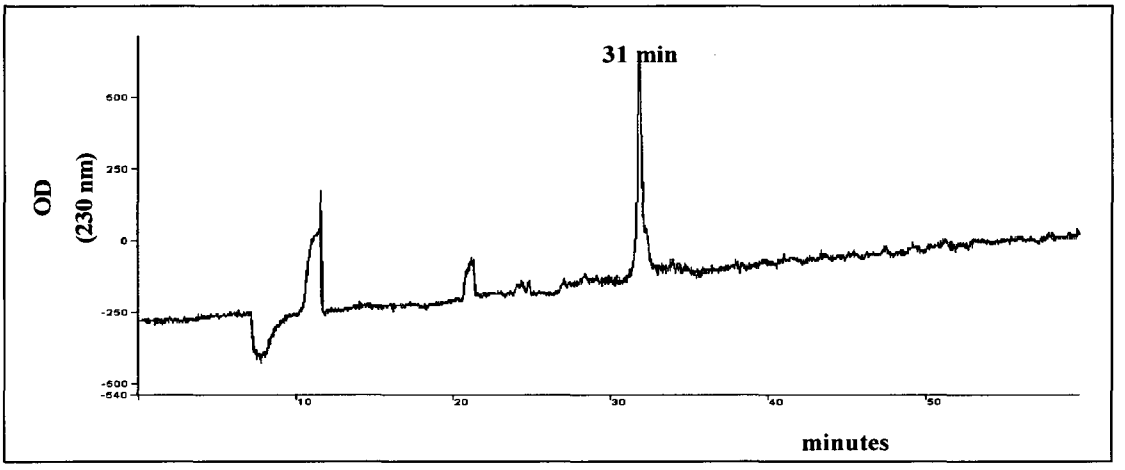

Figure 6.0A: *RP-HPLC chromatogram for RRLLRAIP peptide purification on C18 semi preparative column (Jupiter, Phenomenex; 1 x 25 cm, 10 μ, 300 Å), UV detector with fixed wavelength at 230 nm. Peptide was eluted at 31 min retention time.*

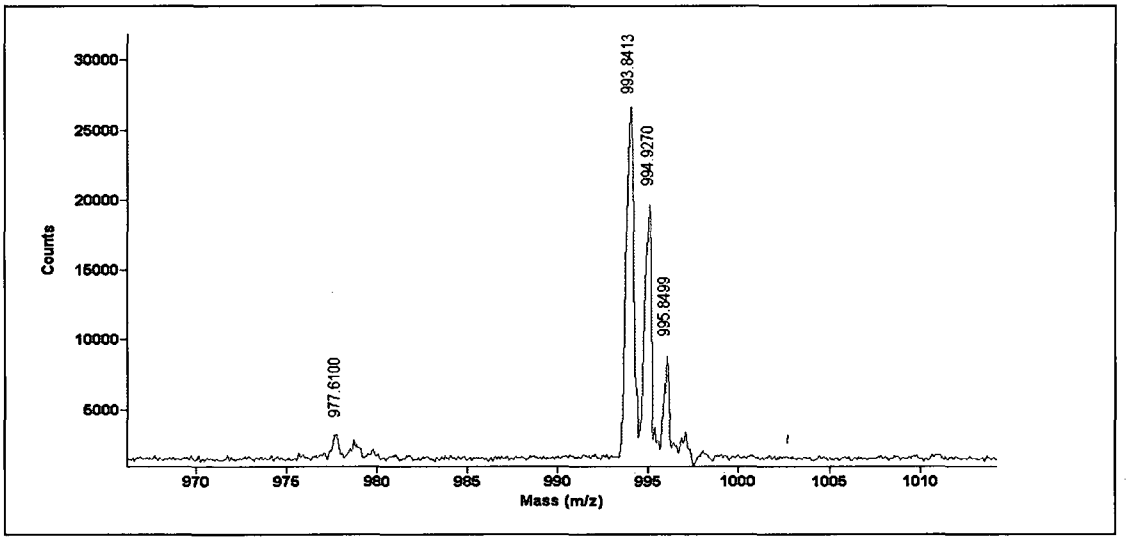

Figure 6.0B: *MALDI-TOF mass spectrum of purified RRLLRAIP peptide, using positive ion detection mode (reflector type) with DHB as matrix. m/z for the mono isotropic ion,* $[M+H]^+$ *of the peptide observed* at *993.8. m/z values for the isotopes were observed at 994.9 and 995.8. Peak at m/z 977.6 was attributed to* NH_2 *(C-terminal) deleted fragment.*

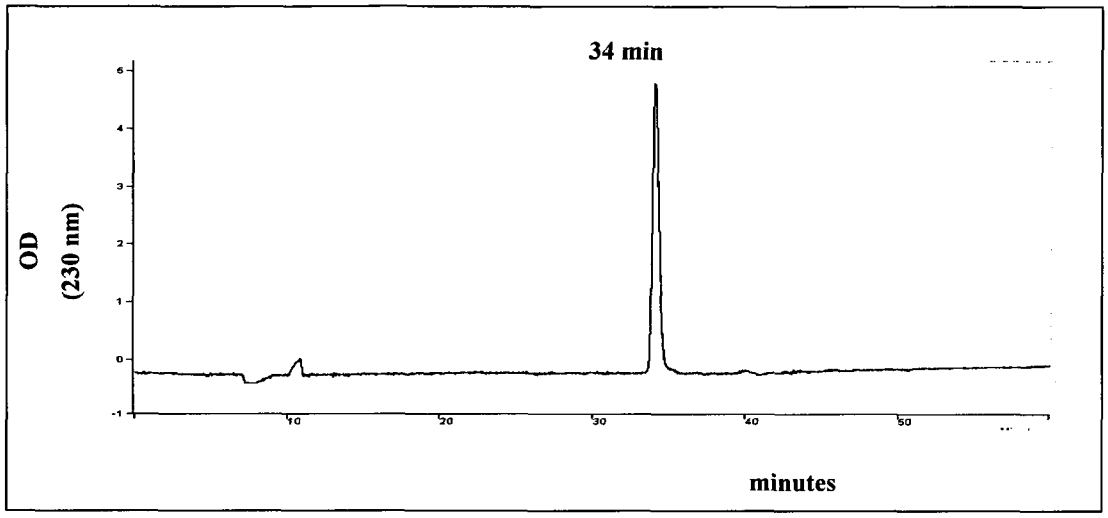

Figure 6.1A: *RP-HPLC chromatogram for the RRLL (Aoa) RAIP pseudo peptide purification on C18 semi preparative column (Jupiter, Phenomenex; 1 x 25 cm, 10 μ, 300 Å),UV detector with fixed wave length at 230 nm. Peptide was eluted at 34 min retention time.*

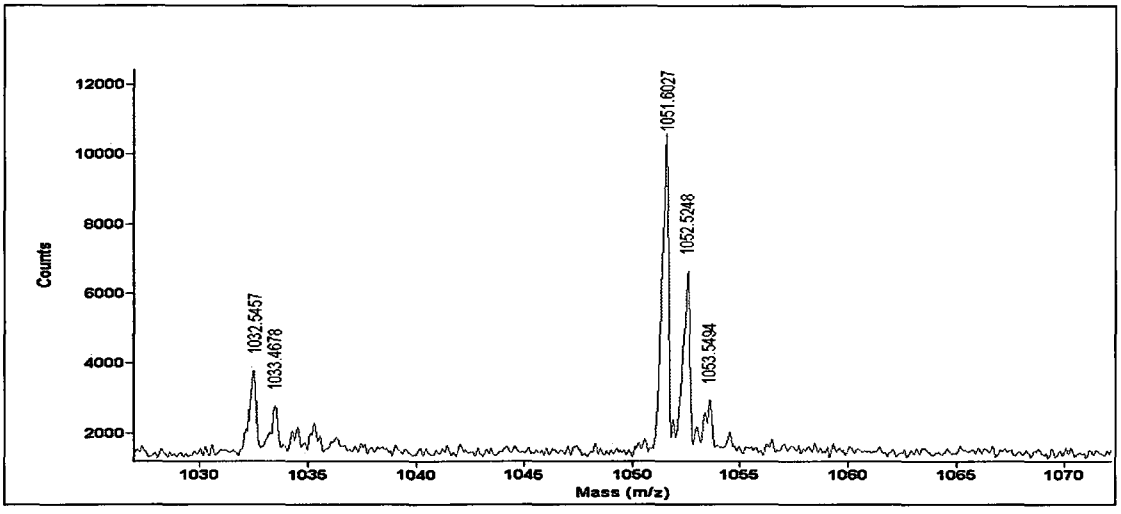

Figure 6.1B: *MALDI-TOF mass spectrum for purified RRLL (Aoa) RAIP peptide, using positive ion detection mode (reflector type) with DHB as matrix. Peak at m/z 1051.6 was attributed to the daughter ion obtained as a loss of NH_2 group from the parent ion. Peaks at m/z 1052.5 and 1053.5 were attributed to isotopes of the daughter ion.*

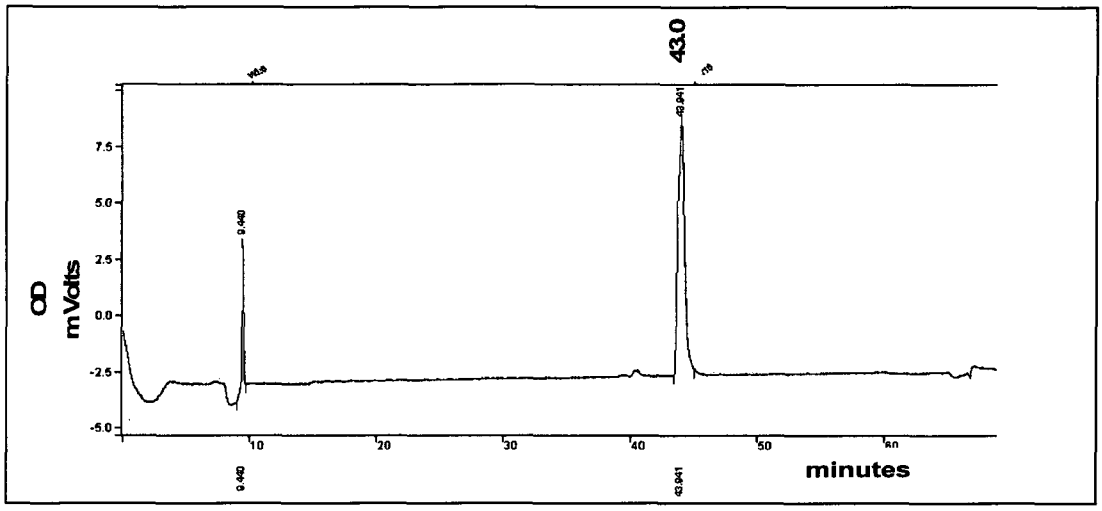

Figure 6.2A: *RP-HPLC chromatogram for fmoc-RRL (Adoa) IP pseudo peptide purification on C18 semi preparative column (Jupiter, Phenomenex; 1 x 25 cm, 10 μ, 300 Å), UV detector with fixed wave length at 214 nm. Peptide was eluted at the 43.0 min retention time.*

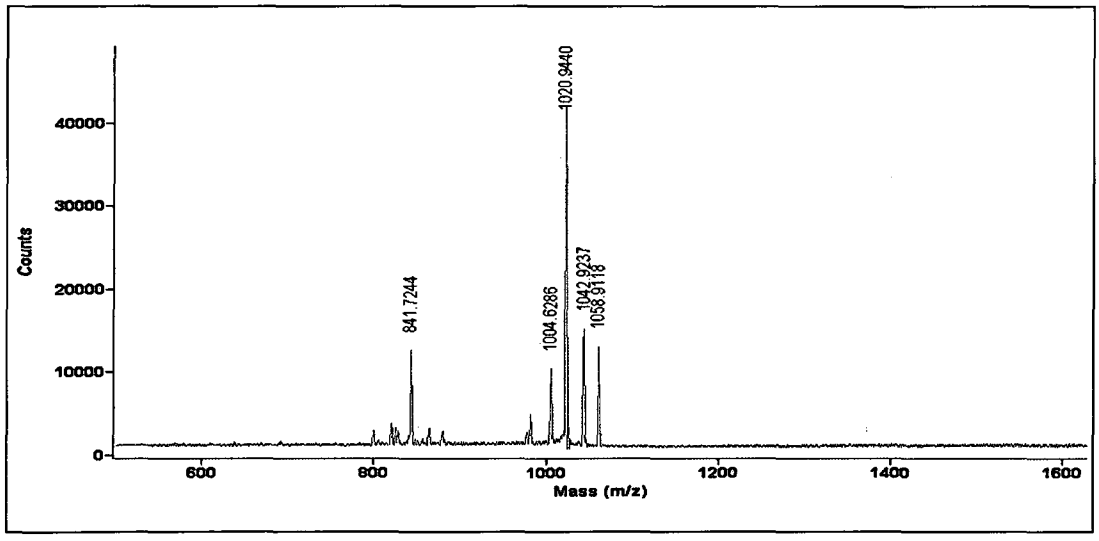

Figure 6.2B: *MALDI-TOF mass spectrum for the purified fmoc-RRL (Adoa) IP pseudo peptide characterization. Positive ion detection mode (reflector type) with CHCA matrix was used. Peak observed at m/z 1020.9 represents the mono isotopic ion of the peptide. Peaks at 1042.9 and 1058.9 were attributed to Na^+ and K^+ adducts respectively of the parent peptide. m/z peak of the fragment of deleted NH_2 group was observed at 1004.6.*

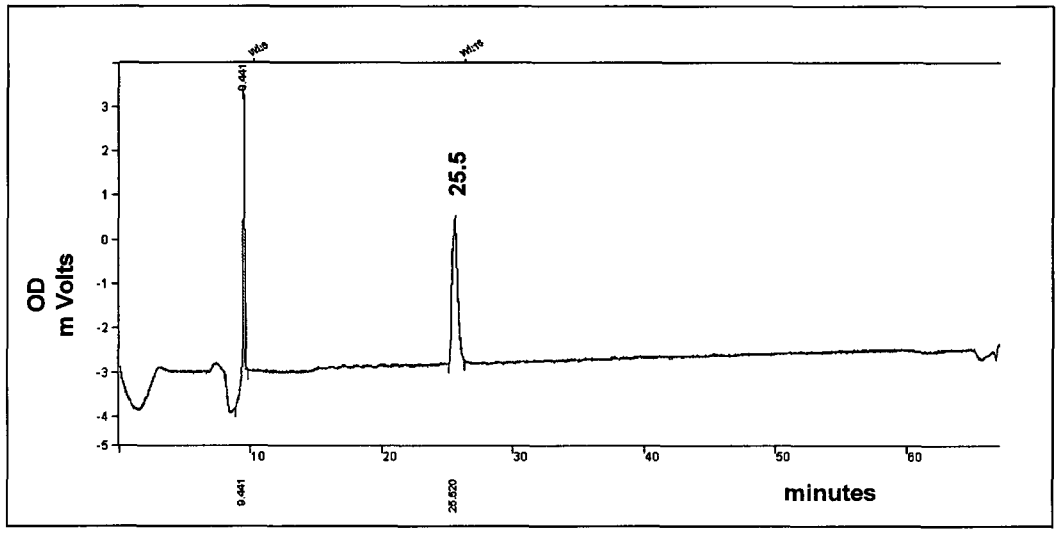

Figure 6.3A: *RP-HPLC chromatogram for RRL (Adoa) AIP pseudo peptide purification on C18 semi preparative column (Jupiter, Phenomenex; 1 x 25 cm, 10 μ, 300 Å), UV detector with fixed wave length at 214 nm. Peptide was eluted at the 25.5 min retention time.*

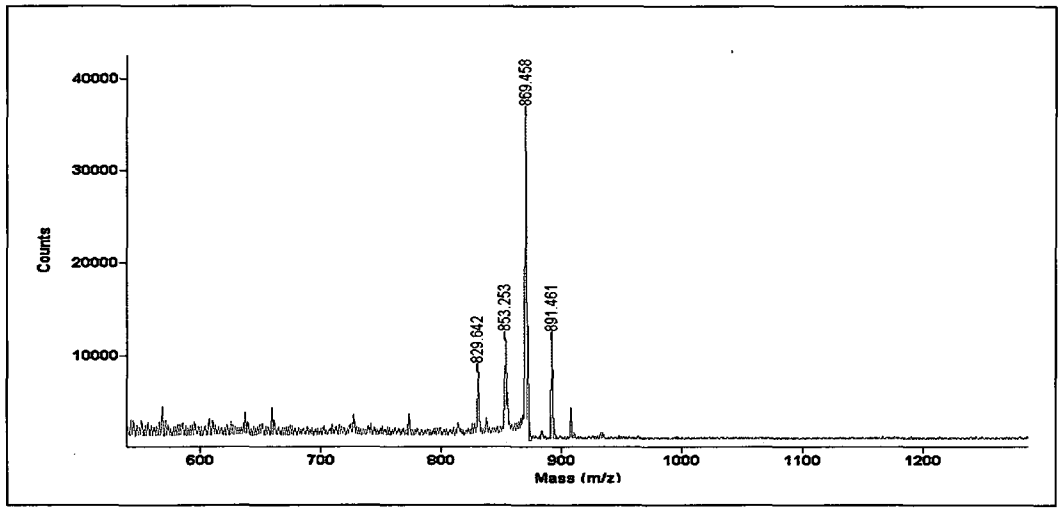

Figure 6.3B: *MALDI-TOF mass spectrum of purified RRL (Adoa) AIP pseudo peptide,* using *positive ion detection mode (reflector type) and CHCA as matrix. M/z peak for the* $[M+H]^+$ *ion of the peptide was observed at 869.5 and the peak at m/z 891.5 was attributed*

to Na^+ adduct of parent peptide. Peak at m/z 853.3 represents NH2 group deleted fragment of the peptide.

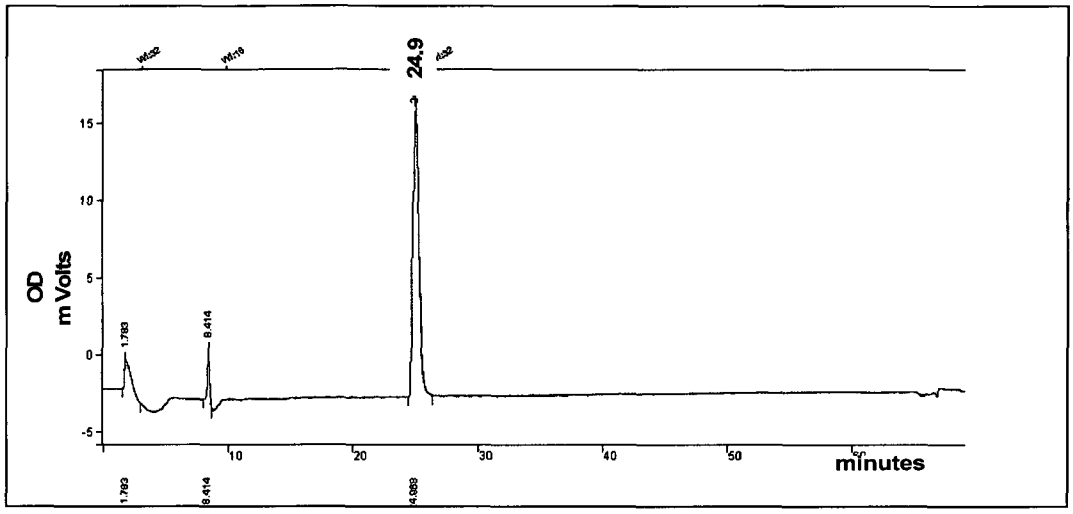

Figure 6.4A: *RP-HPLC chromatogram for GRHSSRRL (Adoa) AIP pseudo peptide purification on C18 semi preparative column (Jupiter, Phenomenex; 1 x 25 cm, 10 μ, 300 Å), UV detector with fixed wave length at 214 nm. Peptide was eluted at 24.9 min retention time.*

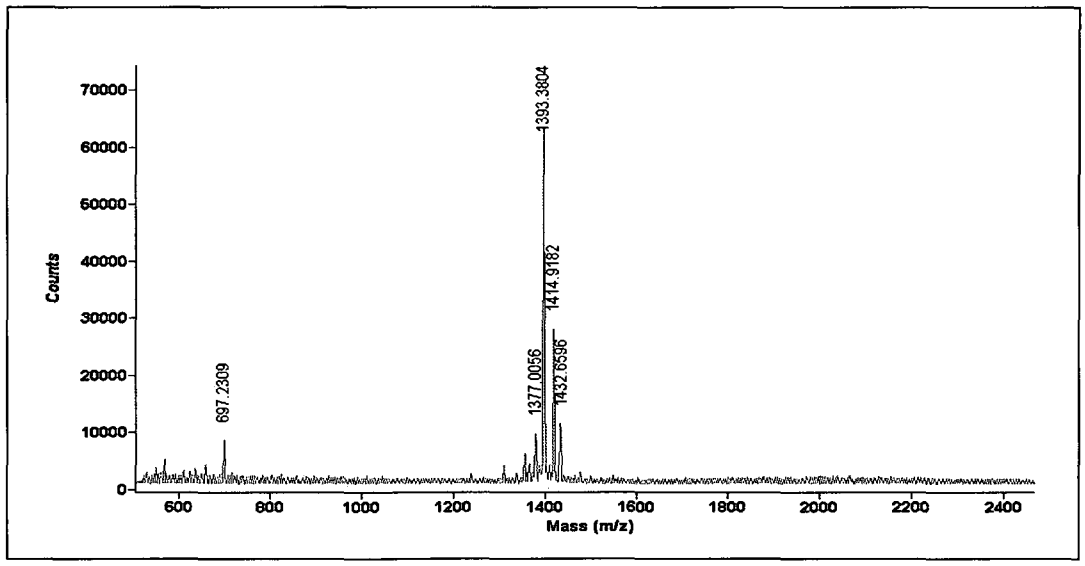

Figure 6.4B: *MALDI-TOF mass spectrum of purified GRHSSRRL (Adoa) AIP pseudo peptide. Positive ion detection mode (reflector type) and CHCA matrix were used for the analysis. M/z peak for $[M+H]^+$ ion of the peptide was observed at 1393.4. Fragmentation*

products for NH_2 group deletion, Na^+ and K^+ adducts of the peptide were observed at m/z 1377.0, 1414.9 and 1432.7 respectively. $[M+2H]^{2+}$ ion was observed at m/z 697.2.

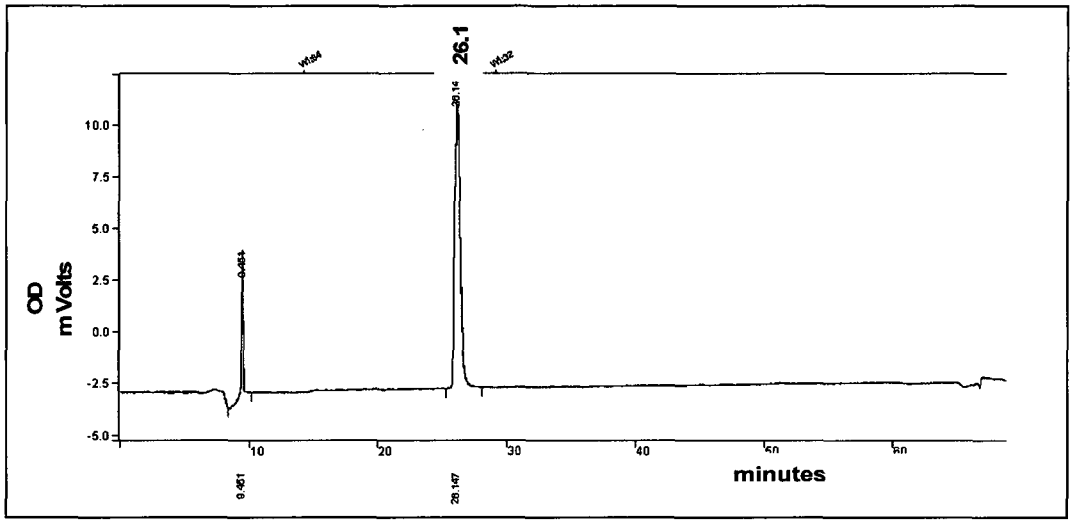

Figure 6.5A: *RP-HPLC chromatogram for GRYSSRRL (Adoa) AIP pseudo peptide purification on C18 semi preparative column (Jupiter, Phenomenex; 1 x 25 cm, 10 μ, 300 Å), UV detector with fixed wave length at 214 nm. Peptide was eluted at the retention time of 26.1 min.*

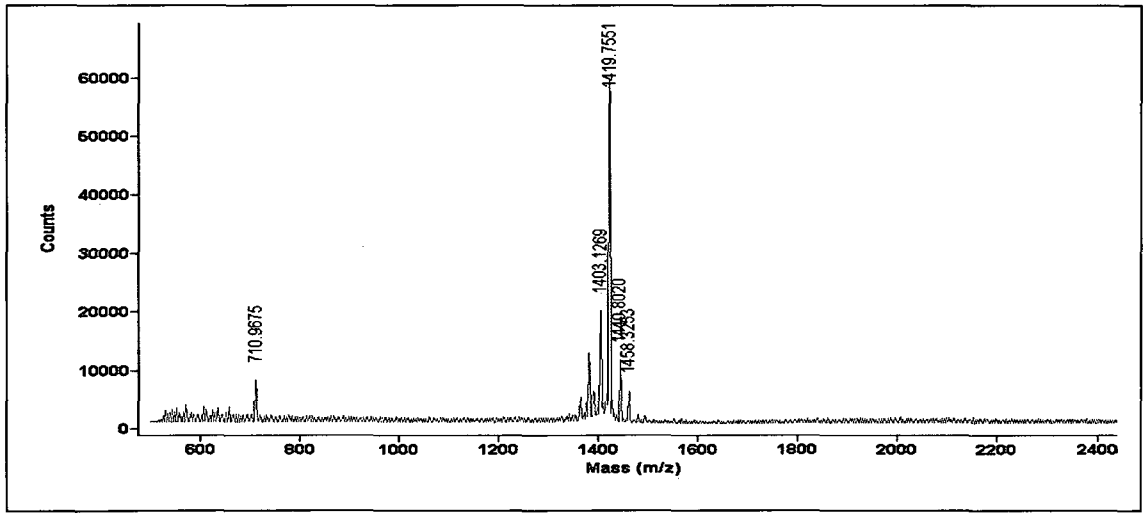

Figure 6.5B: *MALDI-TOF mass spectrum for purified GRYSSRRL (Adoa) AIP pseudo peptide,* using *positive ion detection mode (reflector type) with CHCA as matrix. M/z peaks for $[M+H]^+$ and the $[M+2H]^{2+}$ ions of the peptide were observed at 1419.8 and 710.9*

respectively. Peaks at m/z 1440.8, 1458.3 and 1403.1 were attributed to Na^+, K^+ adducts and NH_2 lacking fragments of the peptide respectively.

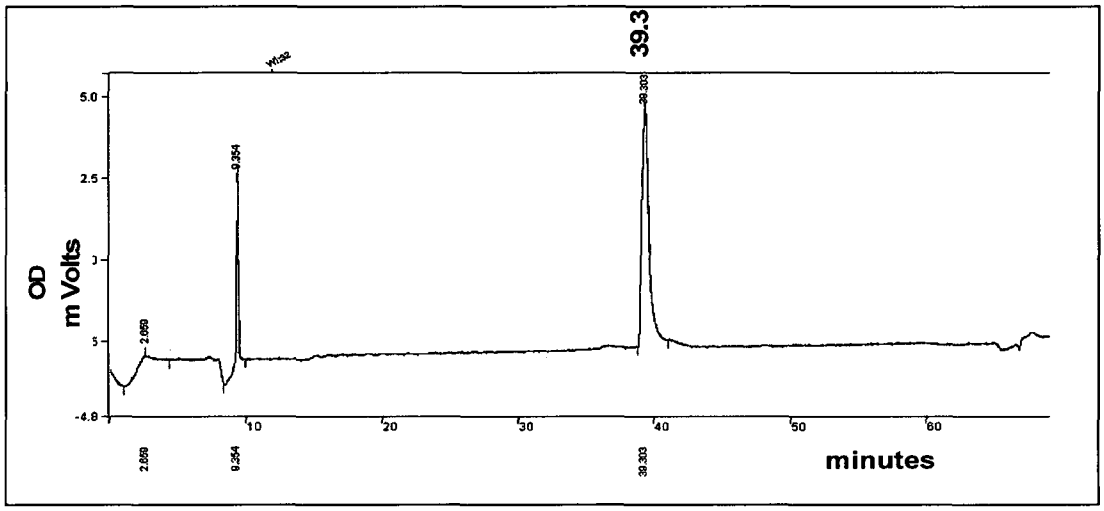

Figure 6.6A: *RP-HPLC chromatogram for fmoc-*^{128}PQRKVFRSLK^{137} *peptide purification on C18 semi preparative column (Jupiter, Phenomenex; 1 x 25 cm, 10 μ, 300 Å), UV detector with fixed wavelength at 214 nm. Peptide was eluted at retention time of 39.3 min.*

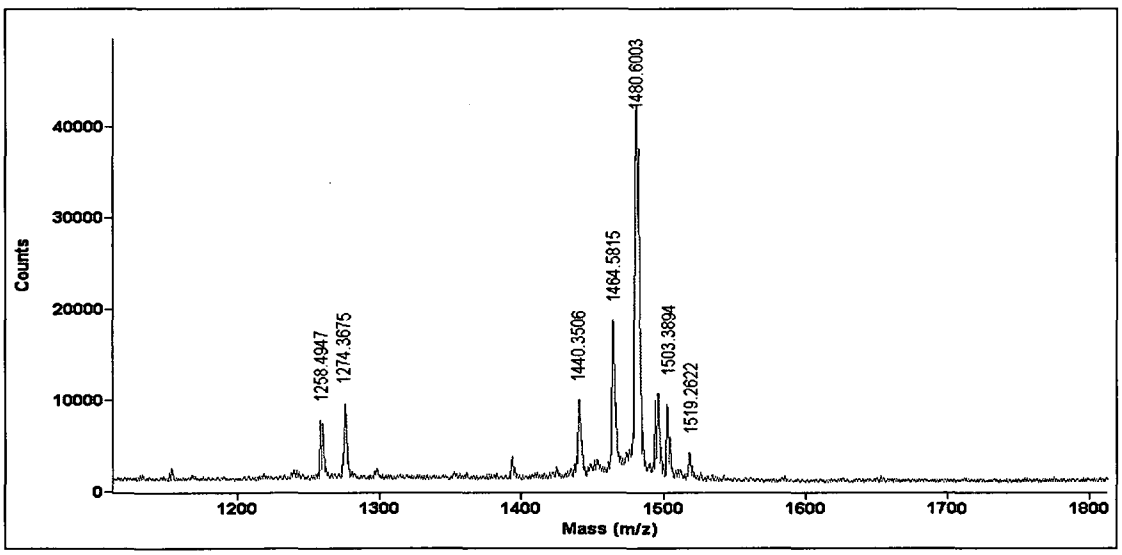

Figure 6.6B: *MALDI-TOF mass spectrum for purified fmoc-*^{128}PQRKVFRSLK^{137} *peptide,* using *positive ion detection mode (reflector type) and sinapic acid as matrix. M/z peak for the $[M+H]^+$ ion of the peptide was observed at 1480.6. Peaks at m/z 1503.4 and 1519.3*

were attributed to Na^+ and K^+ adducts respectively. Fragments of the peptide lacking NH_2 and fmoc groups appeared at m/z 1464.6 and 1258.5 respectively.

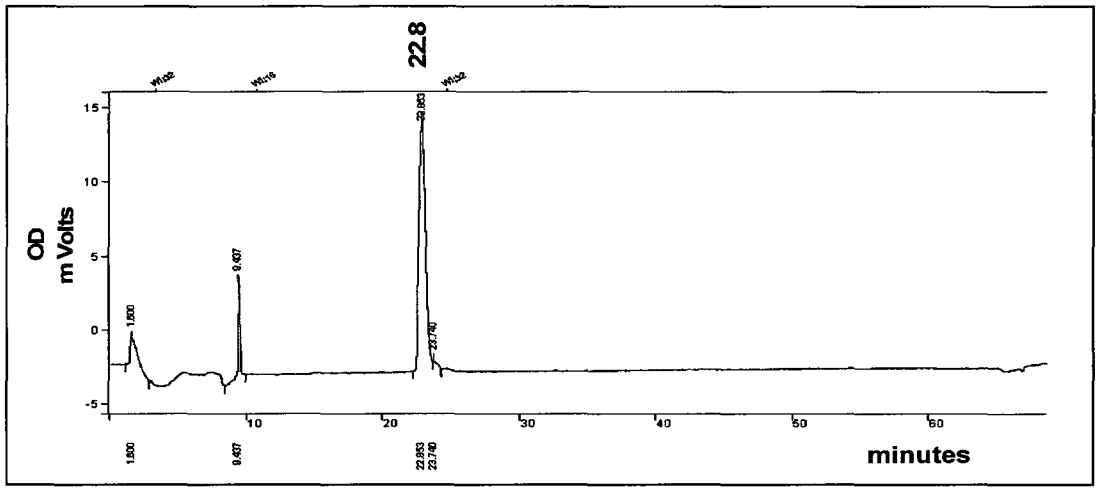

Figure 6.7A: *RP-HPLC chromatogram for linear* ^{128}PQRKVFRSLK^{137} *peptide purification on C18 semi preparative column (Jupiter, Phenomenex; 1 x 25 cm, 10 μ, 300 Å), UV detector with fixed wavelength at 214 nm. Peptide was eluted at the retention time of 22.8 min.*

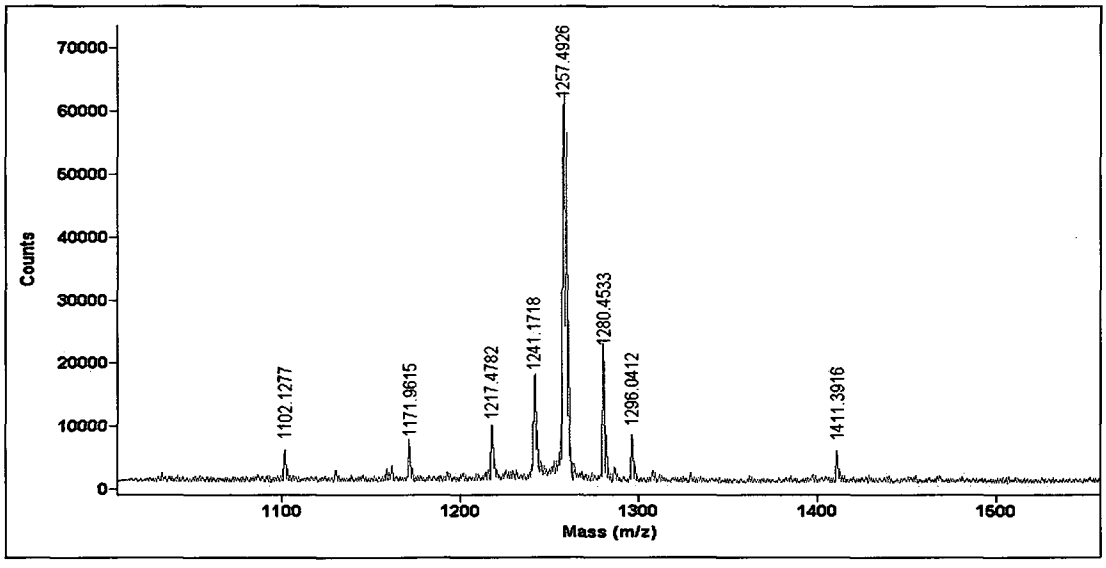

Figure 6.7B: *MALDI-TOF mass spectrum for purified linear* ^{128}PQRKVFRSLK^{137} *peptide,* using *positive ion detection mode (reflector type) with sinapic acid as matrix. M/z peak for the $[M+H]^+$ ion of the peptide was observed at 1257.5. Peaks at m/z 1280.5 and*

1296.0 were attributed to Na^+ and K^+ adducts. Peak for NH_2 deleted fragment was observed at m/z 1241.2.

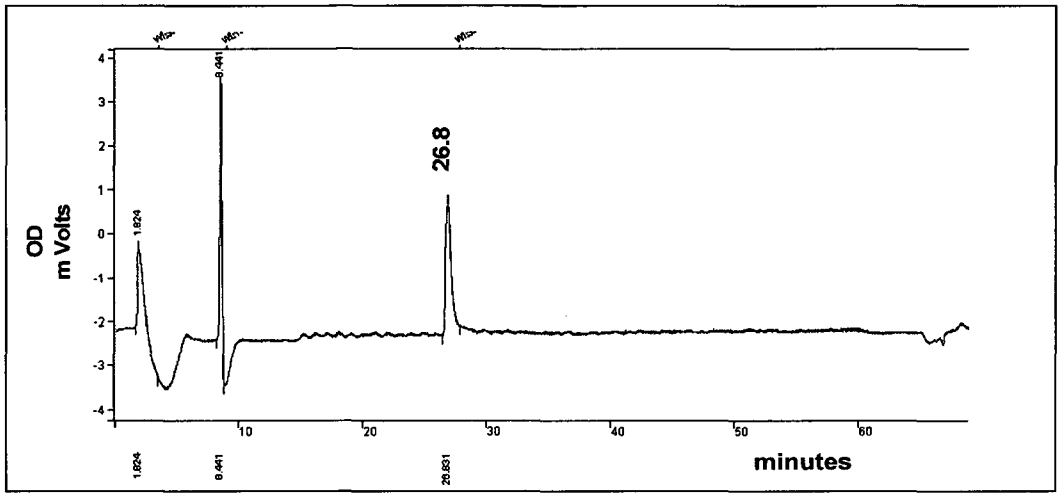

Figure 6.8A: *RP-HPLC chromatogram for (^{128}PQRKVFRSLK^{137})$_2$KA branch peptide purification on C18 semi preparative column (Jupiter, Phenomenex; 1 x 25 cm, 10 μ, 300 Å), UV detector with fixed wave length at 214 nm. Peptide was eluted at retention time of 26.8 min.*

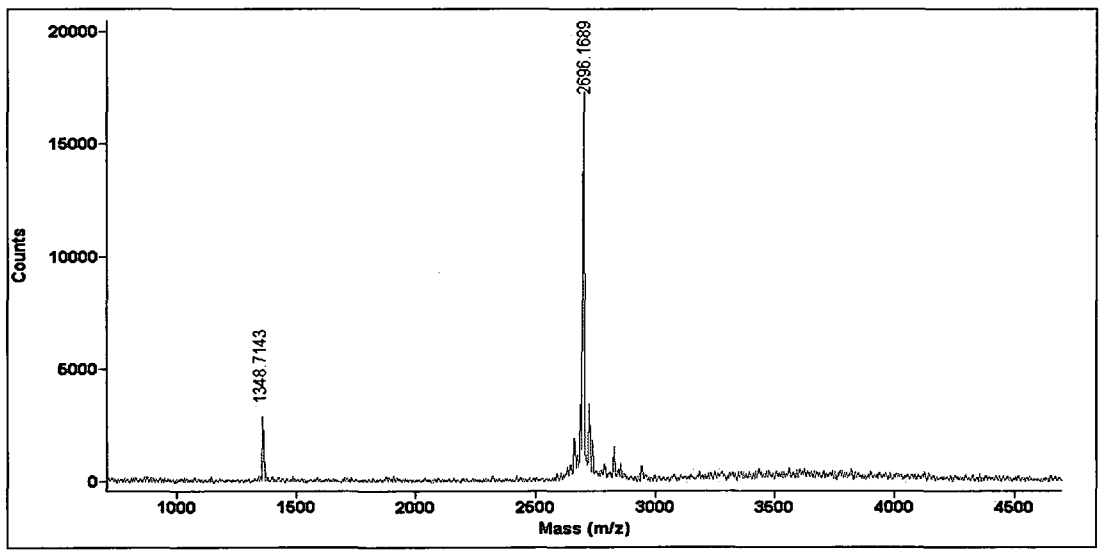

Figure 6.8B: *MALDI-TOF mass spectrum for purified (^{128}PQRKVFRSLK^{137})$_2$KA peptide characterization. Positive ion detection mode (reflector type) and sinapic acid matrix were*

used for the analysis. Peak for $[M+H]^+$ ion were observed at m/z 2696.2. Peak at m/z 1348.7 was attributed $[M+2H]^{2+}$ ion of the peptide.

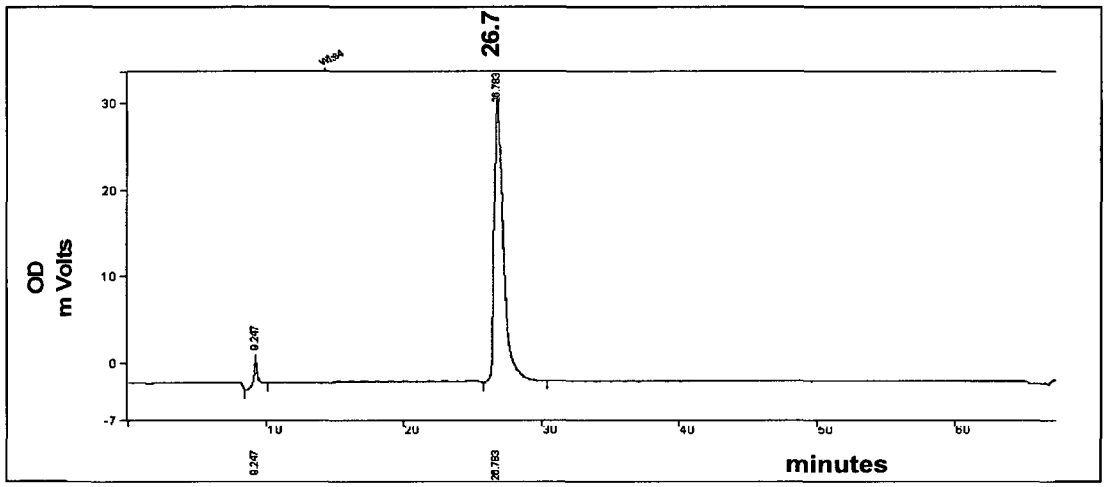

Figure 6.9A; *RP-HPLC chromatogram for $[^{128}PQRKVFRSLK^{137}(Ahx)_2)_2KA$ branch peptide purification on C18 semi preparative column (Jupiter, Phenomenex; 1 x 25 cm, 10 μ, 300 Å), UV detector with fixed wave length at 214 nm. Peptide was eluted at the retention time of 26.7 min.* [ ]

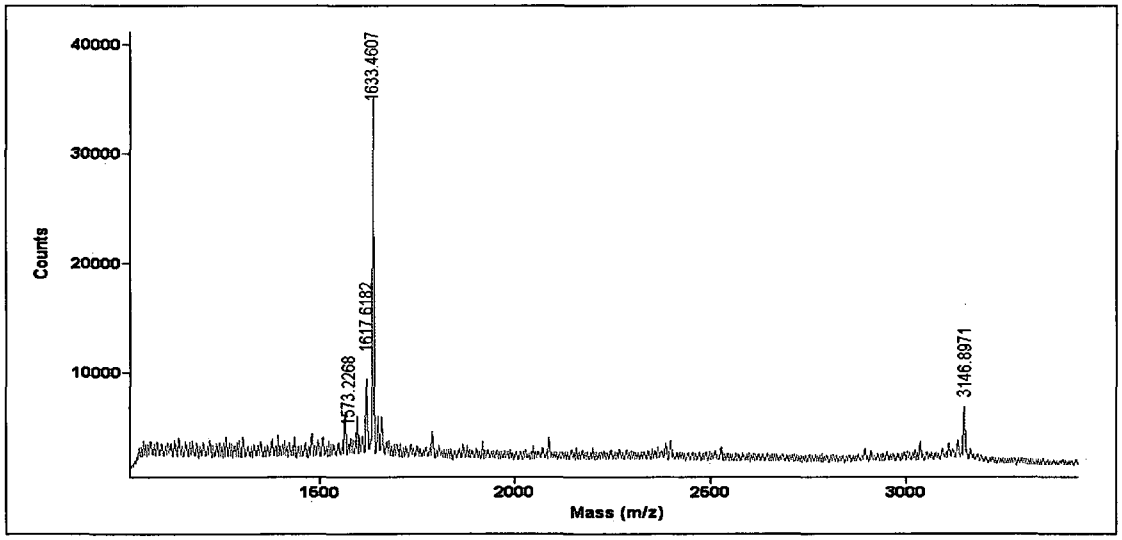

Figure 6.9B: *MALDI-TOF mass spectrum for purified (for $[^{128}PQRKVFRSLK^{137}(Ahx)_2]_2KA$ peptide* using *positive ion detection mode (reflector type)*

with sinapic acid as matrix. Peaks for $[M+H]^+$ and $[M+2H]^{2+}$ ions were observed at m/z 3146.9 and 1573.2 respectively. Peaks at m/z 1633.5 and 1617.6 were attributed to loss of one peptide unit from the parent pepetide and the loss of NH2 group.

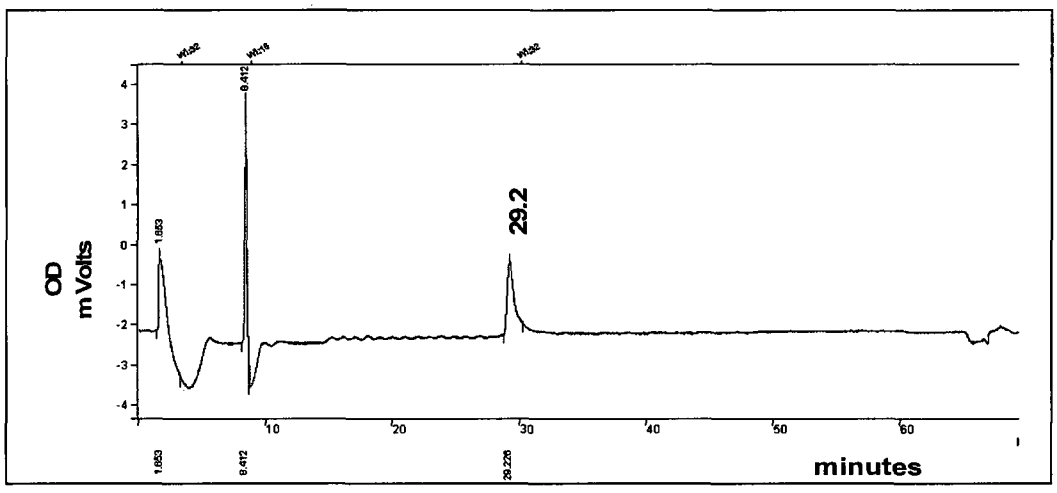

Figure 6.10A: *RP-HPLC chromatogram for $[^{128}PQRKVFRSLK^{137}(Ahx)_2]_4KA$ branch peptide purification on C18 semi preparative column (Phenomenex-Jupiter, 10 μ, 300 Å, 1X 25 Cm), UV detector with fixed wave length at 214 nm. Peptide was eluted at retention time of 29.2 min.*

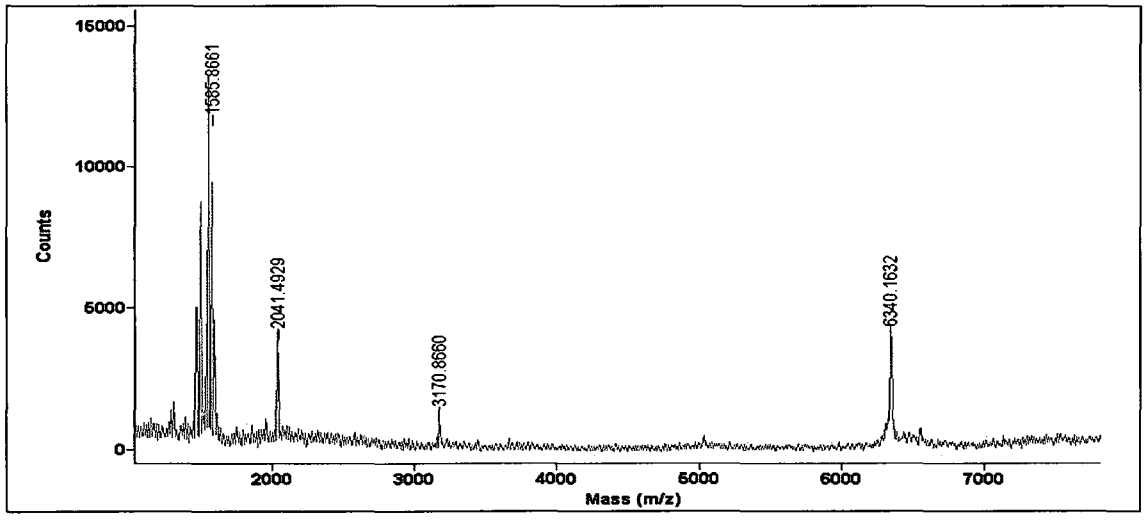

Figure 6.10B: *MALDI-TOF mass spectrum for $[^{128}PQRKVFRSLK^{137}(Ahx)_2]_4KA$ peptide characterization. Positive ion detection mode (reflector type) and sinapic acid matrix were*

used as matrix. The m/z peak for the mono isotopic ion of the peptide was observed at 6340.2. Peaks at m/z 3170.9 and 1585.9 were attributed to $[M+2H]^{2+}$ *and* $[M+4H]^{4+}$ *ions respectively.*

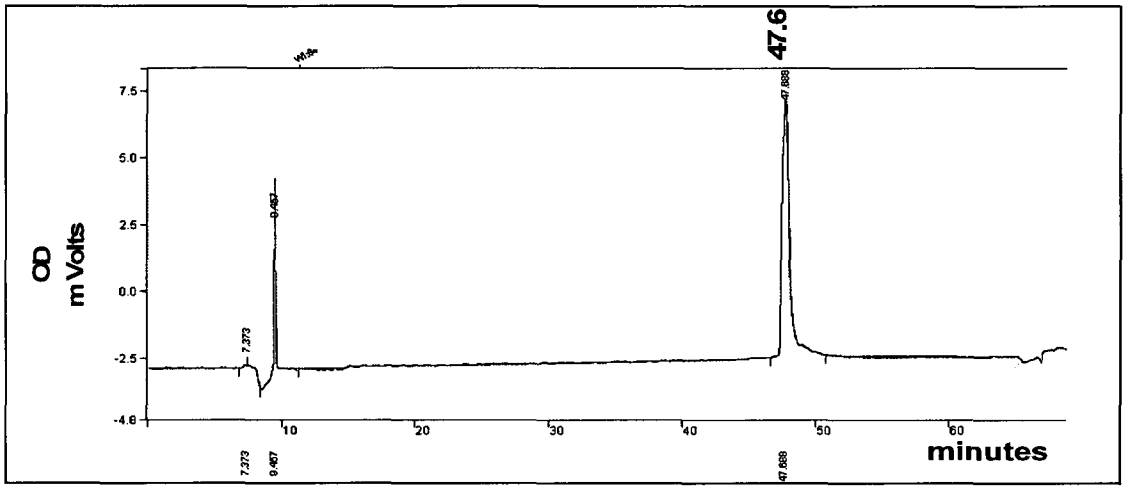

Figure 6.11A: *RP-HPLC chromatogram for fluorogenic Q-GPC substrate purification on C18 semi preparative column (Phenomenex-Jupiter, 10 μ, 300 Å, 1X 25 Cm), UV detector with fixed wave length at 214 nm. Peptide was eluted at the retention time of 47.6 min.*

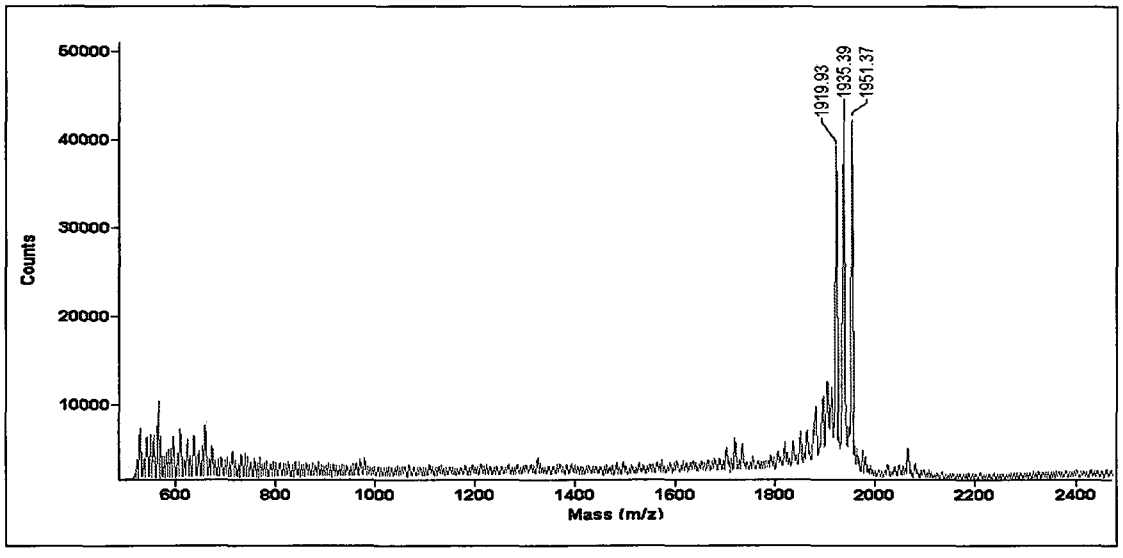

Figure 6.11B: *MALDI-TOF mass spectrum for Q-GPC substrate* using *positive ion detection mode (reflector type) with CHCA as matrix. Peak for the* $[M+H]^{+}$ *ion of the*

peptide was observed at m/z 1951.4. Peaks at m/z 1935.4 and 1919.9 were attributed to consecutive losses of two NH_2 groups.

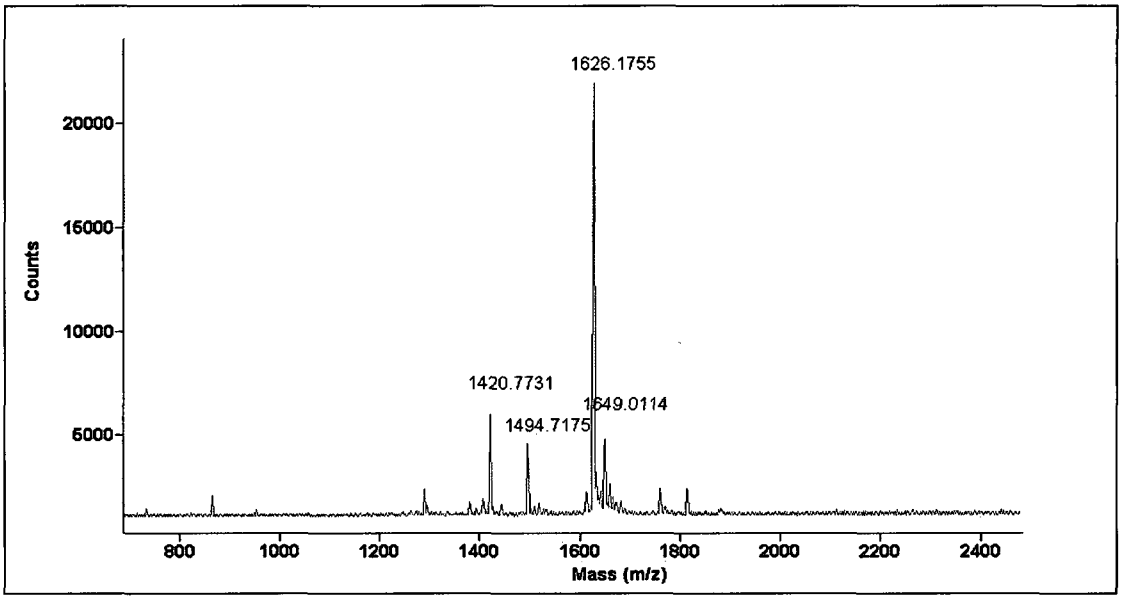

Figure 6.12: *MALDI-TOF mass spectrum for fluorogenic CMV substrate, using positive ion detection mode (reflector type) with CHCA matrix. Major m/z peak at 1626.2 attributed to molecular mass of the mono isotopic ion of the substrate and the peak representing Na^+ adduct was observed at m/z 1649.*

Publications

A. Peer-reviewed articles

1. Basak S*, **Mohottalage D***, and Basak A. Multibranch and Pseudo peptide approach for design of novel inhibitors of Subtilisin Kexin Isozyme-1, *Protein Pept. Letters, 13(9), 863-876, **2006**. (* = equal contribution).*

2. Basak A., Chen A, Scamuffa N, **Mohottalage D**, Basak S and Kahatib A.M Blockade of Furin Activity and Furin-induced Tumor Cells Malignant Phenotypes By The Chemically Synthesized Human Furin Prodomain. *PLoS One (Submitted)*

B. Conferences and book proceedings

1. Basak A, Hao X, **Mohottalage D**, Lotfipour F, Basak S Cellulardelivery and design of Proprotein Convertase Inhibitors. *BIOPOLYMERS, 80(4): 552-552, **2005**.*

2. Basak A, Hao X, **Mohottalage D**, Lotfipour F, Basak S Cellular delivery and design of Proprotein Convertase Inhibitors. Peptides "Understanding Biology Using Peptides, *Proceeding 19th APS (Ed Blondelle, SE), Springer, New York, N, ,pp341-343, **2006.***

3. **Mohottalage D**, Basak S and Basak A. Pseudo and branch-peptide Inhibitors of subtilisin kexin isozyme-1: design, synthesis and biochemical evaluation. *Peptides-Proceedings of 29th European Peptide Society Meeting. Sep 3-8, Gdansk, Poland, **2006.***

4. **Mohottalage D**, Goto N, Basak A "Substilisin Kexin Isozyme-1(SKI-1): Production, purification, inhibitor design and biochemical application" *Peptides for youths, proceedings 20th APS meeting, Montreal, Canada, June 26-30, **2007.***

References

(1) Beyer WR, Popplau D, Garten W et al. Endoproteolytic processing of the lymphocytic choriomeningitis virus glycoprotein by the subtilase SKI-1/S1P. J Virol 2003 March;77(5):2866-72.

(2) Espenshade PJ, Cheng D, Goldstein JL, Brown MS. Autocatalytic processing of site-1 protease removes propeptide and permits cleavage of sterol regulatory element-binding proteins. J Biol Chem 1999 August 6;274(32):22795-804.

(3) Lenz O, ter MJ, Klenk HD et al. The Lassa virus glycoprotein precursor GP-C is proteolytically processed by subtilase SKI-1/S1P. Proc Natl Acad Sci U S A 2001 October 23;98(22):12701-5.

(4) Sakai J. [Site-1 protease: a subtilisin-like serine protease that cleaves SREBPs for controlling the lipid biosynthesis in animal cell]. Nippon Rinsho 2001 February;59 Suppl 2:277-82.

(5) Seidah NG, Mowla SJ, Hamelin J et al. Mammalian subtilisin/kexin isozyme SKI-1: A widely expressed proprotein convertase with a unique cleavage specificity and cellular localization. Proc Natl Acad Sci U S A 1999 February 16;96(4):1321-6.

(6) Ye J, Rawson RB, Komuro R et al. ER stress induces cleavage of membrane-bound ATF6 by the same proteases that process SREBPs. Mol Cell 2000 December;6(6):1355-64.

(7) Sakai J, Rawson RB, Espenshade PJ et al. Molecular identification of the sterol-regulated luminal protease that cleaves SREBPs and controls lipid composition of animal cells. Mol Cell 1998 October;2(4):505-14.

(8) Toure BB, Munzer JS, Basak A et al. Biosynthesis and enzymatic characterization of human SKI-1/S1P and the processing of its inhibitory prosegment. J Biol Chem 2000 January 28;275(4):2349-58.

(9) Rawlings ND, Barrett AJ. Evolutionary families of peptidases. Biochem J 1993 February 15;290 (Pt 1):205-18.

(10) Rawlings ND, Morton FR, Kok CY et al. MEROPS: the peptidase database. Nucleic Acids Res 2008 January;36(Database issue):D320-D325.

(11) Seidah NG, Chretien M. Proprotein and prohormone convertases: a family of subtilases generating diverse bioactive polypeptides. Brain Res 1999 November 27;848(1-2):45-62.

(12) Seidah NG, Benjannet S, Wickham L et al. The secretory proprotein convertase neural apoptosis-regulated convertase 1 (NARC-1): liver regeneration and neuronal differentiation. Proc Natl Acad Sci U S A 2003 February 4;100(3):928-33.

(13) Beynon RJ, Bond JS. Proteolytic Enzymes. Oxford University Press; 1989.

(14) Cheng D, Espenshade PJ, Slaughter CA et al. Secreted site-1 protease cleaves peptides corresponding to luminal loop of sterol regulatory element-binding proteins. J Biol Chem 1999 August 6;274(32):22805-12.

(15) Brown MS, Goldstein JL. A proteolytic pathway that controls the cholesterol content of membranes, cells, and blood. Proc Natl Acad Sci U S A 1999 September 28;96(20):11041-8.

(16) Pullikotil P, Benjannet S, Mayne J, Seidah NG. The proprotein convertase SKI-1/S1P: alternate translation and subcellular localization. J Biol Chem 2007 September 14;282(37):27402-13.

(17) Ellis RJ. Steric chaperones. Trends Biochem Sci 1998 February;23(2):43-5.

(18) Elagoz A, Benjannet S, Mammarbassi A et al. Biosynthesis and cellular trafficking of the convertase SKI-1/S1P: ectodomain shedding requires SKI-1 activity. J Biol Chem 2002 March 29;277(13):11265-75.

(19) Mowla SJ, Farhadi HF, Pareek S et al. Biosynthesis and post-translational processing of the precursor to brain-derived neurotrophic factor. J Biol Chem 2001 April 20;276(16):12660-6.

(20) Okada T, Haze K, Nadanaka S et al. A serine protease inhibitor prevents endoplasmic reticulum stress-induced cleavage but not transport of the membrane-bound transcription factor ATF6. J Biol Chem 2003 August 15;278(33):31024-32.

(21) Schlombs K, Wagner T, Scheel J. Site-1 protease is required for cartilage development in zebrafish. Proc Natl Acad Sci U S A 2003 November 25;100(24):14024-9.

(22) Mouchantaf R, Watt HL, Sulea T et al. Prosomatostatin is proteolytically processed at the amino terminal segment by subtilase SKI-1. Regul Pept 2004 August 15;120(1-3):133-40.

(23) Vincent MJ, Sanchez AJ, Erickson BR et al. Crimean-Congo hemorrhagic fever virus glycoprotein proteolytic processing by subtilase SKI-1. J Virol 2003 August;77(16):8640-9.

(24) Basak S, Mohottalage D, Basak A. Multibranch and pseudopeptide approach for design of novel inhibitors of subtilisin kexin isozyme-1. Protein Pept Lett 2006;13(9):863-76.

(25) Bodvard K, Mohlin J, Knecht W. Recombinant expression, purification, and kinetic and inhibitor characterisation of human site-1-protease. Protein Expr Purif 2007 February;51(2):308-19.

(26) Holskin BP, Bukhtiyarova M, Dunn BM et al. A continuous fluorescence-based assay of human cytomegalovirus protease using a peptide substrate. Anal Biochem 1995 May 1;227(1):148-55.

(27) Basak A, Zhong M, Munzer JS et al. Implication of the proprotein convertases furin, PC5 and PC7 in the cleavage of surface glycoproteins of Hong Kong, Ebola and respiratory syncytial viruses: a comparative analysis with fluorogenic peptides. Biochem J 2001 February 1;353(Pt 3):537-45.

(28) Basak A, Lotfipour F. Modulating furin activity with designed mini-PDX peptides: synthesis and in vitro kinetic evaluation. FEBS Lett 2005 August 29;579(21):4813-21.

(29) Basak A, Shervani NJ, Mbikay M, Kolajova M. Recombinant proprotein convertase 4 (PC4) from Leishmania tarentolae expression system: Purification, biochemical study and inhibitor design. Protein Expr Purif 2008 March 25.

(30) Lecaille F, Weidauer E, Juliano MA et al. Probing cathepsin K activity with a selective substrate spanning its active site. Biochem J 2003 October 15;375(Pt 2):307-12.

(31) Berman Y, Juliano L, Devi LA. Specificity of the dynorphin-processing endoprotease: comparison with prohormone convertases. J Neurochem 1999 May;72(5):2120-6.

(32) Basak A, Chretien M, Seidah NG. A rapid fluorometric assay for the proteolytic activity of SKI-1/S1P based on the surface glycoprotein of the hemorrhagic fever Lassa virus. FEBS Lett 2002 March 13;514(2-3):333-9.

(33) Rawson RB, Zelenski NG, Nijhawan D et al. Complementation cloning of S2P, a gene encoding a putative metalloprotease required for intramembrane cleavage of SREBPs. Mol Cell 1997 December;1(1):47-57.

(34) Duncan EA, Dave UP, Sakai J et al. Second-site cleavage in sterol regulatory element-binding protein occurs at transmembrane junction as determined by cysteine panning. J Biol Chem 1998 July 10;273(28):17801-9.

(35) Brown MS, Goldstein JL. The SREBP pathway: regulation of cholesterol metabolism by proteolysis of a membrane-bound transcription factor. Cell 1997 May 2;89(3):331-40.

(36) Sakai J, Nohturfft A, Goldstein JL, Brown MS. Cleavage of sterol regulatory element-binding proteins (SREBPs) at site-1 requires interaction with SREBP cleavage-activating protein. Evidence from in vivo competition studies. J Biol Chem 1998 March 6;273(10):5785-93.

(37) Biagini G, Avoli M, Marcinkiewicz J, Marcinkiewicz M. Brain-derived neurotrophic factor superinduction parallels anti-epileptic--neuroprotective

treatment in the pilocarpine epilepsy model. J Neurochem 2001 March;76(6):1814-22.

(38) Chen X, Shen J, Prywes R. The luminal domain of ATF6 senses endoplasmic reticulum (ER) stress and causes translocation of ATF6 from the ER to the Golgi. J Biol Chem 2002 April 12;277(15):13045-52.

(39) Paschen W, Mengesdorf T. Cellular abnormalities linked to endoplasmic reticulum dysfunction in cerebrovascular disease--therapeutic potential. Pharmacol Ther 2005 December;108(3):362-75.

(40) Martinez A, Castro A, Gil C, Perez C. Recent strategies in the development of new human cytomegalovirus inhibitors. Med Res Rev 2001 May;21(3):227-44.

(41) Patra D, Xing X, Davies S et al. Site-1 protease is essential for endochondral bone formation in mice. J Cell Biol 2007 November 19;179(4):687-700.

(42) Pullikotil P, Vincent M, Nichol ST, Seidah NG. Development of protein-based inhibitors of the proprotein of convertase SKI-1/S1P: processing of SREBP-2, ATF6, and a viral glycoprotein. J Biol Chem 2004 April 23;279(17):17338-47.

(43) Basak S, Stewart NA, Chretien M, Basak A. Aminoethyl benzenesulfonyl fluoride and its hexapeptide (Ac-VFRSLK) conjugate are both in vitro inhibitors of subtilisin kexin isozyme-1. FEBS Lett 2004 August 27;573(1-3):186-94.

(44) Pasquato A, Pullikotil P, Asselin MC et al. The proprotein convertase SKI-1/S1P. In vitro analysis of Lassa virus glycoprotein-derived substrates and ex vivo validation of irreversible peptide inhibitors. J Biol Chem 2006 August 18;281(33):23471-81.

(45) Rabah N, Gauthier DJ, Gauthier D, Lazure C. Improved PC1/3 production through recombinant expression in insect cells and larvae. Protein Expr Purif 2004 October;37(2):377-84.

(46) Jutras I, Seidah NG, Reudelhuber TL, Brechler V. Two activation states of the prohormone convertase PC1 in the secretory pathway. J Biol Chem 1997 June 13;272(24):15184-8.

(47) Tangrea MA, Bryan PN, Sari N, Orban J. Solution structure of the pro-hormone convertase 1 pro-domain from Mus musculus. J Mol Biol 2002 July 19;320(4):801-12.

(48) Venkatesan N, Kim BH. Synthesis and enzyme inhibitory activities of novel peptide isosteres. Curr Med Chem 2002 December;9(24):2243-70.

(49) Peter E. Pseudo-Peptides in Drug Discovery. Wiley-VCH Verlag GmbH & Co. KGaA; 2003.

(50) Breton P, Monsigny M, Mayer R. Psi[CH2O] pseudodipeptide synthesis. An improved approach which allows absolute configuration determination. Int J Pept Protein Res 1990 April;35(4):346-51.

(51) Rubini E, Gilon C, Selinger Z, Chorev M. Synthesis Of Isosteric Methylene-Oxy psuedopepetide analogues as noval amide bond surrogate units. Tetrahedron 1986;42(21):6039-43.

(52) Basak A, Boudreault A, Chen A et al. Application of the multiple antigenic peptides (MAP) strategy to the production of prohormone convertases antibodies: synthesis, characterization and use of 8-branched immunogenic peptides. J Pept Sci 1995 November;1(6):385-95.

(53) Azuma M, Kojima T, Yokoyama I et al. Antibacterial activity of multiple antigen peptides homologous to a loop region in human lactoferrin. J Pept Res 1999 September;54(3):237-41.

(54) Nomizu M, Yamamura K, Kleinman HK, Yamada Y. Multimeric forms of Tyr-Ile-Gly-Ser-Arg (YIGSR) peptide enhance the inhibition of tumor growth and metastasis. Cancer Res 1993 August 1;53(15):3459-61.

(55) Velazquez-Campoy A, Kiso Y, Freire E. The binding energetics of first- and second-generation HIV-1 protease inhibitors: implications for drug design. Arch Biochem Biophys 2001 June 15;390(2):169-75.

(56) Cornish-Bowden A. Fundamentals of Enzyme Kinetics. Portland Press Ltd; 1995.

(57) Smyth TP. Substrate variants versus transition state analogues as noncovalent reversible enzyme inhibitors. Bioorg Med Chem 2004 August 1;12(15):4081-8.

(58) Bravo IG, Busto F, De AD et al. Application of a normalised plot to the study of uni-uni enzyme-inhibitor systems. Biochim Biophys Acta 2002 July 3;1571(3):183-9.

(59) Tian G, Sobotka-Briner CD, Zysk J et al. Linear non-competitive inhibition of solubilized human gamma-secretase by pepstatin A methylester, L685458, sulfonamides, and benzodiazepines. J Biol Chem 2002 August 30;277(35):31499-505.

(60) Cornish-Bowden A. A Simple Graphical Method for Determining the Inhibition Constants of Mixed, Uncompetitive and Non-Competitive Inhibitors. J Biol Chem 1974;137:143-4.

(61) Kakkar T, Boxenbaum H, Mayersohn M. Estimation of Ki in a competitive enzyme-inhibition model: comparisons among three methods of data analysis. Drug Metab Dispos 1999 June;27(6):756-62.

(62) Leff P, Dougall IG. Further concerns over Cheng-Prusoff analysis. Trends Pharmacol Sci 1993 April;14(4):110-2.

(63) Motoyama A, Xu T, Ruse CI et al. Anion and cation mixed-bed ion exchange for enhanced multidimensional separations of peptides and phosphopeptides. Anal Chem 2007 May 15;79(10):3623-34.

(64) Fugere M, Limperis PC, Beaulieu-Audy V et al. Inhibitory potency and specificity of subtilase-like pro-protein convertase (SPC) prodomains. J Biol Chem 2002 March 8;277(10):7648-56.

(65) Boudreault A, Gauthier D, Rondeau N et al. Molecular characterization, enzymatic analysis, and purification of murine proprotein convertase-1/3 (PC1/PC3) secreted from recombinant baculovirus-infected insect cells. Protein Expr Purif 1998 December;14(3):353-66.

(66) Lamango NS, Zhu X, Lindberg I. Purification and enzymatic characterization of recombinant prohormone convertase 2: stabilization of activity by 21 kDa 7B2. Arch Biochem Biophys 1996 June 15;330(2):238-50.

(67) Zhang J, Kuvelkar R, Wu P et al. Differential inhibitor sensitivity between human recombinant and native photoreceptor cGMP-phosphodiesterases (PDE6s). Biochem Pharmacol 2004 September 1;68(5):867-73.

(68) Brooks SA. Appropriate Glycosylation of Recombinanat Proteins for Human Use: Implications of Choice of Expression System. Molecular Biotechnology 2004;28(16):241-56.

(69) Graham FL, Smiley J, Russell WC, Nairn R. Characteristics of a human cell line transformed by DNA from human adenovirus type 5. J Gen Virol 1977 July;36(1):59-74.

(70) Hoi-Ling Wonga M-XWP-TC. A 3D collagen microsphere culture system for GDNF-secreting HEK293 cells with enhanced protein productivity. Biomaterials 2007;28:5369-80.

(71) Seidah NG, Benjannet S, Hamelin J et al. The subtilisin/kexin family of precursor convertases. Emphasis on PC1, PC2/7B2, POMC and the novel enzyme SKI-1. Ann N Y Acad Sci 1999 October 20;885:57-74.

(72) Lacombe ML, Mercure C, Dikeakos JD, Reudelhuber TL. Modulation of Secretory Granule-targeting Efficiency by Cis and Trans Compounding of Sorting Signals. The Journal of Biological Chemistry 2005;11:4803-7.

(73) Lou H, Smith AM, Coates LC et al. The transmembrane domain of the prohormone convertase PC3: a key motif for targeting to the regulated secretory pathway. Mol Cell Endocrinol 2007 March 15;267(1-2):17-25.

(74) Travis J, Bowen J, Tewksbury D et al. Isolation of albumin from whole human plasma and fractionation of albumin-depleted plasma. Biochem J 1976 August 1;157(2):301-6.

(75) Ahmed N, Barker G, Oliva K et al. An approach to remove albumin for the proteomic analysis of low abundance biomarkers in human serum. Proteomics 2003 October;3(10):1980-7.

(76) Barbour EK, Sagherian V, Talhouk S et al. Evaluation of homeopathy in broiler chickens exposed to live viral vaccines and administered Calendula officinalis extract. Med Sci Monit 2004 August;10(8):BR281-BR285.

(77) Chang BS, Mahoney RR. Enzyme thermostabilization by bovine serum albumin and other proteins: evidence for hydrophobic interactions. Biotechnol Appl Biochem 1995 October;22 (Pt 2):203-14.

(78) Williams AJ, Blacklow SC, Collins T. The zinc finger-associated SCAN box is a conserved oligomerization domain. Mol Cell Biol 1999 December;19(12):8526-35.

(79) Dikeakos JD, Mercure C, Lacombe MJ et al. PC1/3, PC2 and PC5/6A are targeted to dense core secretory granules by a common mechanism. FEBS J 2007 August; 274(16):4094-102.

(80) Garzon MT, Lidon-Moya MC, Barrera FN et al. The dimerization domain of the HIV-1 capsid protein binds a capsid protein-derived peptide: a biophysical characterization. Protein Sci 2004 June;13(6):1512-23.

(81) Mateu MG. Conformational stability of dimeric and monomeric forms of the C-terminal domain of human immunodeficiency virus-1 capsid protein. J Mol Biol 2002 April 26;318(2):519-31.

(82) Xie J, Seto CT. Investigations of linker structure on the potency of a series of bidentate protein tyrosine phosphatase inhibitors. Bioorg Med Chem 2005 April 15;13(8):2981-91.

(83) Gorski JP, Huffman NT, Cui C, Henderson EP, Midura RJ, Seidah NG. Potential role of proprotein convertase SKI-1 in the mineralization of primary bone. Cells Tissues Organs. 2009;189(1-4):25-32. Epub 2008 Aug 26